

Evaluating the Potential Environmental Impacts of Connected and Automated Vehicles

By

Jim Gawron

A thesis submitted in partial
fulfillment of the requirements for the
degree of Masters of Science
(Environment and Sustainability) at
the University of Michigan

April 2019

Thesis Committee:

Professor Gregory A. Keoleian, Chair

Dr. Timothy J. Wallington, Senior Technical Leader, Ford Research and Innovation Center

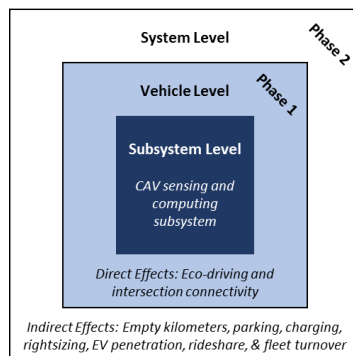
Acknowledgements

I would like to thank Dr. Gregory Keoleian for making this thesis project possible. His vision helped guide the direction of the research and define the scope within the broad topic of autonomous vehicles. His wisdom and support ensured the technical rigor and accuracy of the analysis. Additionally, his work ethic, selflessness, and passion for sustainability helped to inspire the entire team and motivated continued focus throughout the 2.5 year timeline. Dr. Keoleian has been much more than an advisor, but also a mentor, coach, and most importantly, a friend. I would also like to thank the environmental science team members at Ford Motor Company, including Dr. Timothy Wallington, Robert De Kleine, and Dr. Hyung Chul Kim. Their constant support, access to resources, and communication expertise were instrumental to the success of the research. It has been an honor to work with all four of these experts.

This research was supported by the following grants from Ford Motor Company to the Center for Sustainable Systems at the University of Michigan: Ford-University of Michigan Alliance Grant (No. N022546-00) and Ford-Poling Challenge Grant. In addition, I wish to acknowledge the following for their helpful contributions: Morteza Taiebat for his insights on existing autonomous vehicle research and current gaps, Dr. Thomas Stephens at Argonne National Laboratory for sharing his detailed knowledge on autonomous vehicles and scoping recommendations, Dr. Heui Pang at Mcity for sharing information on sensor technology and suppliers, and Geoff Lewis and Helaine Hunscher for their support and advice throughout my graduate school experience.

Preface

While it is clear that future connected and automated vehicles (CAVs) will revolutionize personal mobility, the sustainability and environmental impacts are highly uncertain. The research objective of this thesis is to evaluate the primary energy and life cycle greenhouse gas (GHG) emissions performance of CAVs for a variety of deployment scenarios. The analysis was conducted in two phases: Phase 1 included the subsystem and vehicle levels, while Phase 2 included the system level. The figure below illustrates the relationship between the phases, levels, and autonomous vehicle effects. The scope of Phase 1 focused on a single CAV compared to a human-driven vehicle across six scenarios that varied the powertrain and CAV subsystem. Phase 2 zoomed out to examine an autonomous taxi (AT) fleet across nine scenarios over the long term. Each research phase used life cycle assessment methodology to ensure the inclusion and comprehensive accounting of materials, manufacturing, use, and end of life burdens. The vehicle-level results indicate the addition of CAV subsystems to platform vehicles could increase GHG emissions 3-20%; however, when operational efficiencies from CAV direct effects are included, the net result is up to a 9% reduction. The system-level results indicate the strategic deployment of an electrified AT fleet can reduce cumulative GHG emissions from 2020 to 2050 by 60%. Further reductions up to 87% can be achieved with accelerated electrical grid decarbonization, dynamic ride-share, longer vehicle lifetime, more energy efficient computers, and higher new vehicle fuel consumption rate reductions. Overall, this research highlights the major opportunities for maximizing the environmental performance of this emerging technology.



The work presented in Phase 1 of this thesis was published in the journal Environmental Science and Technology: Gawron, J. H., Keoleian, G. A., De Kleine, R. D., Wallington, T. J., & Kim, H. C. (2018). Life cycle assessment of connected and automated vehicles: Sensing and computing subsystem and vehicle level effects. *Environmental science & technology*, 52(5), 3249-3256.

<https://pubs.acs.org/doi/full/10.1021/acs.est.7b04576#cite>

The work presented in Phase 2 of this thesis was submitted for publication in the journal Transportation Research Part D: Transport and the Environment. The publication decision is still pending at this time.

Table of Contents

List of Tables	8
List of Figures	8
1. Phase 1: Subsystem and Vehicle Levels.....	9
1.1 Abstract.....	9
1.2 Introduction	9
1.3 Methods.....	11
1.4 Product System.....	12
1.5 Results.....	18
1.6 Discussion	24
2. Phase 2: Mobility System Level.....	25
2.1 Abstract.....	25
2.2 Introduction	26
2.3 Methods.....	29
2.3.1 Goal and Scope	31
2.3.2 Fleet Characteristics	32
2.3.3 Vehicles	33
2.3.4 Parking.....	36
2.3.5 Charging Infrastructure.....	36
2.3.6 Fleet Turnover	36
2.4 Results.....	38
2.4.1 Base Case Results	38

2.4.2 Dynamic Ride-sharing.....	42
2.4.3 Sensitivity Analysis.....	43
2.5 Conclusion.....	44
References	47
Appendix A – Phase 1 Supporting Information	54
Appendix B – Phase 2 Supporting Information	55

List of Tables

Table 1: CAV Sensing and Computing Subsystem Architectures	13
Table 2: CAV Component Weight and Power Characteristics	14
Table 3: Individual CAV Direct Effects	18
Table 4: Key characteristics for each of the nine AT fleet scenarios	32
Table 5: Vehicle life-cycle energy and GHG emissions per km	35
Table 6: New vehicle fuel consumption for 2010 to 2050	37

List of Figures

Figure 1: Three CAV impact levels and the boundary of this study	11
Figure 2: Medium CAV subsystem weight and power breakdown	19
Figure 3: Medium CAV subsystem GHG emission breakdown by component	19
Figure 4: Vehicle-level GHG results for the baseline scenario	20
Figure 5: Vehicle-level GHG results for each CAV scenario	22
Figure 6: Tri-level structure for CAV direct and indirect effects	29
Figure 7: Framework for evaluating the environmental impacts of AT fleets	30
Figure 8: Acronym key for the nine scenarios analyzed	31
Figure 9: Monthly GHG emissions from 2020 to 2050	39
Figure 10: Cumulative fleet GHG emissions over the period 2020-2050	40
Figure 11: Expansion of Group A	41
Figure 12: Expansion of Group B	42

1. Phase 1: Subsystem and Vehicle Levels

Phase 1 of this thesis focused on the life cycle energy and greenhouse gas emissions of connected and automated vehicles at the sensing and computing subsystem and vehicle levels. This study was published in *Environmental Science and Technology* under the title “Life Cycle Assessment of Connected and Automated Vehicles: Sensing and Computing Subsystem and Vehicle Level Effects” at DOI 10.1021/acs.est.7b04576.

1.1 Abstract

Although recent studies of connected and automated vehicles (CAVs) have begun to explore the potential energy and greenhouse gas (GHG) emission impacts from an operational perspective, little is known about how the full life cycle of the vehicle will be impacted. We report the results of a life cycle assessment (LCA) of Level 4 CAV sensing and computing subsystems integrated into internal combustion engine vehicle (ICEV) and battery electric vehicle (BEV) platforms. The results indicate that CAV subsystems could increase vehicle primary energy use and GHG emissions by 3–20% due to increases in power consumption, weight, drag, and data transmission. However, when potential operational effects of CAVs are included (e.g., eco-driving, platooning, and intersection connectivity), the net result is up to a 9% reduction in energy and GHG emissions in the base case. Overall, this study highlights opportunities where CAVs can improve net energy and environmental performance.

1.2 Introduction

The connected and automated vehicle (CAV) is an emerging, transformative technology that could fundamentally change the current transportation system due to enhanced travel convenience, coordination with other communication and infrastructure systems, and the development of new mobility business models (Fagnant and Kockelman, 2015). This new mobility future has the potential to either decrease or increase energy consumption and emissions depending on implementation (The Transforming Mobility Ecosystem, 2017). The major factors that will determine CAV energy outcomes include the following:

ecodriving, platooning, lightweighting, and rightsizing, reduced driving to locate parking, ride sharing, congestion mitigation, higher travel demand due to reduced travel cost, increased travel by underserved populations, and faster highway speeds (Brown et al., 2015). When these factors are combined in a travel demand and efficiency framework with a 100% CAV adoption scenario, the resulting impact ranges from a 60% reduction in energy consumption up to a 200% increase (Estimated Bounds and Important Factors, 2016). Integrating these results with EIA reference case projections for the transportation sector produces light duty vehicle energy consumption estimates between 7,000 and 18,000 trillion Btu in 2050 compared to 16,000 trillion Btu in 2016 (Study of the Potential Energy Consumption, 2017).

The existing literature on CAV energy implications referenced above focuses primarily on the operational impact (Estimated Bounds and Important Factors, 2016). However, little is known about the full life cycle implications of CAV deployment. Previous studies have omitted the potential vehicle production life cycle impacts with the rationale that they are smaller in magnitude when compared to the travel related energy consumption, but no work has been done to date to examine this assumption (Wadud et al., 2016).

To fill the gap, this study provides a life cycle assessment (LCA) of CAV sensing and computing subsystems integrated into both internal combustion engine vehicle (ICEV) and battery electric vehicle (BEV) platforms. The LCA quantifies the burdens from the production and use of Level 4 CAV subsystems applied to the vehicle platforms. Level 4 CAVs, as defined by SAE International, conduct the driving task and monitor the driving environment within defined use cases where the human need not take back control (Taxonomy and Definitions, 2016). The potential effect of CAV technology on vehicle operation is modeled based on direct operational effects from the literature to investigate the overall vehicle-level impacts of CAVs. Only direct effects enabled by or directly related to the CAV technology adoption were included. These direct effects were considered to be eco-driving, platooning, intersection connectivity, and faster highway speeds. Broader mobility system shifts that could be indirectly accelerated by CAV technology but are potentially achievable through other means besides CAV deployment (such as congestion mitigation and ride sharing) as well as exogenous influences (such as

new policies and regulations) are not included given the technology-focused approach of this study. An illustration of the three impact levels and the study boundary is provided in Figure 1. Overall, the methodology integrates primary and secondary CAV data and potential direct effects to estimate life cycle energy and greenhouse gas (GHG) emission impacts at the subsystem and vehicle levels. The emerging nature of CAV technology poses unique challenges for the analysis (Miller and Keoleian, 2015). The precision is inherently limited by the available data regarding CAV subsystem architectures, sensor production, and real-world operational efficiencies from direct effects. To address the uncertainties, sensitivity analyses were conducted to evaluate the impacts of potential input parameter variations. Lastly, a set of key design insights was identified to help inform best practices during the early CAV design phases where there is the greatest freedom for improvement.

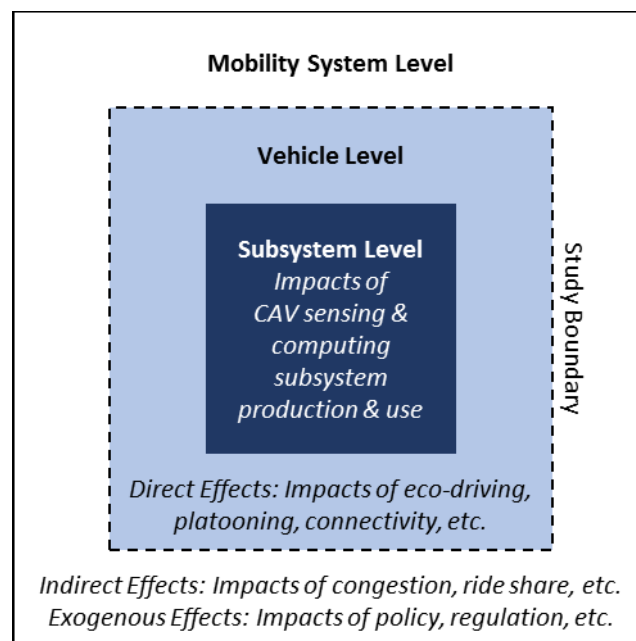


Figure 1. Three CAV impact levels and the boundary of this study

1.3 Methods

This study utilizes LCA methodology to consider life cycle energy use and GHG emissions from cradle to grave (ISO 2006). The analysis is limited to these two metrics due to the lack of available data for other

impacts, such as air pollutant emissions or water consumption, from the production of CAV subsystem components. The life cycle phases included are materials production, manufacturing and assembly, use, and end of life management.

Goal. The goal of this work is to estimate the impacts of CAV sensing and computing subsystems on the vehicle life cycle energy and GHG emissions. The net impact of CAVs is evaluated at the vehicle level after taking into account both direct operational effects and burdens from added component production, use, and shredding at end-of-life management.

Scope. The study provides a comparative analysis between non-CAVs and Level 4 CAVs in the US in multiple scenarios in the near-to-medium term. The scenarios consider BEV and ICEV powertrains as the two bookends of vehicle electrification. The platform vehicles are then paired with CAV subsystems of three different sizes (small, medium, and large) to create the following six scenarios: BEV + Small, BEV + Medium (baseline), BEV + Large, ICEV + Small, ICEV + Medium, and ICEV + Large. The BEV + Medium scenario is selected as the baseline since electric powertrains, and small light detection and ranging sensors (LiDARs) are used in the majority of today's prototype Level 4 CAVs.

1.4 Product System

The BEV platform is modeled as the 2015 Ford Focus Electric and the ICEV platform is modeled as the 2015 Ford Focus 4-Cylinder Automatic. Holding the manufacturer and vehicle model constant illustrates the impact of powertrain variation. Characteristics of the two platform vehicles are provided in Supporting Information (SI) Table S1. The small, medium, and large CAV subsystems are based on the configurations in use on the Tesla Model S, Ford Fusion (AV test vehicles), and Waymo's Chrysler Pacifica, respectively (A Look at Tesla's, Building Ford's Next-Generation, and Introducing Waymo's). The Level 4 CAV subsystem architectures are summarized in Table 1 and include sensors, computer, wire harness, and supporting structures. Images of each CAV subsystem are provided in SI Figure S1. Specific sensor models representing each sensor type were chosen from industry leading suppliers with mature

product offerings; these do not necessarily represent the specific hardware in use on any specific vehicle. Similarly, as details of the computer platforms for automated driving processing and control are typically proprietary for CAV development vehicles, the Nvidia Drive PX2 system was considered for all vehicles given its published product specs. It was assumed that no

additional control hardware is needed beyond the existing drive-by-wire systems of the platform vehicles.

Functional Unit. The functional unit for this study is a passenger car with a service life of 160,000 miles traveled over 12 years (GREET Model, 2015).

Table 1. CAV Sensing and Computing Subsystem Architectures

component	small	medium	large
camera	8	7	9
sonar	12	8	0
radar	1	2	4
large LiDAR	0	0	1
small LiDAR	0	2	4
Global Positioning System (GPS)/Inertial Navigation System (INS)	1	1	1
Dedicated Short Range Communication (DSRC)	1	1	1
computer	2	2	2
wire harness	small	medium	large
structure	negligible	small	large

System Boundary. The life cycle phases included are materials production, manufacturing and assembly, use, and end of life management. CAV indirect and exogenous effects at the mobility system level are excluded. Only operational efficiencies due to direct effects at the vehicle level are included as described in the introduction.

Environmental Impact Indicators. Two indicators are provided in this analysis based on their importance in automotive sustainability assessments (Jasinski et al., 2016). The first is life cycle energy in units of megajoules [MJ]. The second is life cycle GHG emissions in units of kilograms of carbon dioxide equivalent [kg CO₂-eq] on a 100-year GWP basis.

Life Cycle Inventory. An attributional approach was used to produce the life cycle inventory for the six CAV scenarios. Individual component characteristics and inventories are provided in Table 2 with images provided in SI Figure S2. The methods used to estimate each life cycle phase are given below.

Table 2. CAV Component Weight and Power Characteristics

characteristic	camera	radar	sonar	large LiDAR	small LiDAR	GPS/INS	DSRC	CPU
model	Pt. Gray Dragonfly2	Bosch LRR3	Bosch Ultrasonic	Velodyne HDL-64E	Velodyne VLP-16	NovAtel PwrPak7	Cohda MK5	Nvidia Drive PX2
weight (kg)	0.055	0.285	0.054	12.250	0.830	0.640	2.654	5.075
power (W)	2.1	4	0.13	60	8	2	6	96
production (MJ)	50	410	70	2,330	280	370	1,510	1,230
production (kg CO ₂ -eq)	3	24	3	139	17	24	85	81
use (MJ)	60	120	10	1,840	250	60	180	2,940
use (kg CO ₂ -eq)	5	9	1	129	17	5	13	206

Materials. The material breakdowns for each CAV sensing and computing component were sourced from primary data to the extent possible. Publicly available sensor specification sheets were supplemented by supplier interviews when needed (Autonomous Vehicle Uses, NvidiaAI, LRR3, AWG Copper, CohdaWireless, Hacking Automotive, DSRC, Antennas Pinwheel, Enclosures PwrPak7-E1, Dragonfly2, SavariSW-1000, Ultrasonic Sensor, Puck Hi-Res, and HDL-64E). When primary data were not available, materials weights were

estimated based on geometry and material properties. The resulting material breakdowns can be found in SI Table S2. Material energy and GHG emission burdens were taken from the GREET model.¹³ Material burdens for electronic components such as printed wire boards (PWB), integrated circuits (IC), and power supplies were derived from LCAs of desktop computers, laptops, and tablets (Teehan and Kandlikar, 2013). Further details on this method are provided in the Manufacturing section.

Manufacturing. The manufacturing burden for each CAV sensing and computing component was primarily taken from the GREET model. Fabrication processes for steel and aluminum parts include rolling and stamping. Copper parts involve wire drawing. Finally, plastics and polymer composites have injection and blow molding taken into account. Material loss factors of 1.38 and 1.34 (kg of input material/kg of finished part) are applied to manufacturing steps involving aluminum and steel parts,

respectively. For electronics, the estimation of materials and manufacturing burdens was combined according to the electronics LCAs indicated in the Materials section. Data from Teehan and Kandlikar (2013) were used to create component weight allocations specific to small (<0.5 kg), medium (0.5–1 kg), and large (>1 kg) electronics boards. The weight allocation across PWB, power supply, IC package, and IC die components for the small board is 77.8/20.0/2.0/0.2%, for the medium board is 41.3/55.3/3.3/0.1%, and for the large board is 40.6/57.7/1.6/0.1%. The average energy intensities for the PWB, power supply, IC package, and IC die components are 1.1, 0.51, 11, and 350 MJ/gram, respectively. The average GHG emission intensities are 0.060, 0.030, 0.53, and 24 kg CO₂-eq/gram, respectively. Packaging used for shipment of the sensor from the supplier manufacturing site to Dearborn, MI for assembly was estimated based on geometry and included both cardboard and plywood materials. Delivery impacts were estimated based on shipment weight and assuming transport in a Class 8 truck with a fuel intensity of 0.846 gal/100 ton-mile, which was derived from data published by Argonne National Laboratory (Evaluation of Fuel Consumption Potential, 2009).

Use. Four factors need to be considered to assess the usephase contribution of CAV sensing and computing subsystems. First, the CAV components increase the energy consumption of the platform vehicle due to their added electricity demand. On a BEV platform, the components draw electricity from the on-board battery, which is subsequently recharged from the local electrical grid. For this study, the 2015 U.S. Average Mix from the GREET model is assumed (34% coal, 32% natural gas, 20% nuclear, 6% hydro, 5% wind, and 3% other renewable) along with a primary energy to delivered electricity (well to tank) efficiency of 46% (GREET Model, 2015). The corresponding carbon intensity of the delivered electricity is 0.15 kg CO₂-eq/MJ. A 90% battery discharge/charge efficiency is assumed (Cooney et al., 2013). On an ICEV platform, electrical components are powered using gasoline combustion and an alternator. The associated conversion efficiencies are fuel to mechanical energy (30%), belt transmission (98%), and mechanical to electrical energy using the alternator (67%) (Where the Energy Goes and Commission Implementing Decision). Combining these efficiencies produces an overall conversion

efficiency for gasoline combustion energy to electricity of 20%. It is assumed that no additional power distribution systems or batteries are required due to the modest power consumption increases included in this study. The delivered energy (tank to wheel) to gasoline total fuel cycle energy (well to wheel) ratio taken from GREET is 78%. The corresponding well to wheel carbon intensity of the delivered fuel energy is 0.093 kg CO₂-eq/MJ.¹³ The total system on time over the lifetime of the CAV is based on the average time spent driving per person per year of 17,600 min (Cars are Parked 95% and American Driving Survey 2016).

Second, the components increase the weight of the vehicle and increase its fuel consumption. Fuel consumption increase values of 0.073 and 0.27 L equivalent per 100 km per 100 kg were used for the BEV and ICEV based on a physics-based model and the EPA 5-cycle fuel economy test data (Kim and Wallington, 2016).

Third, exterior mounted components increase the aerodynamic drag. Fuel consumption impacts of roof racks were used as a proxy to establish a conservative estimate of drag impacts associated with exterior mounted components. Based on their dimensions and placements on the vehicle, we used the aerodynamic drag from small and large roof racks to characterize the increased drag from medium and large CAV subsystems. The small CAV subsystem has no roof rack effect since all the sensors are integrated into the vehicle body, so no additional drag is assumed. It is estimated that small roof racks mounted on light duty vehicles increase fuel consumption by 0.5% assuming a 55/45 city/highway split (Chen, 2016). The fuel consumption impacts increase to 15.6% for a large roof rack classification.

Fourth, the burdens associated with map data transmission over wireless networks need to be considered. The required map resolution is assumed to be equivalent to typical digital navigation maps. The required data transmission is estimated to be 1.4 MB/mile based on data usage from map applications. The degree to which future vehicles would be able to store or reuse map data is unclear. Therefore, we adopt a conservative approach of assuming no storage and no reuse to give a total requirement of 220 GB over the vehicle lifetime. The primary energy intensity of data transmission over the 4G LTE network is 1.25

MJ/GB, which includes the power consumption of the base station, telecommunications networks, and data centers (The Power of Wireless Cloud, 2013). The 2015 U.S. Average Grid Mix from the GREET model was used to compute GHG emissions associated with transmission of the map data.

End-of-Life. The end-of-life vehicle is assumed to be shredded with its CAV components. The end-of-life management of BEV batteries is the topic of current research but is beyond the scope of, and was not included in, the present work. The energy and GHG intensities of the treatment are 1.08 MJ/kg and 0.076 kg CO₂-eq/kg, respectively (GREET Model, 2015).

CAV Direct Operational Effects. The operational efficiencies from CAV direct effects are included in this study to represent the vehicle-level impacts of the technology. The direct effects that relate to energy intensity at the vehicle level are sourced from a 2016 NREL study and are shown in Table 3 (Estimated Bounds and Important Factors, 2016). The NREL study applied the potential CAV operational efficiencies reported in the literature to the corresponding driving situation and combined the effects assuming that each are independent and therefore have a multiplicative impact with all others. The effects applicable to the scope of this study were combined using a Monte Carlo simulation with triangular random distributions around the median values. The average combined effect is a reduction in fuel consumption of 14% with a range of 5–22%.

The realization of these CAV direct effects in the short to medium term is dependent on the achievement of CAV and supporting infrastructure development timelines and on the effective penetration of CAVs into the fleet. The range of CAV subsystems combined with the potential direct effects provides a wide set of scenarios for this time frame. Also note that faster highway speeds for CAVs is a direct effect because it applies to the individual vehicle and impacts its operational efficiency. However, this would need to be enabled by increasing speed limits. This study assumes the speed limit changes would happen as CAV technology allows for significantly safer travel, thus faster highway speeds are included. If the effect was excluded, the average fuel consumption reduction would increase from 14% to 18%.

Energy and use intensity effects at the mobility system level (e.g., congestion, ridesharing, mode shift, increased travel by underserved populations, etc.) were not included since they are considered indirect effects and therefore out of scope. Potential vehicle lightweighting due to reduced crash protection requirements as a result of enhanced safety and powertrain resizing were also not included since the study scenarios involve addition of a CAV subsystem to an existing platform.

The operational efficiencies from ICEV CAV direct effects are assumed to be applicable to BEV platforms due to the approximately equivalent proportional fuel consumption reduction between the powertrain types. This relationship was reported by Michel et al. through the modeling of ecodriving with varying CAV powertrain types in the Autonomie software environment (Michel et al., 2016).

direct effect	lifetime fuel consumption impact
eco-driving	-7 to -16%
intersection V2V/V2I	-2 to -4%
platooning	-3 to -5%
faster highway speeds	+2 to +8%

Table 3. Individual CAV Direct Effects

1.5 Results

The results of the LCA are provided below in terms of GHG emissions. Life cycle energy data are contained in the SI. In general, energy and emissions trends are consistent.

Baseline Scenario. The results of the BEV + Medium subsystem baseline scenario are first reported at the subsystem level and then combined with the platform to create vehicle level results. The full set of detailed subsystem-level and vehicle-level results for all six scenarios is provided in SI Figures S3–S14.

Subsystem Level. The total added weight and power associated with the medium CAV subsystem in the baseline scenario are 22.4 kg and 240 W, respectively. Breakdowns by component are provided in Figure 2. The computer has the largest share, contributing 45% of the weight and 80% of the power consumption. The supporting structure of the CAV subsystem is also a major weight contributor at 26%.

The life cycle GHG emissions associated with the medium CAV subsystem integrated on a BEV platform are estimated to be 1,300 kg CO₂-eq. Breakdowns by component are provided in Figure 3. The computer is once again the largest contributor, with the fuel consumption increase from the added sensor weight and drag having a notable effect.

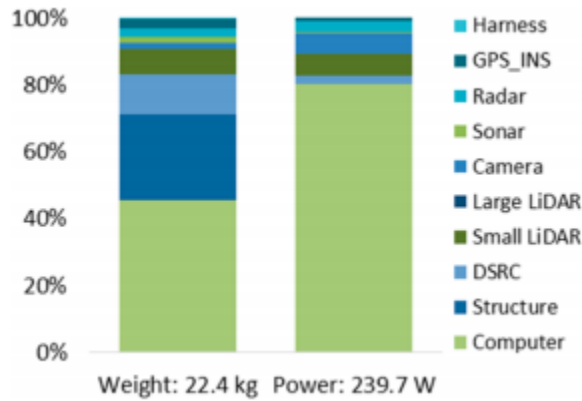


Figure 2. Medium CAV subsystem weight and power breakdown by component

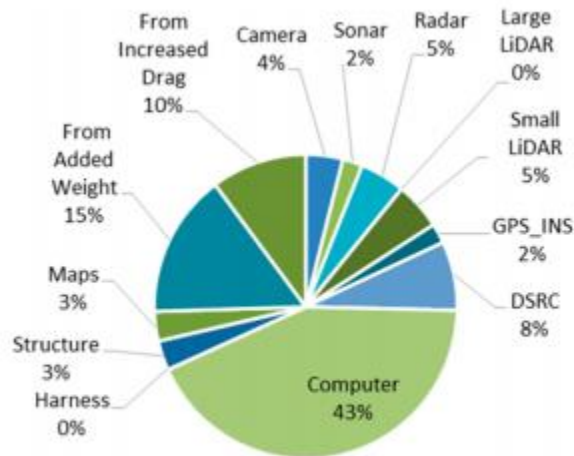


Figure 3. Medium CAV subsystem GHG emission (1,300 kg CO₂-eq) breakdown by component

Vehicle Level. The subsystem-level results are combined with an LCA of the platform vehicle to produce vehicle-level results in Figure 4. The 2015 Ford Focus Electric is the BEV platform and has a production burden of 10,100 kg CO₂-eq (Kim and Wallington, 2016). The fuel consumption of the vehicle is 31.5 kWh/100 miles, resulting in a use phase burden of 27,700 kg CO₂-eq over the 160,000-mile lifetime

(U.S. Department of Energy, 2015). The end-of-life burden is a minimal contributor at 300 kg CO₂-eq. The total life cycle GHG emissions of the BEV platform are therefore 38,100 kg CO₂-eq. Combining the BEV platform results with the medium CAV subsystem results from the previous section gives life cycle GHG emissions of 39,400 kg CO₂-eq. However, an additional step is needed to take into account the CAV direct operational effects. Assuming the 14% reduction in fuel consumption from Table 3, the use phase burden is reduced by 3,700 kg CO₂-eq. This produces a final estimate of 35,700 kg CO₂-eq for the CAV in the baseline scenario, which represents a 6% reduction compared to the BEV platform.

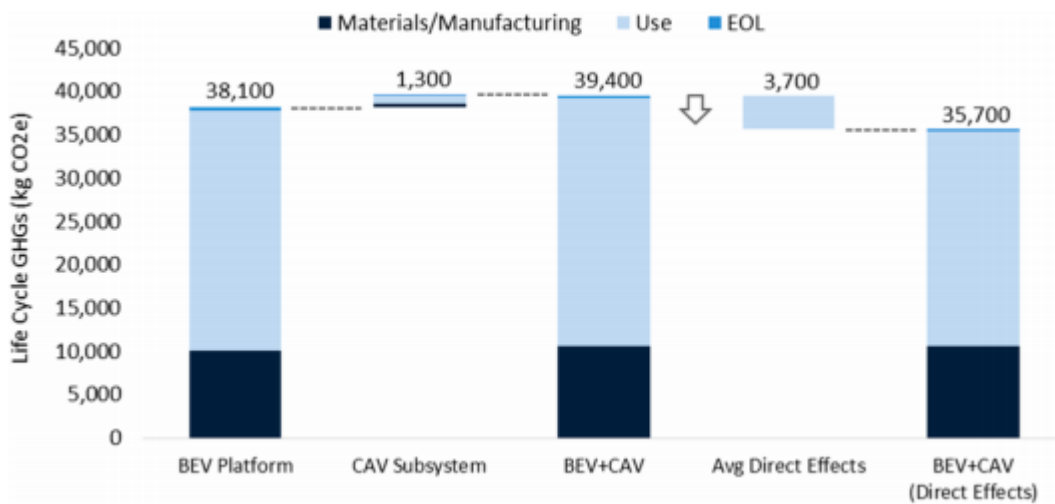


Figure 4. Vehicle-level GHG results for the baseline scenario of BEV + Medium Subsystem.

Scenario Comparison. A comparison across all six scenarios is provided below to illustrate the effects of powertrain and CAV subsystem size.

Subsystem Level. Three CAV subsystem sizes were analyzed in this study: small, medium, and large. The total weights of these subsystems are 16.7, 22.4, and 55.4 kg, respectively. The total power consumptions are 222, 240, and 327 W. Removal of the small LiDARs and supporting structure mainly contributes to the decrease between the medium and small subsystems. The addition of the large LiDAR and a more extensive external supporting structure are the main drivers of the significant increase between the medium and large subsystems. Turning to GHG emission comparisons, holding the CAV subsystem constant, and varying the powertrain illustrate the impacts of the platform. As previously

stated, the BEV + Medium Subsystem scenario has life cycle GHG emissions of 1,300 kg CO₂-eq, while the ICEV + Medium Subsystem is 2× greater at 2,600 kg CO₂-eq. This difference is due to the inefficiency of an ICEV at producing electricity from fuel combustion by the engine and an alternator, as well as the fuel consumption increase from added mass. Therefore, it is shown here that a BEV is a better platform for CAV components compared to an ICEV in terms of minimizing environmental impacts.

Next, holding the BEV platform constant while varying the CAV subsystem size illustrates the impacts of the architecture. The life cycle GHG emissions of the small, medium, and large subsystems are 1,000, 1,300, and 6,300 kg CO₂-eq, respectively. Reduced drag due to the removal of exterior mounted components is the main contributor to the decrease between the medium and small subsystems. The added weight and drag of the exterior mounted sensors and supporting structure are the main drivers of the increases between the medium and large subsystems. Detailed comparisons are provided in SI Figures S15–S18.

Vehicle Level. Looking across the six scenarios, vehicle life cycle GHG emissions increase by 2.8–4.0% after the addition of a small or medium CAV subsystem to a platform vehicle. This modest increase rises to a significant impact of approximately 20% with a large subsystem. Complete details of the impact in each scenario can be found in SI Figures S19 and S20. However, the additional burdens are offset by the operational efficiencies from CAV direct effects. The 2.8–4.0% increase in GHGs from the small and medium CAV subsystems turns into a net reduction of 6–9% after the average direct effects are applied. On the other hand, the 20% increase in GHGs from the large subsystem turns into a modest net increase of 5%. The typical impact of CAV subsystems, however, is a net reduction of life cycle GHG emissions with a worst case of minor increases, assuming the anticipated operational efficiencies are realized. Figure 5 illustrates the vehicle-level GHG results across the six scenarios. Vehicle-level primary energy results can be found in SI Figure S21. The results include the average direct effects and compare the CAV outcomes to the non-CAV platform vehicle.

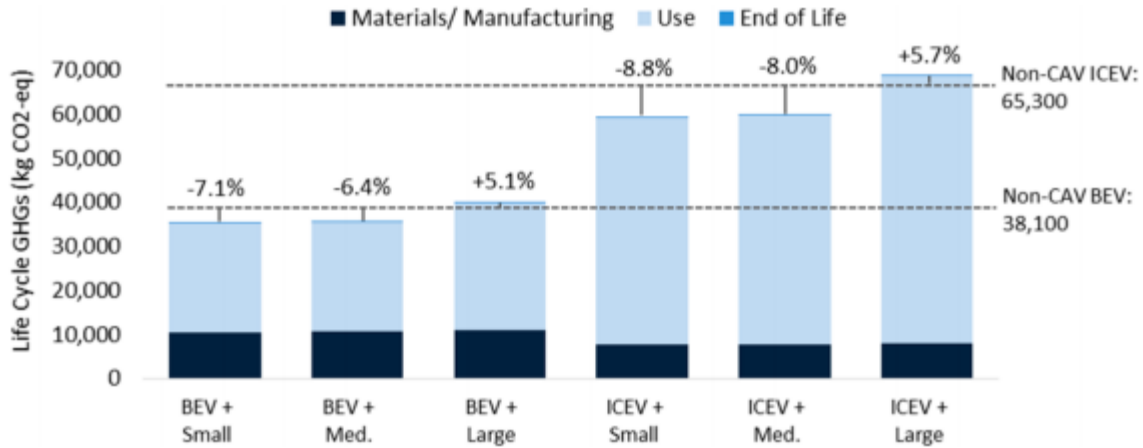


Figure 5. Vehicle-level GHG results for each CAV scenario with average direct effects included. Comparison is given to the non-CAV platform vehicle LCA results to illustrate the net impact of the CAV subsystem addition.

Sensitivity Analysis. A sensitivity analysis was conducted on the baseline scenario to understand the impacts of variations in key parameters. Three special cases were also investigated to illustrate how the net impact of CAVs can become negative with high resource use. Finally, a sensitivity analysis on direct effects is provided to determine the operational efficiency threshold needed to offset CAV subsystem burdens.

Key Parameters. The following six key parameters were varied by $\pm 20\%$ for the purposes of the sensitivity analysis: electrical grid carbon intensity, average vehicle speed, CPU power consumption, drag, structure mass, and map data usage. All parameter variations resulted in $< 0.5\%$ impact on vehicle life cycle GHG emissions with the exception of electrical grid carbon intensity. Just a 2% increase in grid carbon intensity increased CAV GHG impacts by 1.6%. This illustrates the importance of charging BEVs from low carbon sources to achieve their maximum environmental benefit. Additional sensitivity analysis data can be found in SI Figure S22.

Special Cases. Three special cases are included in the sensitivity analysis to illustrate the potential unintended consequences of CAV designs. The first special case focuses on power consumption of the computing platform. The computing platform used in this study consists of redundant Nvidia Drive PX2 modules that together consume approximately 200 W. Other recent studies report CAV computing

platform power consumption on the order of 2,000 W for experimental research and development vehicles (Liu et al., 2017). These prototype power consumption estimates are expected to be reduced by approximately an order of magnitude due to advancements in computer processor unit (CPU) and graphics processing unit (GPU) design (The Power Demands of Self-Driving). However, if 2,000 W is used for the baseline scenario instead of 200 W for illustrative purposes, life cycle GHG emissions increase from 35,700 to 39,600 kg CO₂-eq, completely eliminating the net emissions reductions. The second special case focuses on aerodynamic drag from the exterior CAV components. The design of the medium CAV subsystem is analogous to a small roof rack, which has been shown to increase fuel consumption by 0.5% (Chen, 2016). If the medium subsystem instead resembled a large roof rack, life cycle GHG emissions would increase to 39,200 kg CO₂-eq, eliminating the net emissions reductions. The third and final special case focuses on the data transmission over 4G LTE networks to support onboard maps. This study assumed typical navigation maps would be sufficient for the operation of future Level 4 CAVs. However, other recent studies highlight the potential need for high definition (HD) maps for precise localization (Seif and Hu, 2016). These HD maps could require on the order of 600 MB/mile of data to be transmitted to the CAV over wireless communication networks. That amounts to approximately 100,000 GB over the lifetime of the vehicle. If this large amount of data were transmitted over a 4G LTE network, the CAV life cycle GHG emissions would increase to 54,800 kg CO₂-eq, resulting in a large net increase in emissions. New 5G networks may be operational by the time Level 4 CAVs are deployed, but it is not clear if 5G will be less energy and carbon intensive compared to 4G. A plot of the special case data contained in this section is available in SI Figure S23. Direct Effects. Throughout this study, the direct effect of CAVs is assumed to be a 14% reduction in fuel consumption due to a net increase in operational efficiency. However, the full range produced by the Monte Carlo simulation is 5–22%. Applying this range to the model results in a ±7% variation from the baseline scenario GHG emission results. The threshold for when net emissions reductions are eliminated occurs when the direct effects are reduced from 14% to 5%. This high sensitivity highlights the need for CAV efficiencies such as eco-

driving and platooning to be prioritized in order to achieve environmental benefits from the technology. An illustration of the variation in direct effects can be found in SI Figure S24.

1.6 Discussion

We present the first detailed assessment of the contribution of CAV sensing and computing subsystems to vehicle life cycle energy use and GHG emissions. Five key insights can be drawn from the results of this study.

First, due to the higher GHG burden associated with generating electricity onboard an ICEV compared to the U.S. grid mix and the greater sensitivity of fuel consumption to increased mass for an ICEV, the CAV subsystem burden is approximately a factor of 2 less for BEVs than for ICEVs. Looking at the vehicle-level results, CAVs with electrical powertrains have 40% lower life cycle GHG emissions compared to a conventional powertrain.

Second, wireless data transmission for live maps is a significant contributor to life cycle burdens. Limiting transmission to existing standard maps results in 35% lower GHG emissions compared to HD maps assuming transmission over a 4G LTE network.

Third, the results are highly sensitive to assumptions for the direct benefits realized in CAV operation. Achieving a 14% reduction in fuel consumption due to the operational efficiencies of CAVs produces significant environmental benefits in the baseline scenario. However, these benefits erode if only a 5% reduction is achieved. This highlights the importance of eco-driving algorithms in CAV design since drive cycle smoothing can reduce life cycle GHG emissions by 7–16% compared to typical human-controlled drive cycles.

Fourth, the added weight and power demand from the computing platform produces significant impacts. At 10 kg and 200 W, the computer contributes nearly half of the total CAV subsystem burden in the baseline scenario. If the power demand were instead 2,000 W, as reported for some prototype or developmental CAVs, then the contribution would rise and environmental benefits would be eliminated.

Fifth, large exterior-mounted CAV components have the potential to significantly increase aerodynamic drag. The fuel consumption increase due to drag was found to contribute up to 70% of the large CAV subsystem burden, which offsets the environmental benefits. CAV technology is at an early stage of development; sensing and computing components will continue to be miniaturized and packaged more compactly, but in the near-term the size and shape of exterior-mounted equipment will have tangible impacts.

CAVs are a disruptive technology that will likely transform personal mobility and the built urban landscape in the coming decades. Impacts on life cycle energy consumption and GHG emissions from the indirect effects of CAV adoption are likely to be significant. Some effects such as shared mobility and optimized routing will decrease energy use and emissions, while other effects such as increased mobility demand will increase energy use and emissions. The current analysis of CAV subsystem- and vehicle-level impacts provides an important foundation for future work to explore the broader indirect effects at the mobility system level and to develop a more comprehensive sustainability assessment of CAV impact on the transportation system.

2. Phase 2: Mobility System Level

Phase 2 of this thesis focused on the life cycle energy and greenhouse gas emissions of connected and automated vehicles at the mobility system level. This study was submitted for publication to Transportation Research Part D under the title “Deep Decarbonization from Electrified Autonomous Taxi Fleets: Life Cycle Assessment and Case Study in Austin, TX.”

2.1 Abstract

Although recent studies of autonomous taxis (ATs) have begun to explore potential environmental implications of fleet deployment, little is known about their impacts over the long term. We present a holistic life-cycle assessment framework that incorporates both direct and indirect effects of ATs at the subsystem, vehicle, and mobility-system levels. Eco-driving and intersection connectivity are the direct

effects analyzed along with indirect effects that include empty kilometers, parking, charging infrastructure, powertrain rightsizing, electric vehicle adoption, ride-sharing, and fleet-turnover rates. A case study of an AT fleet in Austin, Texas from 2020 to 2050 with constant travel demand indicates the strategic deployment of an electrified AT fleet can reduce cumulative energy and greenhouse gas (GHG) emissions by 60% in the base case, with a majority of this benefit resulting from electrified powertrains. Further reductions up to 87% can be achieved with accelerated electrical grid decarbonization, dynamic ride-share, longer vehicle lifetime, more energy efficient computers, and higher new-vehicle fuel-consumption rate reductions. We highlight the major opportunities for maximizing the environmental performance of AT fleets over the long term.

2.2 Introduction

Light-duty vehicles were responsible for 1,083 million metric tons CO₂-eq in 2015, making up 60% of U.S. transportation emissions and 16% of total U.S. emissions (U.S. EPA, 2017). An emerging technology that could reduce these emissions and create a more sustainable transportation system (Sweeting and Winfield, 2012) is the connected and automated vehicle (CAV) (Greenblatt and Shaheen, 2015). Once deployed at scale, CAVs will create ripple effects across the mobility ecosystem that could eventually result in wide-reaching societal implications such as changes in energy consumption, safety, and social equity (Milakis et al. 2017 and Taiebat et al. 2018). For example, the bounds on nationwide energy impacts from CAV deployment have been estimated to be anywhere between a 60% decrease to a 200% increase (Stephens et al. 2016 and Wadud et al. 2016). CAVs also have natural synergies with electric vehicles (EVs) (Greenblatt and Saxena, 2015) and transportation as a service (TaaS) business models (Ford, 2012) that could further amplify societal implications. Many of the economic and technical barriers to EV adoption (Lieven et al., 2011) can be ameliorated by CAV-enabled mobility services since the higher upfront vehicle cost achieves quicker payback from lower operational costs with higher utilization. In addition, charging time and driving range issues can be addressed with fleet management

(Kley et al., 2011). Similarly, TaaS business models are more easily implemented due to the profitability and fleet repositioning advantages achieved when using CAVs (Kang et al., 2017).

One potential deployment scenario for CAVs that can combine automated driving technology with EVs and TaaS business models is a fleet of autonomous taxis (ATs), also known as shared autonomous vehicles (SAVs). ATs are defined as fully autonomous vehicles that are capable of driving passengers to their destinations on a demand-responsive basis (Brownell and Kornhauser, 2014). Numerous studies have investigated the potential for AT fleets to meet urban travel demand using agent-based modeling and traffic-flow simulations. Some examples include Burns et al. (2013), who analyzed the performance of an AT fleet in three distinct city environments, and Chen et al. (2016), who examined the operation of a fleet of electric ATs and the corresponding charging infrastructure in Austin, TX. The key metrics reported across each of the AT studies include the fleet size, wait times for passengers, and vehicle kilometers traveled (VKT). Results varied substantially due to the differences in modeling assumptions such as location, travel demand profile, relocation strategy, powertrain, refueling, congestion modeling, and dynamic ride-sharing (i.e. traveler pooling) capability (Fagnant and Kockelman, 2016). The fleet size was reduced in every scenario, with each AT replacing between 3 and 10 human-driven vehicles while maintaining average wait times between 3 and 30 minutes (Bischoff and Maciejewski 2016, Boesch et al. 2016, Burns et al. 2013, Chen et al. 2016, Kornhauser 2013, Loeb et al. 2018, Spieser et al. 2014, Wang et al. 2006). Total fleet VKT decreased by up to 24% compared to the human-driven vehicle baseline when dynamic ride-sharing was included and increased by 8-71% with no ride-share, resulting in higher levels of congestion (Burghout et al. 2015, Fagnant and Kockelman 2014, Fagnant et al. 2015, Farhan and Chen 2018, Levin et al. 2016, Martinez and Crist 2015, Rigole 2014).

The environmental implications of AT fleet deployment could be significant due to the changes in fleet size, VKT, utilization, vehicle type, congestion, and dynamic ride-sharing observed in previous research. Several studies have attempted to quantify the impacts on energy consumption and greenhouse gas (GHG) emissions over the short term using published life cycle assessment (LCA) data for human-driven

vehicles. Fagnant and Kockelman (2014) took the human-driven vehicle life-cycle inventory estimates provided by Chester and Horvath (2009) and applied them to their AT scenario results. They found a 12% reduction in life-cycle energy and 5.6% reduction in GHG emissions. Fagnant et al. (2015) applied a similar approach to AT scenarios that made use of more realistic travel-demand profiles and found a 14% and 7.6% reduction in energy and emissions, respectively. Rigole (2014) used internal combustion engine vehicle (ICEV) life-cycle inventory estimates from Hawkins et al. (2013) and found a large range of GHG impacts across the six SAV scenarios that included ride-share. Results ranged from a 72% increase compared to the business-as-usual case with human-driven vehicles when no travel-time increase was allowed, to a 24% decrease when up to a 50% increase in travel time was allowed. This range narrowed substantially to a 69%-84% decrease when EVs were modeled. However, these methods focus on the short term and do not take into account the added burden from the CAV sensing and computing subsystem (Gawron et al. 2018) or operational efficiencies from CAV direct effects such as eco-driving and intersection connectivity (Stephens et al. 2016). Greenblatt and Saxena (2015) investigated the environmental impacts of electric ATs over the long term by taking into account future decreases in electrical-grid carbon intensity and the potential for vehicle rightsizing within the fleet. The results show an 87%-94% decrease in US per-mile GHG emissions by 2030; however, this analysis focused only on the use phase and ignores fleet characteristics such as materials and manufacturing burdens, empty kilometers, parking, and charging infrastructure. Finally, Chen et al. (2017) estimated the fuel-consumption impact of CAVs using a data-rich approach that includes fleet turnover and fuel-efficiency improvement, but the study does not include life-cycle impacts and omits electrification.

To address these gaps in the literature, we provide a holistic LCA framework for evaluating the energy use and GHG emissions of AT fleets over the long term. The framework builds on the results presented by Gawron et al. (2018) and includes both direct and indirect effects at the subsystem, vehicle, and mobility-system levels. These effects are tailored to an urban environment, where ATs are predicted to be first deployed, and include the CAV sensing and computing subsystem, eco-driving, intersection

connectivity, empty kilometers, parking, charging infrastructure, powertrain rightsizing, EV adoption, ride-share, and fleet turnover. The tri-level structure and corresponding direct and indirect effects are summarized in Figure 6. The framework is then used in a case study to answer the question: what is the most environmentally sustainable AT fleet design over the long term?

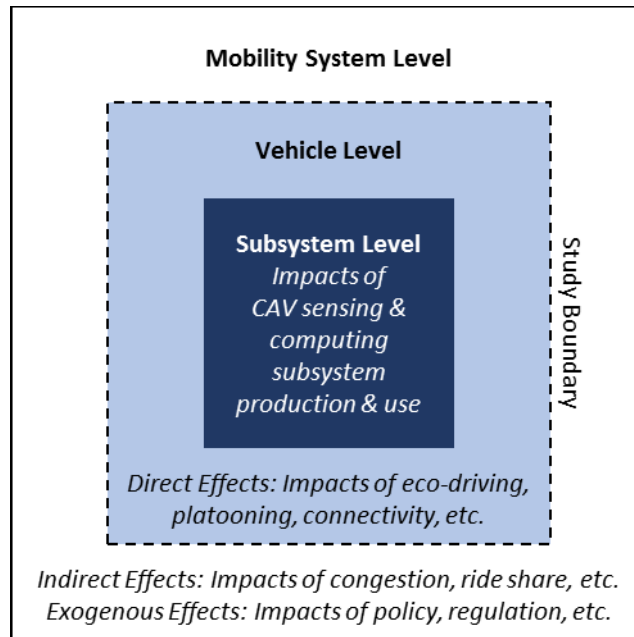


Figure 6. Tri-level structure for CAV direct and indirect effects

2.3 Methods

We evaluate CAV direct and indirect effects and create a framework that evaluates AT fleet energy use and GHG emissions from “cradle to grave”. LCA methodology offers a systematic approach to calculate the environmental impacts across the materials production, manufacturing and assembly, use, and end-of-life management phases (ISO, 2006). The framework is illustrated in Figure 7 and the analysis consists of four steps and six main components. First, define the goal and scope to constrain the analysis. This includes identifying the functional unit, impact indicators, and system boundary. The functional unit is the quantified description of the performance requirements that must be fulfilled, which for the AT fleet includes the travel-demand profile, wait time, and the scenario timeframe. The impact indicators include

the environmental metrics for evaluation (e.g. energy use and GHG emissions). The system boundary defines the specific CAV direct and indirect effects for inclusion across the four main life-cycle phases. Second, determine the characteristics of the fleet capable of meeting the functional unit through simulation or collection of real-world fleet data. Dynamic ride-share can be included to enhance the efficiency of the fleet. The key data include the fleet VKT per day, total number of fleet vehicles, and the charging infrastructure if the fleet is electrified. Third, calculate the relevant characteristics of the fleet vehicles including the impact indicator per distance (e.g. GHG emissions per kilometer) and estimated vehicle lifetime, then determine the impacts of the parking and charging infrastructure. Fourth, simulate the fleet over the scenario timeframe taking into account fleet turnover, annual improvements in vehicle fuel consumption, and electrical grid decarbonization if using EVs.

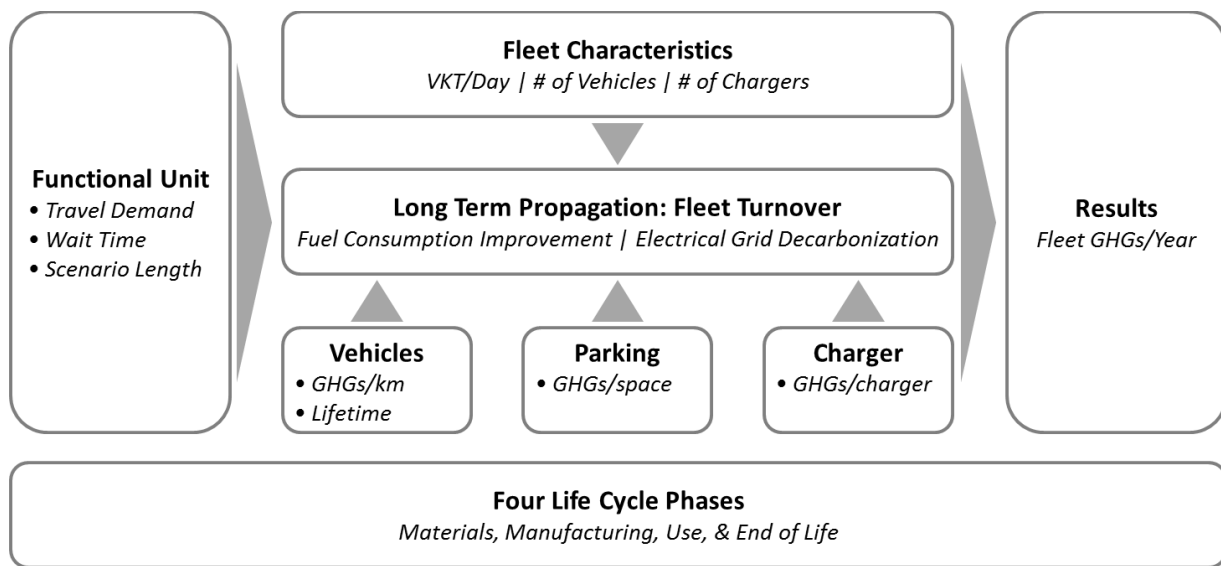


Figure 7. Framework for evaluating the environmental impacts of AT fleets. Each component is discussed in the subsections below.

The framework was applied to a case study evaluation of the AT fleet scenarios for Austin, TX presented in Chen et al. (2016). The following subsections provide details on the application of the framework components to the case study.

2.3.1 Goal and Scope

The goal is to estimate the CAV direct and indirect impacts of AT fleets on energy use and GHG emissions over the period 2020-2050 in Austin, TX. The scope includes a comparative analysis between the current human-driven vehicle baseline in Austin, three modified human-driven vehicle scenarios, and the five AT fleet scenarios contained in Chen et al. (2016). The scenarios vary the autonomy, powertrain, range, charging type, and vehicle lifetime. The nine scenarios along with an acronym key are provided in Figure 8.

Key		
Parameters	Options	Description
Autonomy	HV	Human-driven vehicle (Personal ownership)
	AT	Autonomous taxi (Shared fleet)
Powertrain	IC	Internal combustion engine vehicle (Compact car)
	EV	Battery electric vehicle (Compact car)
Range	SR	Short range (24 kWh, 137 km)
	LR	Long range (68 kWh, 322 km)
Charger	II	Level II charging
	DC	DC fast charging
Lifetime	257	257,495 km (U.S. DOT)
	321	321,869 km (NYC cab fleet)
	643	643,738 km (Sensitivity)

Scenarios		
Internal Combustion Engine	Short Range Electric	Long Range Electric
1: Baseline	4: HV-EV_SR-II (257)	7: HV-EV_LR-II (257)
2: HV-IC (257)	5: AT-EV_SR-II (321)	8: AT-EV_LR-II (321)
3: AT-IC (321)	6: AT-EV_SR-DC (321)	9: AT-EV_LR-DC (321)

Figure 8. Acronym key (top) for the nine scenarios (bottom) analyzed

The functional unit is to service 10% of the current travel demand in Austin with less than 10-minute average wait time over a 2020-2050 time period. The service size and wait-time constraints were selected based on the modeling parameters used in Chen et al. (2016). The 30-year scenario timeframe was chosen to include multiple fleet turnovers and to provide an analysis window to 2050 to facilitate comparison with literature studies. The system boundary for the case study includes the following life-cycle phases:

materials production, manufacturing and assembly, use, and end-of-life management. All CAV direct and indirect effects listed in Figure 6 are included. Platooning and faster highway travel, which are effects that have been considered in other work (Stephens et al. 2016), are excluded from the direct effects since they are not applicable to an urban environment where the AT fleet operates. Consistent with Chen et al. (2016), travel demand was assumed to be static, and changes in congestion were not considered. The selected environmental impact indicators are energy use in units of megajoules [MJ] and GHG emissions in units of kilograms of carbon dioxide equivalent [kg CO₂-eq] on a 100-year GWP basis. The analysis focuses on these metrics due to their importance in assessing automotive sustainability (Jasinski et al., 2016) and due to the limited availability of data for other impacts, such as other air pollutants or water consumption.

2.3.2 Fleet Characteristics

The key characteristics of the AT fleet scenarios capable of meeting the functional unit defined in Section 2.1 are shown in Table 4. These data were derived from the agent-based modeling results provided in Chen et al. (2016) and were used directly in the framework to determine the environmental impact indicators. Note that 2%-4% of trips were unserved across the scenarios when using a 30-minute wait time threshold in the modeling.

Table 4. Key characteristics for each of the nine AT fleet scenarios derived from Chen et al. (2016).

	1: Baseline	2: HV-IC (257)	3: AT-IC (321)	4: HV-EV_SR-II (257)	5: AT-EV_SR-II (321)	6: AT-EV_SR-DC (321)	7: HV-EV_LR-II (257)	8: AT-EV_LR-II (321)	9: AT-EV_LR-DC (321)
Fleet Size	217,703	217,703	29,939	217,703	57,279	39,593	217,703	41,179	31,859
# of Chargers ¹	0	0	0	2,245	30,129	16,510	2,245	16,554	2,389
Average VKT Per Vehicle Per Day	52	52	417	52	211	317	52	306	388
Average VKT Per Vehicle Per Year ²	19,312	19,312	152,139	19,312	76,951	115,712	19,312	111,608	141,565
Fleet VKT Per Day ³	11,281,182	11,281,182	12,479,177	11,281,182	12,075,792	12,552,595	11,281,182	12,591,523	12,356,574
Average Vehicle Lifetime in Years ⁴	13.3	13.3	2.1	13.3	4.2	2.8	13.3	2.9	2.3

- 1: Fueling infrastructure for the ICEV scenarios not included since it is assumed it already exists
- 2: Human-driven vehicle (HV) scenarios are assigned 19,312 VKT per vehicle per year since it is assumed that some rural travel will occur in addition to the 52 km of urban travel per day. For another data point, the average annual VKT for cars, SUVs, and light trucks over their first 14 years of life is approximately 19,473 km (U.S. DOT, 2009).
- 3: Includes empty kilometers for AT scenarios
- 4: Lifetimes based on 257,495 VKT lifetime of CV and 321,869 VKT lifetime of AT

2.3.3 Vehicles

Vehicle life-cycle energy and GHG emissions data for the baseline scenario were sourced from the GREET Model (ANL, 2016a and 2016b). These data for various 2005 vehicle models were combined into a single baseline using a weighted average consistent with the U.S. average fleet of 47.2% passenger cars, 42.2% SUVs, and 10.7% pickup trucks (U.S. EPA, 2017). The 2005 vehicle models are consistent with the average age for U.S. light-duty passenger vehicles of approximately 13 years (Culver, 2016). AT vehicle data were derived from Gawron et al. (2018). These data include the burden from the platform vehicle, baseline (medium) CAV sensing and computing subsystem, and the impact of operational efficiencies from CAV direct effects. The AT fleets are assumed to be comprised of compact cars (i.e. C-segment cars) similar to either the 2015 Ford Focus or Focus Electric vehicles adapted for the short-range and long-range scenarios. The five-person capacity is sufficient to accommodate common dynamic ride-share scenarios (Farhan and Chen, 2018). It is possible that AT fleets will include other vehicle types. Thus, fleets may offer further rightsizing opportunities, which would result in lower energy and GHG emissions. Several vehicle factors were modified from the Gawron et al. (2018) study to customize the data for the urban environment of Austin. First, city fuel consumption rates of 9.1 and 2.0 Le/100 km were used for the Focus and short range Focus Electric, respectively, instead of the original combined rates of 7.5 and 2.2 Le/100 km (U.S. DOE, 2015). Second, the fuel-consumption increase from the medium CAV subsystem aerodynamic drag was changed from 0.5% to 0% due to the lower speeds of city

driving. Third, the platooning and faster highway travel direct effects were excluded in this analysis since these do not apply in the urban environment. Finally, the CAV subsystem computer power consumption was changed from 192 W to an exponentially decreasing trend between 2020 and 2050. In the base case, the power consumption begins at 2,000 W in 2020 and decreases to 192 W in 2039, after which it remains constant through 2050. These beginning and ending values were chosen based on the sensitivity-analysis bounds from Gawron et al. (2018). Recent data suggest that peak-computation energy efficiency doubles every 2.7 years (Kooimey et al., 2017). We consider that some efficiency gains will be offset by the desire to process higher fidelity data as Level 4 software matures, thus we assume a doubling in CAV computation efficiency every 5.4 years. In the optimistic scenario, the power consumption begins at the same starting value of 2,000 W in 2020, but decreases by half every 2.7 years to a value of 192 W in 2030. Power consumption data for both the conservative and optimistic scenarios can be found in Tables A4 and A5 in the Supplementary Material.

The battery electric vehicle (BEV) scenarios consist of both 137 km short-range and 322 km long-range powertrain options. The short-range BEV includes a 24 kWh battery and a fuel consumption rate of 2.0 Le/100 km (U.S. DOE, 2015). The long-range BEV includes a 68 kWh battery with a higher fuel consumption rate of 2.4 Le/100 km due to the added 555 kg from the larger battery and a fuel increase rate of 0.073 Le/(100 km 100 kg) (Kim et al., 2016a). The added 44 kWh of battery capacity also increases the production burden by 85,836 MJ and 6,233 kg CO₂eq (Kim et al., 2016b). Larger batteries may be used in ATs in the future; however, the two battery sizes included in this case study successfully illustrate the impacts from the tradeoff between battery size and recharging frequency. The lithium nickel-cobalt manganese oxide (NCM) battery assumed in this study has a predicted lifetime of 3,000 cycles (Majeau-Bettez et al., 2011). If each cycle uses an average of 80% of its total range, then the battery lifetime will be 321,869 km for the short-range BEV and 772,485 km for the long-range BEV. The lifetime for conventionally driven ICEV and BEV powertrains is assumed to be 257,495 km (160,000 miles) (U.S. DOT, 2006 and ANL, 2016b). The lifetime for ATs is assumed to be 321,869 km (200,000

miles) for the conservative scenario used in the base case due to the higher mileage typically achieved with fleet vehicles (NYC, 2013 and Greenblatt & Saxena, 2015). A sensitivity analysis is included where the lifetime is increased to miles 643,738 km (400,000 miles) in an optimistic scenario to account for the time-based dependency for high-utilization vehicles in addition to mileage. For example, the time-based lifetime in Scenario 3 increases from 2.1 years to 4.2 years when the mileage-based lifetime increases from 321,869 to 643,738 km, which may be more consistent with daily cycle fatigue capability. The 643,738-km lifetime results in one battery replacement being required for the short-range BEV powertrain based on the battery lifetimes listed above. No battery replacement is required for the long-range BEV powertrain due to fewer charge/discharge cycles. Note that BEV powertrains may be more likely to achieve the 643,738 km lifetime compared to ICEV powertrains; however, further research using empirical data is required to fully characterize this relationship.

The vehicle energy use and GHG emissions for each of the nine scenarios are provided in Table 5. These data assume a 0.1821 kg CO₂eq / MJ electrical grid carbon intensity for the U.S. Central and Southern Plains region in 2020 from the GREET model, which is chosen as an approximation for Austin (ANL, 2016a). Impacts due to a reduction in grid carbon intensity through 2050 are discussed in Section 2.6.

Table 5. Vehicle life-cycle energy and GHG emissions per km in 2020 for each of the nine AT Fleet scenarios included in the case study. Vehicle data for Scenario 1 were sourced from ANL (2016a and 2016b), while data for Scenarios 2 to 9 were derived from Gawron et al. (2018).

	1: Baseline	2: HV-IC (257)	3: AT-IC (321)	4: HV-EV_SR-II (257)	5: AT-EV_SR-II (321)	6: AT-EV_SR-DC (321)	7: HV-EV_LR-II (257)	8: AT-EV_LR-II (321)	9: AT-EV_LR-DC (321)
Life-Cycle Energy (MJ / km)									
Materials & Manufacturing	0.445	0.393	0.337	0.541	0.455	0.455	0.874	0.722	0.722
Use	4.886	3.718	4.402	1.615	1.923	1.923	1.944	2.205	2.205
End of Life	0.016	0.016	0.012	0.016	0.012	0.012	0.021	0.017	0.017
Total	5.347	4.129	4.751	2.172	2.390	2.390	2.839	2.943	2.943
Life-Cycle GHG Emissions (kg CO ₂ eq / km)									
Materials & Manufacturing	0.033	0.028	0.024	0.039	0.033	0.033	0.063	0.052	0.052
Use	0.355	0.269	0.318	0.116	0.138	0.138	0.140	0.158	0.158
End of Life	0.001	0.001	0.001	0.001	0.001	0.001	0.001	0.001	0.001
Total	0.389	0.298	0.342	0.157	0.171	0.171	0.204	0.212	0.212

2.3.4 Parking

A surface parking spot has an estimated life-cycle energy and GHG emissions burden of 926 MJ/m² and 76 kg CO₂eq/m², respectively (Horvath, 2003). A typical parking spot has an area of 16.7 m² (Parking facility, 2016). Therefore, a parking space burden is 15,480 MJ/space and 1,270 kg CO₂eq/space. This burden was applied to the total number of parking spots required in each scenario to determine the overall impact of parking. Each conventional vehicle and autonomous taxi was assumed to require one parking spot. Parking burden reduction due to smaller fleet size was assumed to be realized through reduced demand for construction of new parking spaces as urban populations increase.

2.3.5 Charging Infrastructure

The BEV charging infrastructure consists of both Level II and DC fast chargers. Level II chargers produce a charging time of 240 minutes in the Chen et al. (2016) model, while DC fast chargers reduce the charging time to just 30 minutes. The Level II charger assumed in this study is 1,255 kg, rated at 22 kW, and has a lifetime of 6 years. Its associated burden is 4,290 MJ/charger and 250 kg CO₂eq/charger (Lucas et al., 2012). In contrast, the DC fast charger has a weight of 3,250 kg, rated power of 50 kW, lifetime of 12 years, and burdens of 54,300 MJ/charger and 2,500 kgCO₂eq/charger (Lucas et al., 2012). The burdens for the chargers were applied to the required infrastructure in each scenario while taking into account the estimated lifetime of the charger and the scenario timeframe. Note that frequent DC fast charging may accelerate battery degradation and reduce battery lifetime. This secondary effect was not included in the modeling since the extent of the impacts is still being studied. The production burden of gas stations was not included since it is assumed this refueling network already exists for the baseline scenario.

2.3.6 Fleet Turnover

Fleet turnover is included in the framework since the vehicle lifetime is shorter than the 30-year scenario timeframe from 2020 to 2050. Replacement of the entire fleet was assumed when the vehicles reach their design lifetimes. This assumption works well for the AT scenarios since the service would most likely

begin on a given start date with a new fleet of vehicles. To account for the heterogeneous fleet in the baseline scenario, older model-year vehicles from ANL (2016a and 2016b) were used. When fleet turnover occurs, the replacement vehicles have lower use-phase fuel-consumption rates due to technology maturation. This leads to step changes in use-phase burden with a frequency dependent on vehicle lifetime. The annual reduction (Reduction) was applied to the initial fuel consumption (FC₀) using Equation 1 to obtain the estimated future fuel consumption (FCT) in year T.

Equation 1:
$$FC_T = FC_0 * (1 + Reduction)^T$$

The annual reductions for new ICEV and BEV fuel consumption rates through 2050 are provided in Table 6. The conservative scenario is used in the base case, while the optimistic scenario is used in the sensitivity analysis.

Table 6. New vehicle fuel consumption for 2010 to 2050 for conservative and optimistic scenarios (Committee on Transitions et al., 2013).

Powertrain Type	Fuel Consumption (L _e /100 km)			2010-2030 Annual Reduction	2030-2050 Annual Reduction
	2010	2030	2050		
Conservative					
ICEV	7.60	3.67	2.70	3.6%	1.5%
BEV	1.62	1.25	0.96	1.4%	1.2%
Optimistic					
ICEV	7.60	3.18	2.14	4.3%	2.0%
BEV	1.62	1.11	0.80	2.1%	1.5%

The anticipated decarbonization of the electrical grid will reduce the use phase burden over time for the BEV scenarios. In the conservative scenario used in the base case, the current carbon intensity for the U.S. Central and Southern Plains region of 0.1821 kg CO₂eq/ MJ undergoes a 22% reduction by 2050, which is consistent with the predicted reduction for the U.S. Mix in that same timeframe (ANL, 2016a). In the optimistic scenario used in the sensitivity analysis, the current carbon intensity undergoes a 92% reduction by 2050, which is consistent with the “Stretch Tech, CP20” scenario reported in Appendix A of U.S. DOE (2017). Further data on electrical grid carbon intensity and primary energy predictions can be found in Tables A1 to A3 in the Supplementary Material.

2.4 Results

The GHG-emission results for the base case are provided in Section 2.4.1. The base case uses the conservative AT lifetime, annual new-vehicle fuel-consumption rate reduction, computer power-consumption reduction, and electrical-grid decarbonization rate inputs outlined in Section 2.3. In contrast, the baseline scenario refers to the current fleet of human-driven vehicles in Austin. Energy data are contained in Figures A4 and A5 in the Supplementary Material and the energy and emissions trends are consistent. Section 2.4.2 discusses the implications of adding dynamic ride-share to the case study. Finally, Section 2.4.3 provides a sensitivity analysis that discusses the impacts of using the optimistic inputs. The impacts of varying other key parameters, such as CAV-subsystem size and direct effects, are also reported.

2.4.1 Base Case Results

The base case results begin with a time series to illustrate fleet turnover, then breaks down the results for each scenario by direct and indirect effect to determine the major drivers. Figure 9 provides the GHG emissions in a time series from 2020 to 2050. Production and end-of-life emissions are amortized over the life of the vehicle while the use-phase emissions are attributed to the time of generation. The step changes are due to fleet turnover since the replacement vehicles have reduced fuel-consumption rates and computer-power consumption according to the conservative scenario in Section 2.3.6. The frequency of the step changes for the AT fleets is much higher than for the human-driven vehicle scenarios due to the higher utilization rates and corresponding shorter lifetimes. The gradual decrease evident in the BEV scenarios is a function of the conservative electrical-grid decarbonization for Austin discussed in Section 2.3.6. Also note that the AT scenarios initially have higher monthly GHG emissions in the 2020-2026 timeframe due to the high CAV-subsystem computer-power consumption. However, these emissions levels drop below the human-driven vehicle scenarios after 2026 due to more energy-efficient computing.

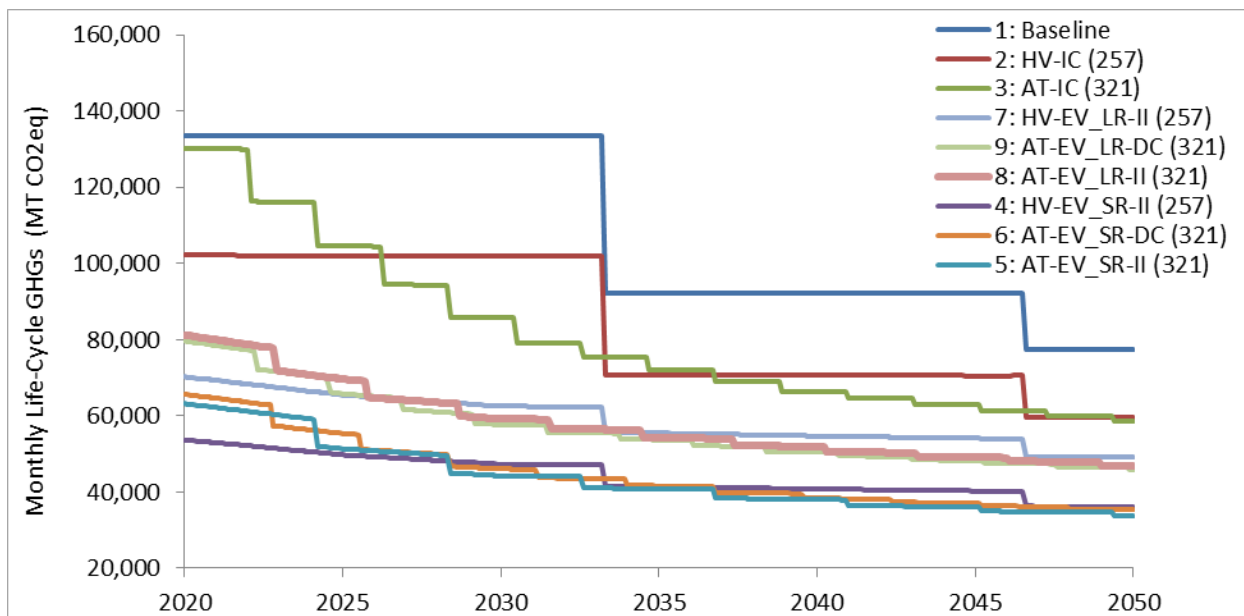


Figure 9. Monthly GHG emissions from 2020 to 2050 modeled using the conservative fleet turnover and electrical-grid decarbonization inputs for the base case. Legend listed in order of decreasing GHG emissions.

The cumulative GHG emissions for each scenario over the 30-year scenario timeframe are provided in Figure 10. The results are broken out by life-cycle phase as well as the contributions from parking and charging infrastructure. The ICEV scenarios (Group A) have lower production burden compared to the BEV scenarios (Groups B-E) primarily due to the addition of the battery. However, the ICEV use-phase burden is significantly higher since BEV powertrain technology is more energy efficient. Parking burden is reduced when transitioning from human-driven vehicles to AT scenarios due to the smaller fleet size. Charging-infrastructure burden only applies to the BEV scenarios, is negligible, and is hardly discernable in Figure 10. Overall, the cumulative GHG emissions decrease by 60% when transitioning from the Baseline to Scenario 5.

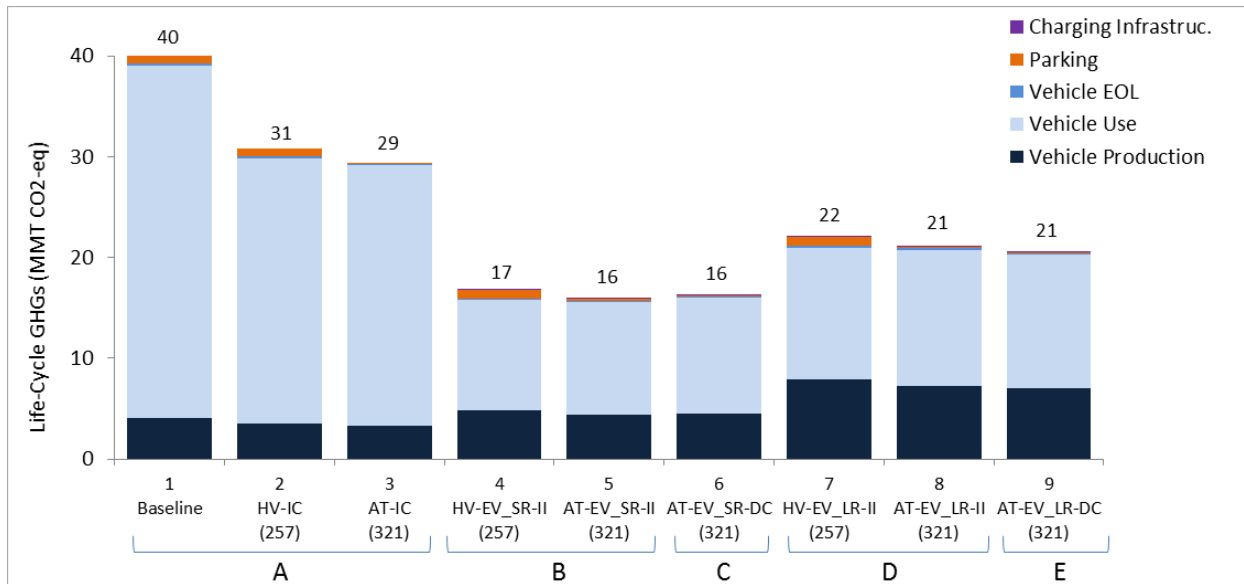


Figure 10. Cumulative fleet GHG emissions over the period 2020-2050 broken out by life-cycle phase. Groups A and B are expanded in Figures 11 and 12, respectively. Groups C, D, & E details are contained in Figures A1 to A3 in the Supplementary Material.

An expansion of Group A is provided in Figure 11 to show the main differences between Scenarios 1, 2, and 3. The waterfall starts with the transition between the Baseline and Scenario 2. Shifting from a heterogeneous fleet of cars, SUVs, and trucks in the Baseline to a uniform fleet of compact cars in Scenario 2 results in decreasing GHGs across all life-cycle phases. Next, transitioning from Scenario 2 to 3 first results in increasing GHGs due to additional VKT from empty kilometers and due to the added burden from the CAV sensing and computing subsystem. However, this is offset by the operational efficiencies from CAV direct effects, less parking due to the smaller fleet, and the longer life of the AT allowing the production burden to be amortized over more VKT. Finally, transitioning from Scenario 3 with a conservative 321,869 km lifetime to an optimistic 643,738 km lifetime first results in increasing GHGs since the longer lifetime reduces fleet turnover. However, the increase is more than offset by amortizing the production burden over the longer lifetime. Overall, the GHG emissions decrease by 7% when transitioning from Scenario 2 to Scenario 3 with the 643,738-km lifetime.

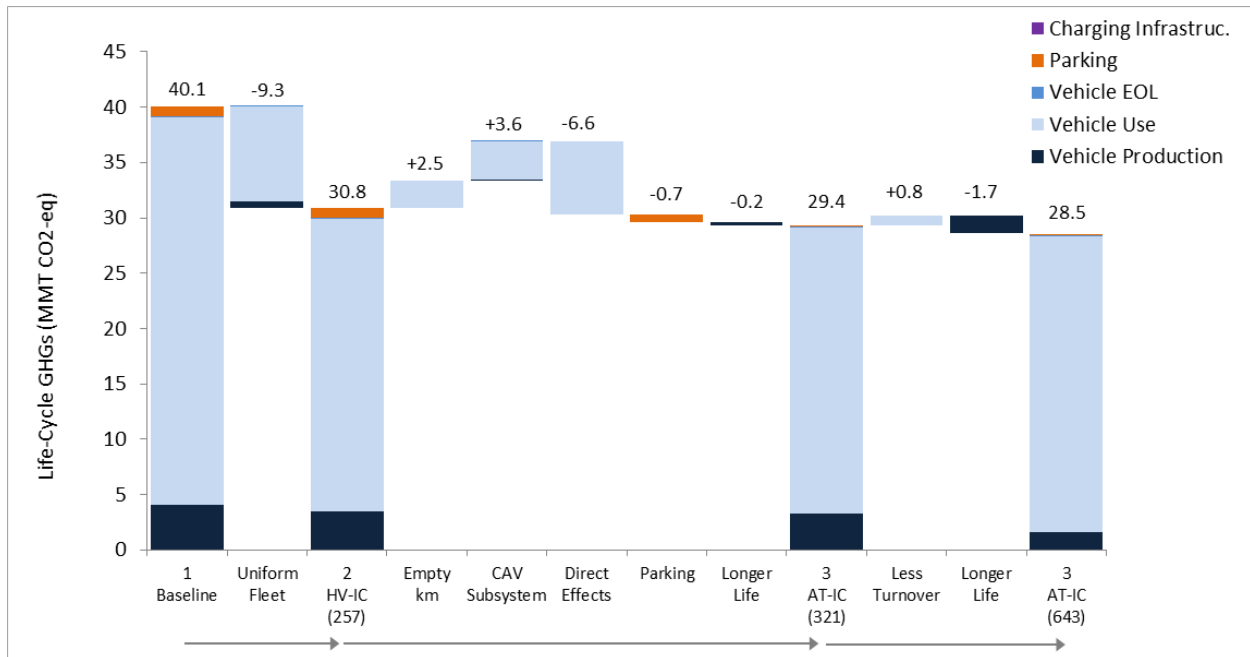


Figure 11. Expansion of Group A showing the impacts of direct and indirect effects. Includes Scenarios 1 to 3, as well as a special sensitivity case for Scenario 3 with a 643,738 km lifetime.

An expansion of Group B is provided in Figure 12 to show the main differences between Scenarios 4 and 5. The waterfall follows a similar pattern as for Group A. The empty kilometers have less of an impact than in the ICEV scenarios since BEVs are more efficient in the use phase. The CAV subsystem also adds less burden because the electricity required to run the sensors and computer has lower GHG burden on BEV platforms. The direct effects for BEVs are less than for ICEVs because BEVs are already more efficient and have less to gain. The longer life of BEVs has a greater impact due to the higher production burden that can be amortized over the additional VKT. The charging-infrastructure burden is the only new indirect effect, which is reduced because less chargers are needed with a smaller AT fleet. Transitioning from Scenario 5 with a 321,869 km lifetime to an optimistic 643,738 km lifetime has a similar impact as in Group A. However, the effect from less fleet turnover is smaller due to the lower annual new-vehicle fuel-consumption rate reduction. Overall, the GHG emissions decrease by 12% when transitioning from Scenario 4 to Scenario 5 with the 643,738 km lifetime. Expansions of Groups C, D, and E are provided in Figures A1 to A3 in the Supplementary Material.

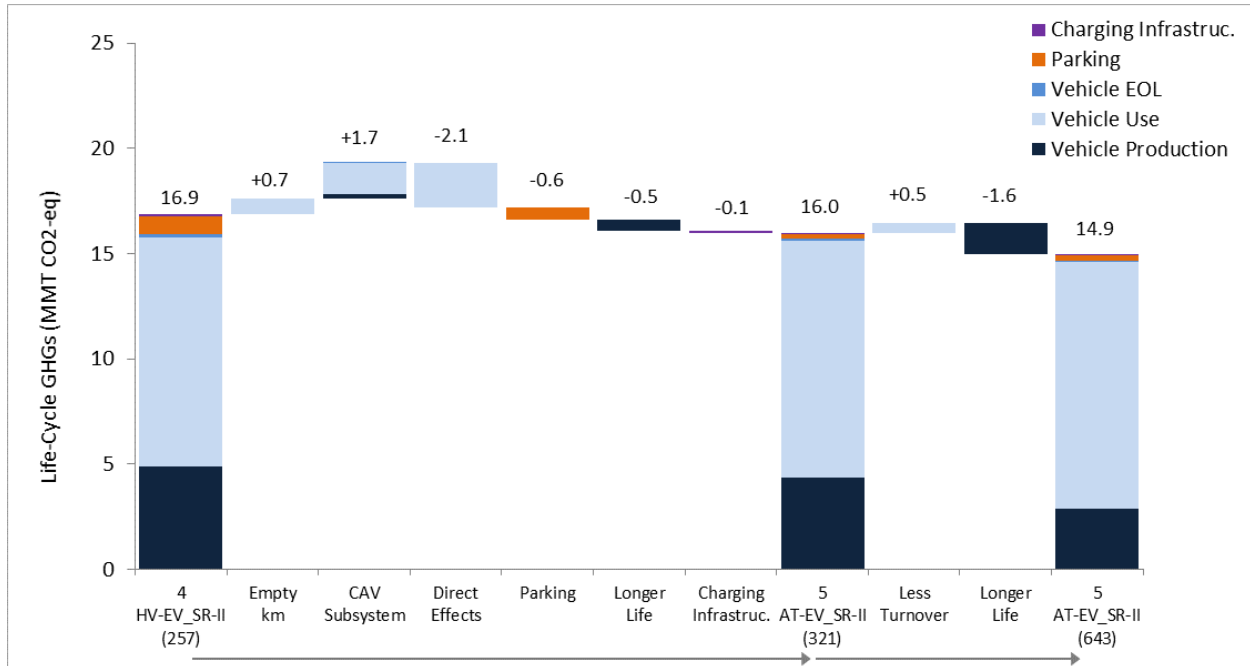


Figure 12. Expansion of Group B showing the impacts of direct and indirect effects specific to BEV powertrains. Includes Scenarios 4 and 5, as well as a special sensitivity case for Scenario 5 with a 643,738 km lifetime.

2.4.2 Dynamic Ride-sharing

Dynamic ride-sharing involves the pooling of multiple travelers with similar origins, destinations, and departure times in the same vehicle to further reduce AT fleet size and VKT (Fagnant and Kockelman, 2016). The results reported above do not include the impact of dynamic ride-sharing since the input data derived from Chen et al. (2016) did not incorporate ride-share in the modeling process. Instead, each trip was carried out by one AT from origin to destination. After dropping off the passenger, the AT would then relocate to the next trip request, resulting in up to an 11% increase in total fleet VKT due to empty kilometers. However, AT studies that did include a dynamic ride-sharing feature report decreases in VKT. For example, Farhan and Chen (2018) reported up to a 22% decrease in fleet VKT using an agent-based model and Austin, TX case study scenario similar to Chen et al. (2016).

To illustrate the potential impact of dynamic ride-sharing, the life-cycle energy and GHG emissions for the short-range electric AT scenarios from Farhan and Chen (2018) were modeled using the framework

developed for this study. These three scenarios are identical to Scenario 5 from Chen et al. (2016) except for the inclusion of dynamic ride-sharing. The AT ride-share capacity varies across the three scenarios from two to four passengers, resulting in VKT reductions from 18% to 22%, respectively. Overall, implementing dynamic ride-share with an AT capacity of four passengers in Scenario 5 reduces GHG emissions by 23% compared to Scenario 5 with no ride-share. Results for all three scenarios from Farhan and Chen (2018) in comparison to Scenario 5 from Chen et al. (2016) can be found in Figure A6 in the Supplementary Material.

2.4.3 Sensitivity Analysis

Several key inputs included in the base case were varied in a sensitivity analysis to better understand their impacts. The first parameter is the CAV subsystem size as reported in Gawron et al. (2018). If a small CAV subsystem is used instead of the medium size, the impact on the cumulative life-cycle GHG emissions is small at less than 1%. However, the impact from using the large subsystem is much greater at 8%-10%. The second parameter is the CAV direct effects. The average fuel-consumption reduction of 14% due to direct effects is assumed throughout this study. However, if the full range from 9% -19% is examined from Stephens et al. (2016), the impact on the cumulative GHG emissions is $\pm 5\%$. The third parameter is the amount of empty kilometers that increase total fleet VKT. The scenarios modeled in this case study include up to an 11% increase in VKT due to empty kilometers. However, if VKT increased by up to 50% due to empty kilometers, GHG emissions for Scenario 5 would increase by 38% compared to the base case. The fourth parameter is the lifetime of the AT fleet vehicles, which was varied between the conservative 321,869 km (200,000 miles) in the base case to 643,738 km (400,000 miles). Overall, GHG emissions are reduced 3% -8% by increasing the lifetime to 643,738 km, with the BEV powertrains seeing more benefit due to the amortization of the higher production burden. The fifth parameter is the annual new-vehicle fuel-consumption rate reduction. If optimistic reductions are used instead of the conservative reductions, then AT fleets with higher turnover are further rewarded since the replacement vehicles are even more energy efficient. For example, Scenario 3 from the base case has a further 6% decrease in life-

cycle GHG emissions when using the optimistic reductions. The sixth parameter is the CAV-subsystem computer power consumption. If optimistic reductions are used following Moore's Law instead of the conservative assumptions, then GHG emissions are reduced 2% -3% across the AT scenarios. The final parameter is the electrical-grid decarbonization rate. The base case assumed the conservative scenario where the Austin electrical-grid carbon intensity undergoes a 30% reduction by 2050. If the optimistic scenario is used instead, then the BEV scenarios will be further rewarded in the use phase due to accelerated decarbonization. For example, the comparison between the Baseline and Scenario 5 would change from a 60% decrease in GHG emissions under the base case to a 79% decrease by assuming stretch technology assumptions with an escalating carbon price (U.S. DOE, 2017). Taking the sensitivity one step further, if dynamic ride-share with an AT capacity of four passengers is combined with the optimistic AT lifetime, annual new-vehicle fuel-consumption rate reductions, and electrical-grid decarbonization rate from the sensitivity analysis, then emissions in Scenario 5 are 87% below the Baseline. Further details on the sensitivity analysis can be found in Figures A7 to A14 in the Supplementary Material.

2.5 Conclusion

We present a holistic LCA framework for evaluating the life-cycle energy and GHG emissions of AT fleets over the long term. The framework incorporates both direct and indirect effects at the subsystem, vehicle, and mobility-system levels. To demonstrate its capabilities, a case study was conducted of an AT fleet design in Austin, TX. In the base case, transitioning from a baseline scenario with the current fleet of human-driven vehicles to a scenario with a fleet of electric ATs results in a 60% reduction in GHG emissions. This reduction is primarily due to electrification (57% decrease compared to the baseline) and less parking (1.5% decrease). Additional scenarios were modeled to achieve a further reduction of up to 87% compared to the baseline. The scenarios include accelerated electrical-grid decarbonization of 92% by 2050 (48% decrease compared to the base case), dynamic ride-sharing to reduce VKT up to 22% (27% decrease), longer AT lifetime up to 643,738 km (5% decrease), high operational efficiencies of 19% from

CAV direct effects (5% decrease), higher new-vehicle fuel-consumption rate reductions for BEVs up to 2% (4% decrease), optimistic CAV-subsystem computer power consumption (2% decrease) and small CAV subsystems (1% decrease). The results provide important policy and design implications for maximizing the environmental sustainability of AT fleets by focusing on some of the largest levers such as electrification and dynamic ride-share.

While our modeling elucidates many complex interactions between key model parameters, several limitations exist with this study. First, congestion was excluded from the indirect effects since it was not included in the Chen et al. (2016) modeling. Congestion could amplify the impact of empty kilometers and increase GHG emissions due to longer travel times and the need for larger AT fleets. Second, travel demand was assumed to be constant over the 30-year scenario timeframe for tractable modeling purposes and due to uncertainty in consumer behavior. On one side, rebound effects from the lower cost of travel promised by AT fleets could increase overall travel demand. The resulting fleet VKT may or may not increase depending on how the AT fleet optimizes for dynamic ride-sharing and repositioning.

Conversely, travel demand increases may be offset by consumers' tendency to reduce travel in a pay-as-you-go business model that makes the marginal cost of travel more apparent (Chen and Kockelman, 2016). Third, parking reduction was assumed to have a direct relationship with fleet size. However, the vehicle replacement rate from ATs may not directly translate to a parking impact due to multi-modal travel, as discussed in Chen and Kockelman (2016). This may be partially offset by a higher parking space to car ratio of 3.4 to 1 for the conventional vehicles that do end up being eliminated (Chester et al. 2010). Fourth, the CAV direct effects on BEV platforms are not yet fully understood. Previous analysis of eco-driving and intersection connectivity was conducted for ICEVs. Michel et al. (2016) showed that efficiency gains are consistent across powertrains. However, this may vary depending on the engine and motor efficiency profile assumed. Finally, the case study assumed a uniform AT fleet of compact cars. Further work could be undertaken to assess the impacts of AT-fleet vehicle size and powertrain. Right-sizing with a heterogeneous fleet could also be incorporated as was done by Greenblatt and Saxena

(2015). Suggested future work that could address these limitations involves incorporating this framework directly into AT fleet agent-based modeling to optimize the fleet design for environmental outcomes in addition to wait time and service level parameters. The charging options could also be expanded to include inductive charging. Overall, we illustrate how deep decarbonization and energy-consumption reductions can be achieved across the full life-cycle in the transportation sector through the strategic deployment of electrified AT fleets.

References

- A look at Tesla's new Autopilot hardware suite. <https://electrek.co/2016/10/20/tesla-new-autopilot-hardware-suite-camera-nvidiatesla-vision/> (accessed Jan 27, 2018).
- American Driving Survey: 2014–2015; AAA Foundation for Traffic Safety: Washington, DC, 2016. <http://publicaffairsresources.aaa.biz/wp-content/uploads/2016/09/AmericanDrivingSurvey2015.pdf> (accessed Jan 27, 2018).
- Antennas Pinwheel OEM Version 5. www.Novatel.com (accessed Jan 27, 2018).
- Argonne National Laboratory (ANL). (2016a). The Greenhouse Gases, Regulated Emissions, and Energy Use in Transportation (GREET) Model Software: GREET 1. Version 2011 Copyright © 1999 UChicago Argonne, LLC.
- Argonne National Laboratory (ANL). (2016b). The Greenhouse Gases, Regulated Emissions, and Energy Use in Transportation (GREET) Model Software: GREET 2. Version 2.7 Copyright © 2007 UChicago Argonne, LLC.
- Autonomous Vehicle Uses Dragonfly2 and Firefly MV Cameras for Vision. <https://www.ptgrey.com/case-study/id/10393> (accessed Jan 27, 2018).
- AWG Copper Wire Size Table and Data Chart. http://www.engineersedge.com/copper_wire.htm (accessed Jan 27, 2018).
- Bischoff, J., & Maciejewski, M. (2016). Simulation of City-wide Replacement of Private Cars with Autonomous Taxis in Berlin. *Procedia Computer Science*, 83, 237-244. doi:10.1016/j.procs.2016.04.121
- Boesch, P. M., Ciari, F., & Axhausen, K. W. (2016). Autonomous Vehicle Fleet Sizes Required to Serve Different Levels of Demand. *Transportation Research Record: Journal of the Transportation Research Board*, 2542, 111-119. doi:10.3141/2542-13
- Brown, A.; Gonder, J.; Repac, B. An Analysis of Possible Energy Impacts of Automated Vehicle. *Road Vehicle Automation Lecture Notes in Mobility 2014*, 137–153.
- Brownell, C., & Kornhauser, A. (2014). A Driverless Alternative. *Transportation Research Record: Journal of the Transportation Research Board*, 2416, 73-81. doi:10.3141/2416-09
- Building Ford's Next-Generation Autonomous Development Vehicle. <https://medium.com/@ford/building-fords-next-generation-autonomous-development-vehicle-82a6160a7965> (accessed Jan 27, 2018).
- Burghout, W., Rigole, P. J., & Andreasson, I. (2015). Impacts of shared autonomous taxis in a metropolitan area. In *Proceedings of the 94th annual meeting of the Transportation Research Board*, Washington DC, 2015.
- Burns, L., William, J., Scarborough, B., 2013. *Transforming Personal Mobility*. The Earth Institute – Columbia University, New York.

- Cars are parked 95% of the time. Let's check! <http://www.reinventingparking.org/2013/02/cars-are-parked-95-of-time-letscheck.html> (accessed Jan 27, 2018).
- Chen, T. D., & Kockelman, K. M. (2016). Carsharing's life-cycle impacts on energy use and greenhouse gas emissions. *Transportation Research Part D: Transport and Environment*, 47, 276-284. doi:10.1016/j.trd.2016.05.012
- Chen, T. D., Kockelman, K. M., & Hanna, J. P. (2016). Operations of a shared, autonomous, electric vehicle fleet: Implications of vehicle & charging infrastructure decisions. *Transportation Research Part A: Policy and Practice*, 94, 243-254. doi:10.1016/j.tra.2016.08.020
- Chen, Y., Gonder, J., Young, S., & Wood, E. (2017). Quantifying autonomous vehicles national fuel consumption impacts: A data-rich approach. *Transportation Research Part A: Policy and Practice*. doi:10.1016/j.tra.2017.10.012
- Chen, Y.; Meier, A. Fuel consumption impacts of auto roof racks. *Energy Policy* 2016, 92, 325–333.
- Chester, M., & Horvath, A. (2009). Life-cycle Energy and Emissions Inventories for Motorcycles, Diesel Automobiles, School Buses, Electric Buses, Chicago Rail, and New York City Rail. UC Berkeley: Center for Future Urban Transport: A Volvo Center of Excellence. Retrieved from <https://escholarship.org/uc/item/6z37f2jr>
- Chester, M., Horvath, A., & Madanat, S. (2010). Parking infrastructure: Energy, emissions, and automobile life-cycle environmental accounting. *Environmental Research Letters*, 5(3), 034001. doi:10.1088/1748-9326/5/3/034001
- Commission Implementing Decision (EU) 2016/588 of 14 April 2016. OJ L 101/25, 2016. <http://eur-lex.europa.eu/legalcontent/EN/TXT/?uri=CELEX%3A32016D0588> (accessed Jan 27, 2018).
- Cooney, G.; Hawkins, T. R.; Marriott, J. Life cycle assessment of diesel and electric public transportation buses. *J. Ind. Ecol.* 2013, 17, 689–99.
- Cohda Wireless MK5 OBU Specification Version 1.4. www.cohdawireless.com (accessed Jan 27, 2018).
- Committee on Transitions to Alternative Vehicles and Fuels, Board on Energy and Environmental Systems, Division on Engineering and Physical Sciences, & National Research Council. (2013). *Transitions to Alternative Vehicles and Fuels*. The National Academies Press. doi:10.17226/18264
- Culver, M. (2016, November 22). Vehicles Getting Older: Average Age of Light Cars and Trucks in U.S. Rises Again in 2016 to 11.6 Years, IHS Markit Says. Retrieved June 23, 2018, from <http://news.ihsmarkit.com/press-release/automotive/vehicles-getting-older-average-age-light-cars-and-trucks-us-rises-again-201>
- Dragonfly2 Technical Reference Manual Revision 2.5. www.ptgrey.com (accessed Jan 27, 2018).
- DSRC Spring Mounted Mobile Antennas 5.9 GHz. www.mobilemark.com (accessed Jan 27, 2018).
- Enclosures PwrPak7-E1 Version 0B. www.Novatel.com (accessed Jan 27, 2018).

- Estimated Bounds and Important Factors for Fuel Use and Consumer Costs of Connected and Automated Vehicles; National Renewable Energy Laboratory: Golden, CO, 2016.
<http://www.nrel.gov/docs/fy17osti/67216.pdf> (accessed Jan 27, 2018).
- Evaluation of Fuel Consumption Potential of Medium and Heavy Duty Vehicles through Modeling and Simulation; Contract DEPS-BEES001; Argonne National Laboratory: Lemont, IL, 2009.
http://www.autonomie.net/docs/6%20-%20Papers/nas_mediumheavyduty_2009.pdf (accessed Jan 27, 2018).
- Fagnant, D. J., & Kockelman, K. M. (2014). The travel and environmental implications of shared autonomous vehicles, using agent-based model scenarios. *Transportation Research Part C: Emerging Technologies*, 40, 1-13. doi:10.1016/j.trc.2013.12.001
- Fagnant, D. J., Kockelman, K. M., & Bansal, P. (2015). Operations of Shared Autonomous Vehicle Fleet for Austin, Texas, Market. *Transportation Research Record: Journal of the Transportation Research Board*, 2536, 98-106. doi:10.3141/2536-12
- Fagnant, D. J., & Kockelman, K. M. (2016). Dynamic ride-sharing and fleet sizing for a system of shared autonomous vehicles in Austin, Texas. *Transportation*, 45(1), 143-158. doi:10.1007/s11116-016-9729-z
- Farhan, J., & Chen, T. D. (2018). Impact of ridesharing on operational efficiency of shared autonomous electric vehicle fleet. *Transportation Research Part C: Emerging Technologies*, 93, 310-321. doi:10.1016/j.trc.2018.04.022
- Fagnant, D. J.; Kockelman, K. Preparing a nation for autonomous vehicles: opportunities, barriers and policy recommendations. *Transportation Research Part A: Policy and Practice* 2015, 77, 167–181.
- Ford, H. J. (2012). *Shared autonomous taxis: Implementing an efficient alternative to automobile dependency*. Princeton University.
- Gawron, J. H., Keoleian, G. A., Kleine, R. D., Wallington, T. J., & Kim, H. C. (2018). Life Cycle Assessment of Connected and Automated Vehicles: Sensing and Computing Subsystem and Vehicle Level Effects. *Environmental Science & Technology*, 52(5), 3249-3256. doi:10.1021/acs.est.7b04576
- Greenblatt, J. B., & Saxena, S. (2015). Autonomous taxis could greatly reduce greenhouse-gas emissions of US light-duty vehicles. *Nature Climate Change*, 5(9), 860-863. doi:10.1038/nclimate2685
- Greenblatt, J. B., & Shaheen, S. (2015). Automated Vehicles, On-Demand Mobility, and Environmental Impacts. *Current Sustainable/Renewable Energy Reports*, 2(3), 74-81. doi:10.1007/s40518-015-0038-5
- Hacking Automotive Ultrasonic Sensors. <http://www.instructables.com/id/Hacking-Automotive-Ultrasonic-Sensors/> (accessed Jan 27, 2018).
- Hawkins, T. R., Singh, B., Majeau-Bettez, G., & Strømman, A. H. (2012). Comparative Environmental Life Cycle Assessment of Conventional and Electric Vehicles. *Journal of Industrial Ecology*, 17(1), 53-64. doi:10.1111/j.1530-9290.2012.00532.x
- HDL-64E. www.velodynelidar.com (accessed Jan 27, 2018).

- Horvath, A. (2003). Life-Cycle Environmental and Economic Assessment of Using Recycled Materials for Asphalt Pavements. UC Berkeley: University of California Transportation Center. Retrieved from <https://escholarship.org/uc/item/5jz3x91z>
- Introducing Waymo's suite of custom-built, self-driving hardware. <https://medium.com/waymo/introducing-waymos-suite-of-custom-built-self-driving-hardware-c47d1714563> (accessed Jan 27, 2018).
- ISO 2006: Environmental Management – Life Cycle Assessment – Principles and Framework; 14040; International Organization for Standardization: Geneva, Switzerland. <http://www.iso.org> (accessed Jan 27, 2018).
- Jasiński, D., Meredith, J., & Kirwan, K. (2016). A comprehensive framework for automotive sustainability assessment. *Journal of Cleaner Production*, 135, 1034-1044. doi:10.1016/j.jclepro.2016.07.027
- Kang, N., Feinberg, F. M., & Papalambros, P. Y. (2016). Autonomous Electric Vehicle Sharing System Design. *Journal of Mechanical Design*, 139(1), 011402. doi:10.1115/1.4034471
- Kim, H. C., & Wallington, T. J. (2016a). Life Cycle Assessment of Vehicle Lightweighting: A Physics-Based Model To Estimate Use-Phase Fuel Consumption of Electrified Vehicles. *Environmental Science & Technology*, 50(20), 11226-11233. doi:10.1021/acs.est.6b02059
- Kim, H. C., Wallington, T. J., Arsenault, R., Bae, C., Ahn, S., & Lee, J. (2016b). Cradle-to-gate emissions from a commercial electric vehicle Li-ion battery: a comparative analysis. *Environmental science & technology*, 50(14), 7715-7722. doi: 10.1021/acs.est.6b00830
- Kley, F., Lerch, C., & Dallinger, D. (2011). New business models for electric cars—A holistic approach. *Energy Policy*, 39(6), 3392-3403. doi:10.1016/j.enpol.2011.03.036
- Koomey, J, and Naffziger, S. (2015, March 31). Moore's Law Might Be Slowing Down, But Not Energy Efficiency. Retrieved September 15, 2018 from <https://spectrum.ieee.org/computing/hardware/moores-law-might-be-slowing-down-but-not-energy-efficiency>
- Kornhauser, A. L. (2013). PRT Statewide Application: Conceptual Design of a Transit System Capable of Serving Essentially All Daily Trips. *Urban Public Transportation Systems 2013*. doi:10.1061/9780784413210.032
- Levin, M. W., Li, T., Boyles, S. D., & Kockelman, K. M. (2016). A general framework for modeling shared autonomous vehicles. In 95th Annual Meeting of the Transportation Research Board.
- Lieven, T., Mühlmeier, S., Henkel, S., & Waller, J. F. (2011). Who will buy electric cars? An empirical study in Germany. *Transportation Research Part D: Transport and Environment*, 16(3), 236-243. doi:10.1016/j.trd.2010.12.001
- Liu, S.; Tang, J.; Zhang, Z.; Gaudiot, J. CAAD: Computer Architecture for Autonomous Driving. Institute for Electrical and Electronics Engineers; 2017. <https://arxiv.org/ftp/arxiv/papers/1702/1702.01894.pdf> (accessed Jan 27, 2018).

- Loeb, B., Kockelman, K. M., & Liu, J. (2018). Shared autonomous electric vehicle (SAEV) operations across the Austin, Texas network with charging infrastructure decisions. *Transportation Research Part C: Emerging Technologies*, 89. doi: 10.1016/j.trc.2018.01.019
- Lucas, A., Silva, C. A., & Neto, R. C. (2012). Life cycle analysis of energy supply infrastructure for conventional and electric vehicles. *Energy Policy*, 41, 537-547. doi:10.1016/j.enpol.2011.11.015
- LRR3: 3rd generation Long-Range Radar Sensor. http://products.bosch-mobility-solutions.com/media/db_application/downloads/pdf/safety_1/en_4/lrr3_datenblatt_de_2009.pdf (accessed Jan 27, 2018).
- Martinez, L., & Crist, P. (2015). Urban Mobility System Upgrade—How shared self-driving cars could change city traffic. In *International Transport Forum*, Paris.
- Majeau-Bettez, G., Hawkins, T. R., & Strømman, A. H. (2011). Life Cycle Environmental Assessment of Lithium-Ion and Nickel Metal Hydride Batteries for Plug-In Hybrid and Battery Electric Vehicles. *Environmental Science & Technology*, 45(10), 4548-4554. doi:10.1021/es103607c
- Michel, P., Karbowski, D., & Rousseau, A. (2016). Impact of Connectivity and Automation on Vehicle Energy Use (No. 2016-01-0152). SAE Technical Paper. doi:10.4271/2016-01-0152
- Milakis, D., Arem, B. V., & Wee, B. V. (2017). Policy and society related implications of automated driving: A review of literature and directions for future research. *Journal of Intelligent Transportation Systems*, 21(4), 324-348. doi:10.1080/15472450.2017.1291351
- Miller, S. A.; Keoleian, G. A. Framework for Analyzing Transformative Technologies in Life Cycle Assessment. *Environ. Sci. Technol.* 2015, 49, 3067–3075.
- New York City Taxi & Limousine Commission. (2013). Take Charge: A Roadmap to Electric New York City Taxis. Retrieved February 17, 2018 from <http://www.nyc.gov/html/tlc/downloads/pdf/electric_taxi_task_force_report_20131231.pdf>.
- Nvidia AI Driving Platform and SI Supercomputer
Xavier. <https://www.gputechconf.jp/assets/files/1062.pdf> (accessed Jan 27, 2018).
- Parking facility layout and dimensions. (2016). Retrieved May 15, 2018, from http://qcode.us/codes/temecula/view.php?topic=17-17_24-17_24_050
- Puck Hi-Res. www.velodynelidar.com (accessed Jan 27, 2018).
- Rigole, P. J. (2014). Study of a Shared Autonomous Vehicles Based Mobility Solution in Stockholm. Retrieved from <http://www.diva-portal.org/smash/record.jsf?pid=diva2%3A746893&dswid=-6143>
- Ultrasonic Sensor. http://products.bosch-mobility-solutions.com/en/de/_technik/component/CO_PC-CV_DA_Side-ViewAssist_CO_CV_Driver-Assistance_2197.html?compId=1157 (accessed Jan 27, 2018).
- U.S. Department of Energy (DOE) and U.S. Environmental Protection Agency (EPA). (2015). Fuel Economy Guide. Retrieved January 27, 2018 from <https://www.fueleconomy.gov/feg/download.shtml>.

- U.S. Department of Energy (COE). (2017). Energy CO2 Emissions Impacts of Clean Energy Technology Innovation and Policy. Retrieved May 2, 2018 from <https://www.energy.gov/sites/prod/files/2017/01/f34/Energy%20CO2%20Emissions%20Impacts%20of%20Clean%20Energy%20Technology%20Innovation%20and%20Policy.pdf>
- U.S. Department of Energy and U.S. Environmental Protection Agency Model Year. Fuel Economy Guide; 2015. <https://www.fueleconomy.gov/feg/download.shtml> (accessed Jan 27, 2018).
- U.S. Department of Transportation (DOT), Federal Highway Administration. (2009). 2009 National Household Travel Survey. Retrieved April 12, 2018 from <https://nhts.ornl.gov>.
- U.S. Department of Transportation (DOT), National Highway Traffic Safety Administration. (2006). Vehicle Survivability and Travel Mileage Schedules. DOT HS 809 952.
- U.S. Environmental Protection Agency (EPA). (2017). Inventory of U.S. Greenhouse Gas Emissions and Sinks: 1990-2015. Retrieved March 26, 2018 from <https://www.epa.gov/ghgemissions/inventory-us-greenhouse-gas-emissions-and-sinks-1990-2015>
- SavariSW-1000 Road-Side-Unit (RSU). www.savari.net (accessed Jan 27, 2018).
- Seif, H. G.; Hu, X. Autonomous Driving in the iCity-HD Maps as a Key Challenge of the Automotive Industry. *Engineering* 2016, 2, 159–162.
- Spieser, K., Treleaven, K., Zhang, R., Frazzoli, E., Morton, D., & Pavone, M. (2014). Toward a Systematic Approach to the Design and Evaluation of Automated Mobility-on-Demand Systems: A Case Study in Singapore. *Road Vehicle Automation Lecture Notes in Mobility*, 229-245. doi:10.1007/978-3-319-05990-7_20
- Stephens, T. S., Gonder, J., Chen, Y., Lin, Z., Liu, C., & Gohlke, D. (2016). Estimated Bounds and Important Factors for Fuel Use and Consumer Costs of Connected and Automated Vehicles. NREL (National Renewable Energy Laboratory (NREL), Golden, CO (United States)). Retrieved from <http://www.nrel.gov/docs/fy17osti/67216.pdf>
- Study of the Potential Energy Consumption Impacts of Connected and Automated Vehicles; United States Energy Information Administration: Washington, DC, 2017. https://www.eia.gov/analysis/studies/transportation/automated/pdf/automated_vehicles.pdf (accessed Jan 27, 2018).
- Sweeting, W. J., & Winfield, P. H. (2012). Future transportation: Lifetime considerations and framework for sustainability assessment. *Energy Policy*, 51, 927-938. doi:10.1016/j.enpol.2012.09.055
- Taiebat, M., Brown, A. L., Safford, H. R., Qu, S., & Xu, M. (2018). A Review on Energy, Environmental, and Sustainability Implications of Connected and Automated Vehicles. *Environmental Science & Technology*. doi:10.1021/acs.est.8b00127
- Taxonomy and Definitions for Terms Related to Driving Automation Systems for On-Road Motor Vehicles; J3016; SAE International: Warrendale, PA, 2016. https://saemobilus.sae.org/content/j3016_201609 (accessed Jan 27, 2018).

Teehan, P.; Kandlikar, M. Comparing Embodied Greenhouse Gas Emissions of Modern Computing and Electronics Products. *Environ. Sci. Technol.* 2013, 47, 3997–4003.

The Transforming Mobility Ecosystem: Enabling an Energy-Efficient Future; United States Department of Energy, Energy Efficiency & Renewable Energy: Washington, DC, 2017.
https://energy.gov/sites/prod/files/2017/01/f34/The%20Transforming%20Mobility%20EcosystemEnabling%20an%20Energy%20Efficient%20Future_0117_1.pdf (accessed Jan 27, 2018).

The Power Demands of Self-Driving Technology. <http://www.autobeatdaily.com/articles/the-power-demands-of-self-drivingtechnology> (accessed Jan 27, 2018).

The Power of Wireless Cloud; Centre for Energy-Efficient Telecommunications: Melbourne, Australia, 2013. <http://www.ceet.unimelb.edu.au/publications/ceet-white-paper-wireless-cloud.pdf> (accessed Jan 27, 2018).

Wadud, Z., MacKenzie, D., & Leiby, P. (2016). Help or hindrance? The travel, energy and carbon impacts of highly automated vehicles. *Transportation Research Part A: Policy and Practice*, 86, 1-18. doi:10.1016/j.tra.2015.12.001

Wang, F., Yang, M., & Yang, R. (2006). Dynamic fleet management for cybercars. 2006 IEEE Intelligent Transportation Systems Conference. doi:10.1109/itsc.2006.1707393

Where the Energy Goes: Gasoline Vehicles. <https://www.fueleconomy.gov/feg/atv.shtml> (accessed Jan 27, 2018).

Appendix A – Phase 1 Supporting Information

Supporting Information

Life Cycle Assessment of Connected and Automated Vehicles (CAVs): Sensing and Computing Subsystem and Vehicle Level Effects

James H. Gawron, Gregory A. Keoleian, Robert De Kleine, Timothy J. Wallington, and Hyung Chul Kim

Supporting Information Includes:

Table S1: Characteristics of CAV platform vehicles	S2
Figure S1: Images of CAV subsystem basis	S3
Figure S2: CAV sensor models	S4
Table S2: Materials breakdowns of CAV sensing and computing components	S5
Figure S3-S8: Weight, power, life cycle energy, and GHG emissions for the six scenarios	S6 - S11
Figure S9-S14: Vehicle-level life cycle energy and GHG emissions results for the six scenarios	S12 - S17
Figure S15-S18: Weight, power, life cycle energy, and GHG emissions comparisons for the six scenarios	S18 - S21
Figure S19-S20: Impact of CAV subsystem additions at the vehicle level	S22 - S23
Figure S21: Comparison between vehicle life cycle energy of non-CAVs and CAVs across the six scenarios	S24
Figure S22-S24: Sensitivity analysis	S25 – S27

Table S1: Characteristics of the battery electric vehicle (BEV) and internal combustion engine vehicle (ICEV) platforms.¹⁻³



Characteristic	BEV	ICEV
Picture		
Model	2015 Ford Focus Electric	2015 Ford Focus
Curb Weight (lb)	3,690	3,055
Combined Fuel Economy (mpge)	107	31
FRV (Le / 100 km 100 kg)	0.073	0.27
Production Burden: CED (MJ)	139,372	101,132
Production Burden: GWP (kg CO ₂ -eq)	10,121	7,241



Figure S1. Basis for the small CAV sensing and computing subsystem is the Tesla Model S (top), medium subsystem is the Ford Fusion (middle), and large subsystem is the Waymo Pacifica (bottom).⁴⁻⁶

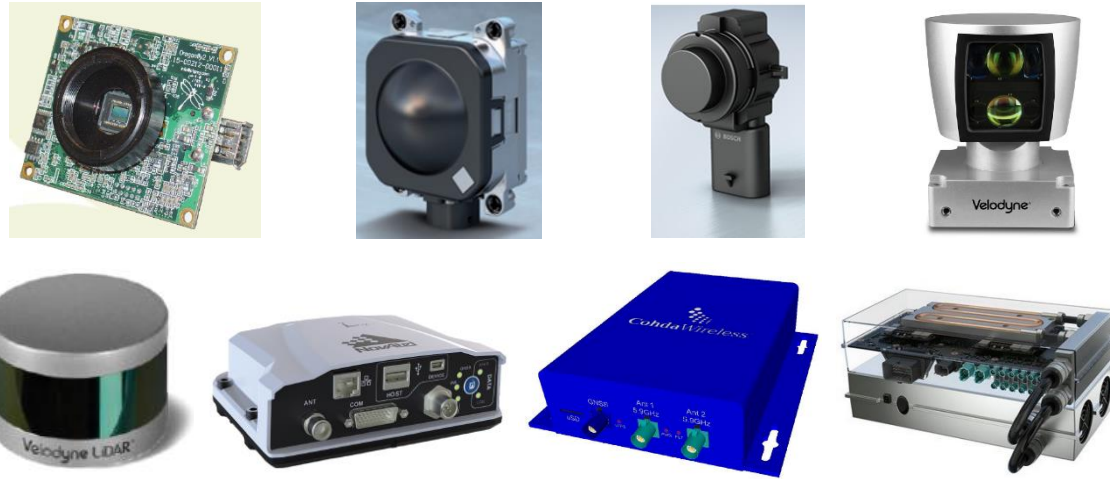


Figure S2. CAV sensors and components. From top left to bottom right: Point Greg Dragonfly 2, Bosch LRR3, Bosch Ultrasonic, Velodyne HDL-64E, Velodyne VLP-16 Puck, NovAtel PwrPak7-E1, Cohda MK5 OBU, and Nvidia Drive PX2.⁷⁻²⁰

Table S2. Materials breakdowns for each CAV component.⁷⁻²¹

Material	Camera	Sonar	Radar	L. LiDAR	S. LiDAR	GPS/INS	DSRC	Computer	Harness	Structure
Steel							13%			
Cast Iron				7%	1%			2%		
Aluminum				61%	60%		48%	70%		49%
Copper				6%	1%		1%	6%	100%	
Glass	9%			5%	8%					
Plastic	45%	50%	30%	7%	17%	45%	3%	4%		51%
Rare Earth				6%	1%			2%		
Electronics*	46%	50%	70%	5%	12%	55%	35%	16%		

*Electronic weight further allocated to PWB, power supply, IC package, and IC die components according to Teehan et al. 2013

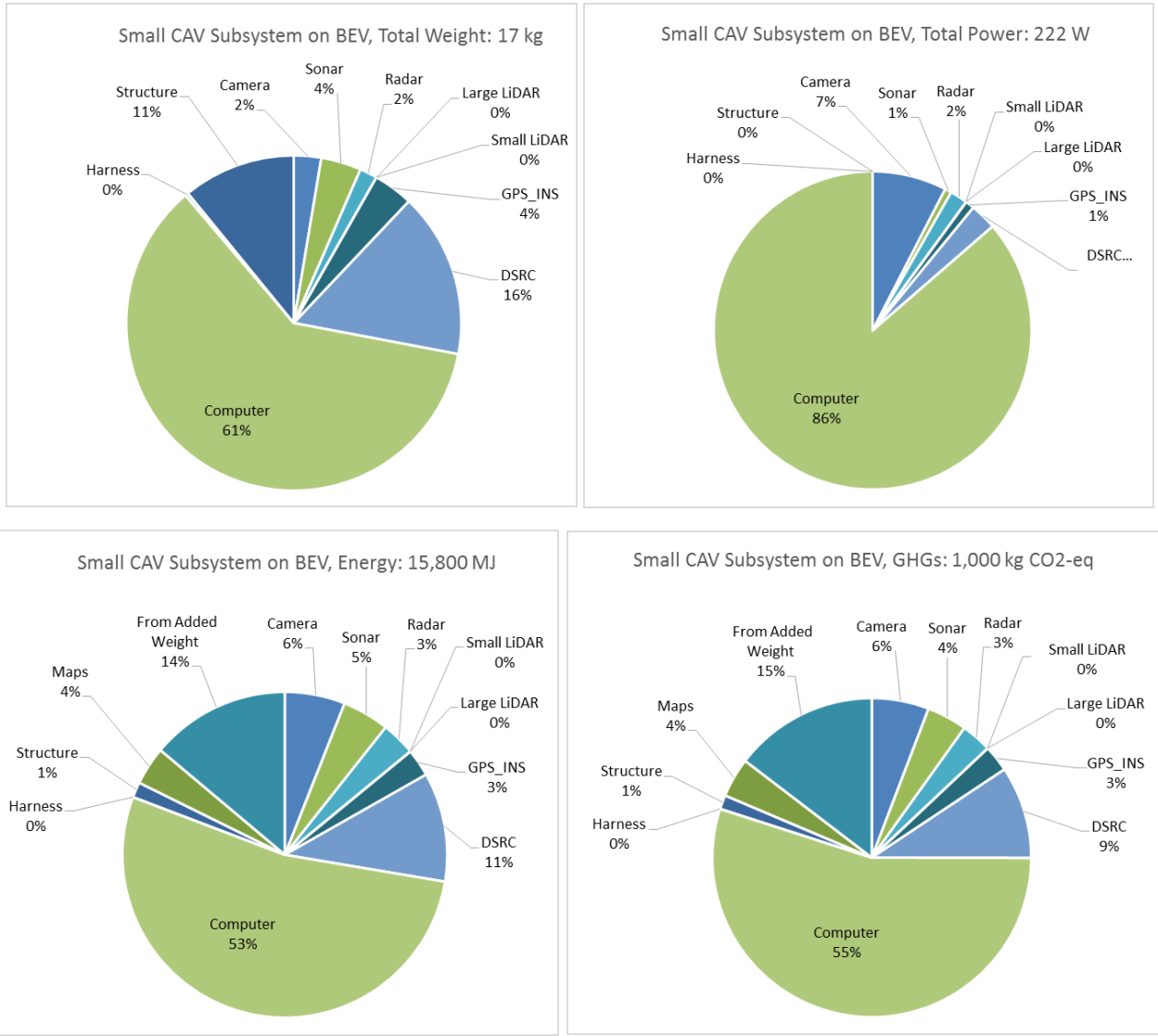


Figure S3. Weight, power, life cycle energy, and GHG emissions for the small CAV subsystem on a BEV

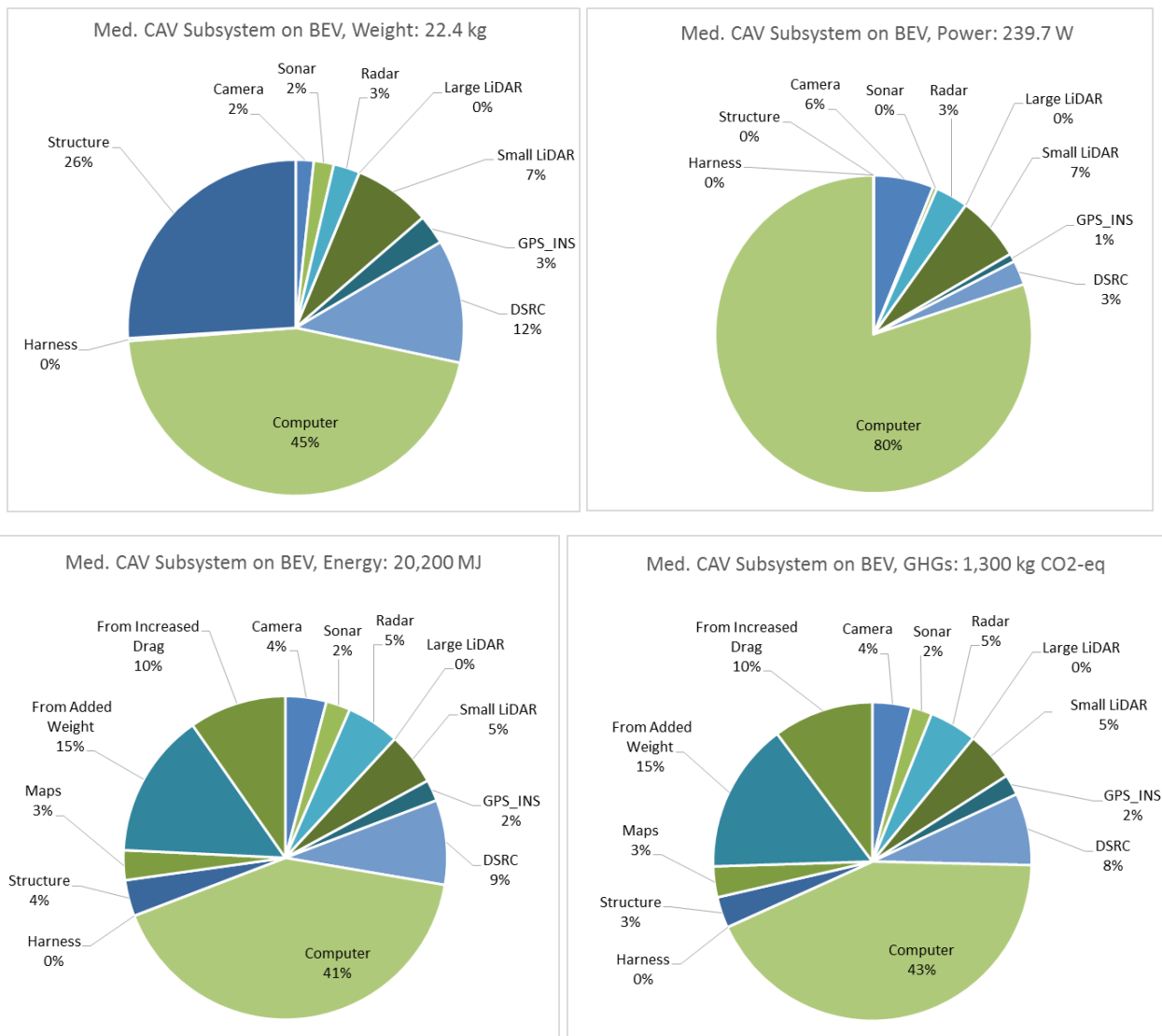


Figure S4. Weight, power, life cycle energy, and GHG emissions for the medium CAV subsystem on a BEV

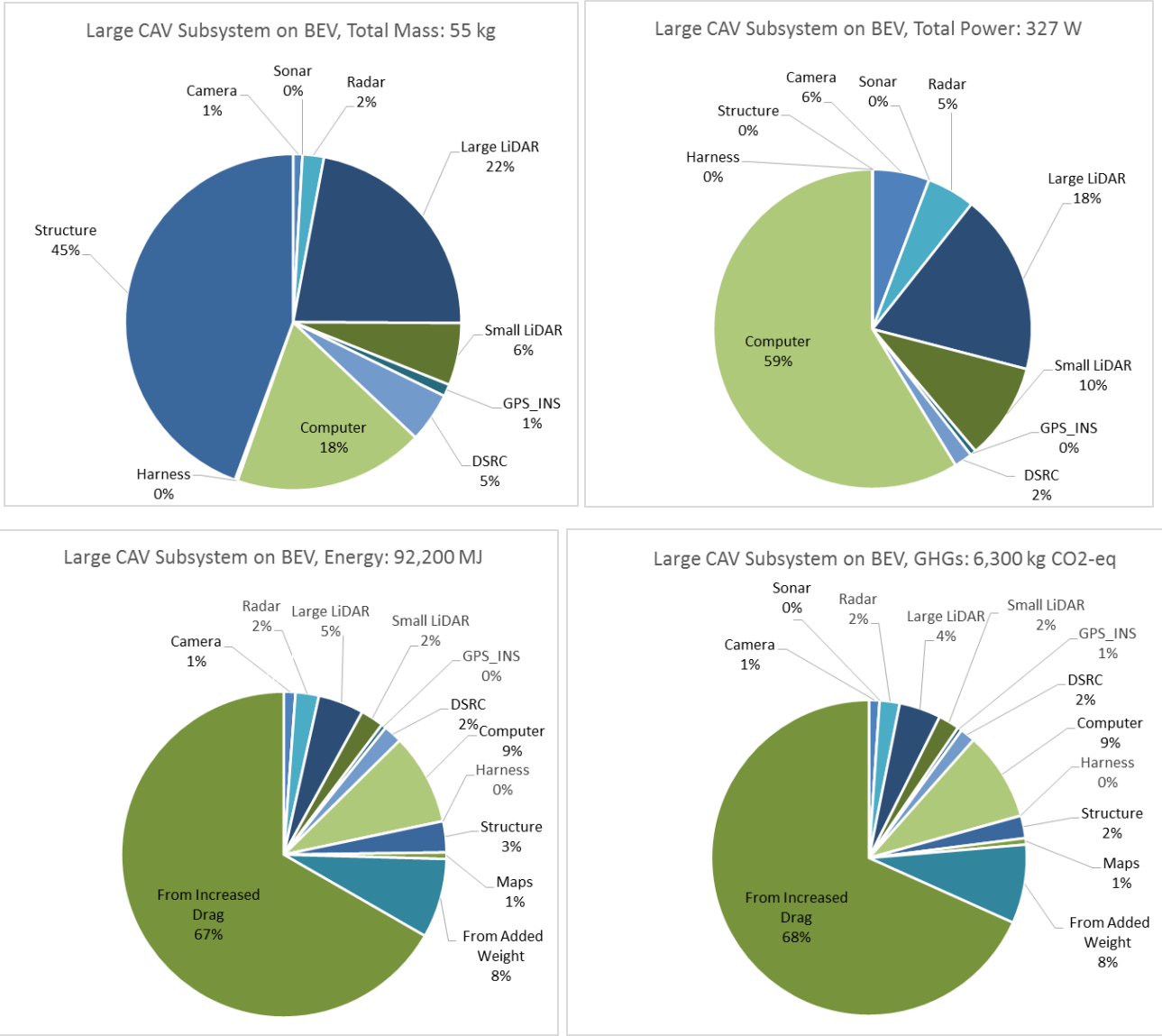


Figure S5. Weight, power, life cycle energy, and GHG emissions for the large CAV subsystem on a BEV

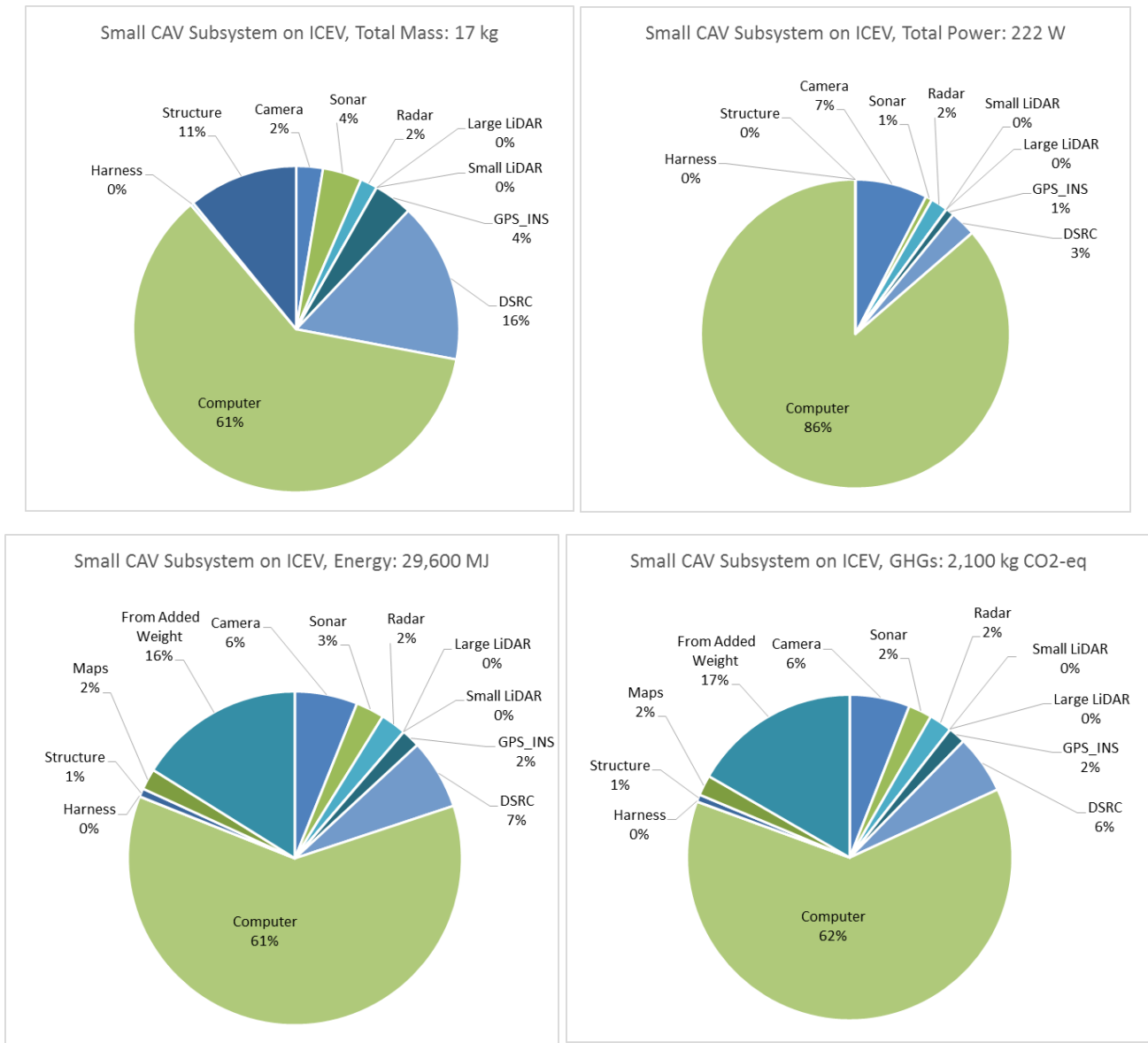


Figure S6. Weight, power, life cycle energy, and GHG emissions for the small CAV subsystem on an ICEV

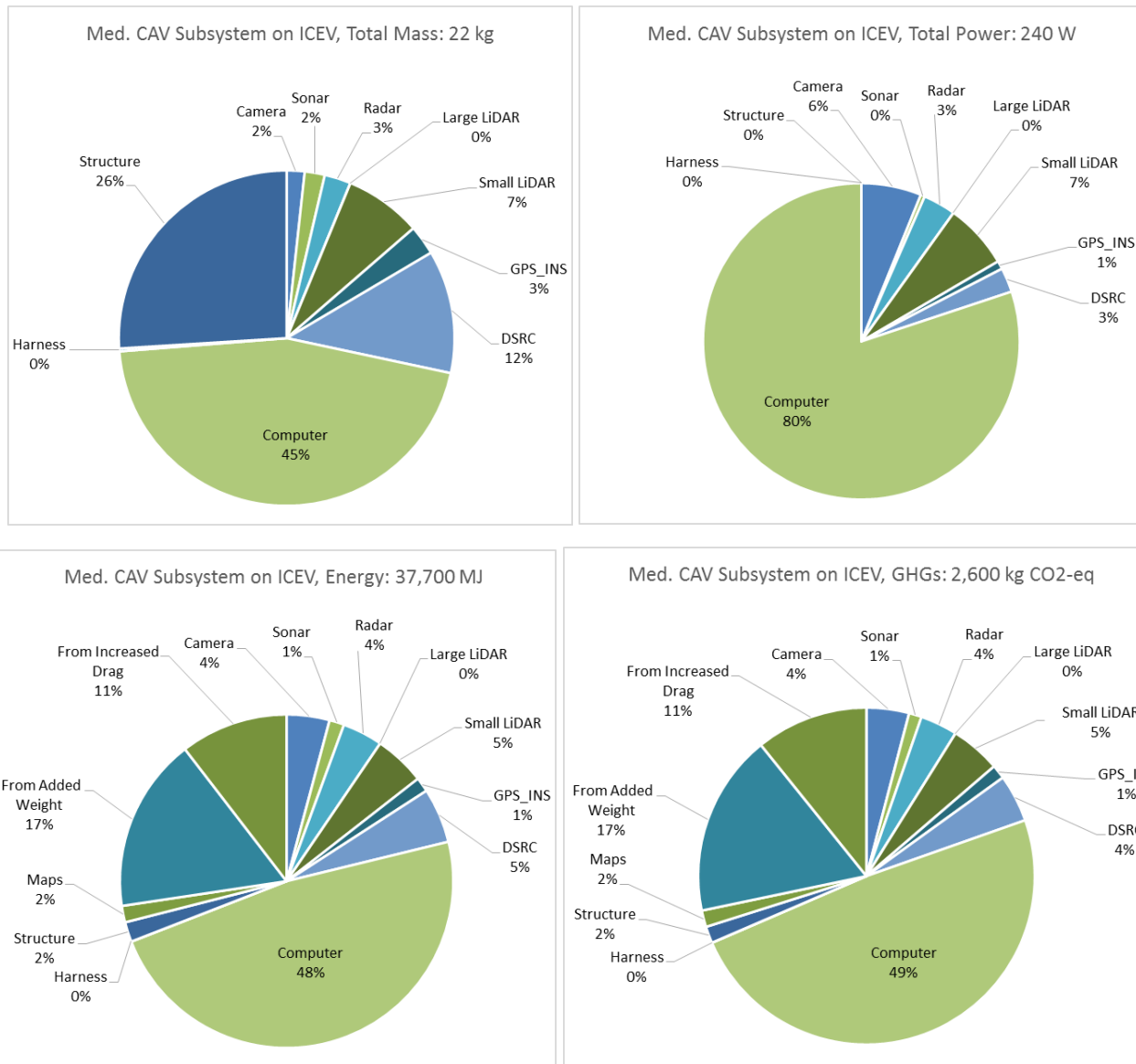


Figure S7. Weight, power, life cycle energy, and GHG emissions for the medium CAV subsystem on an ICEV

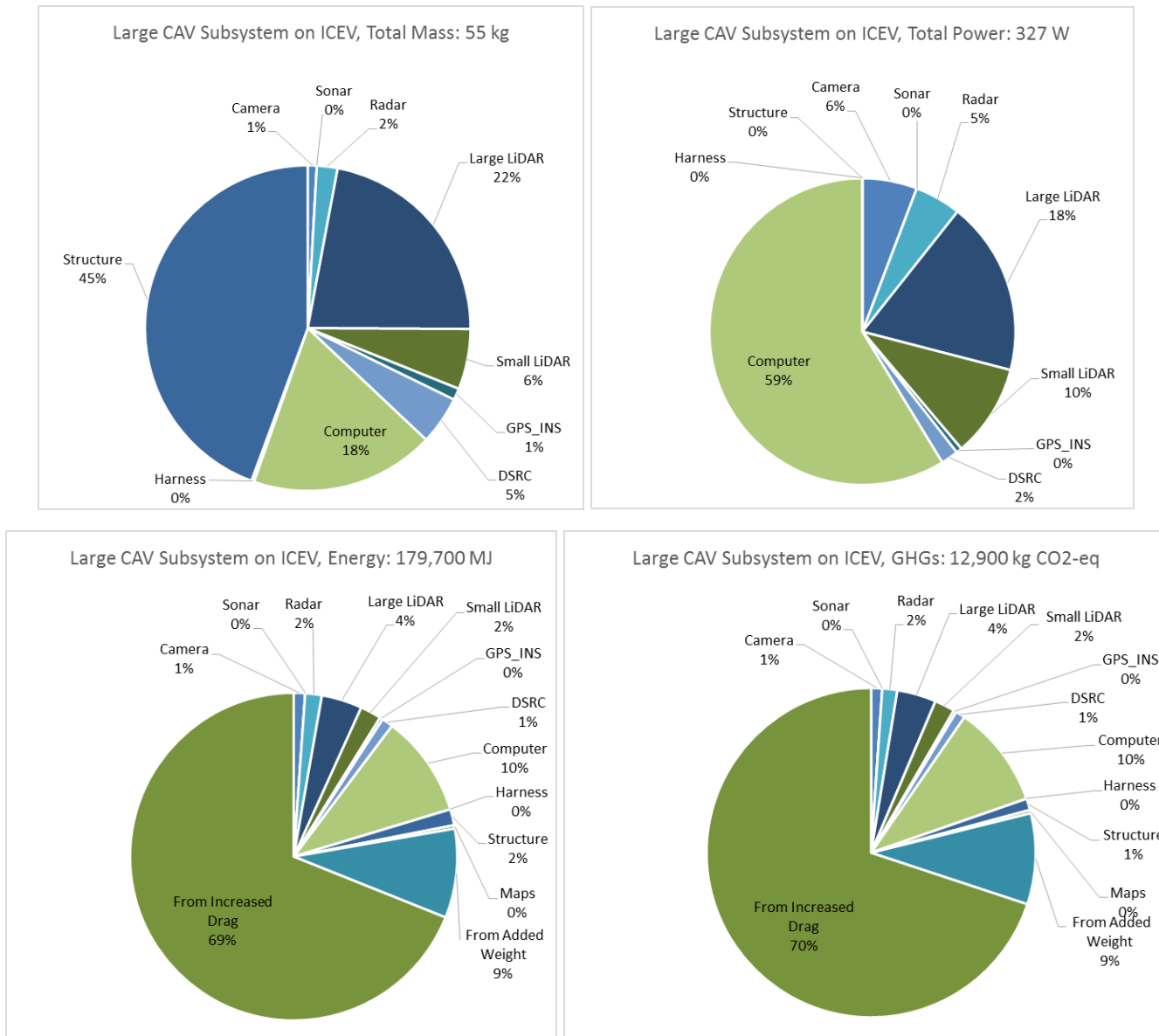


Figure S8. Weight, power, life cycle energy, and GHG emissions for the large CAV subsystem on an ICEV

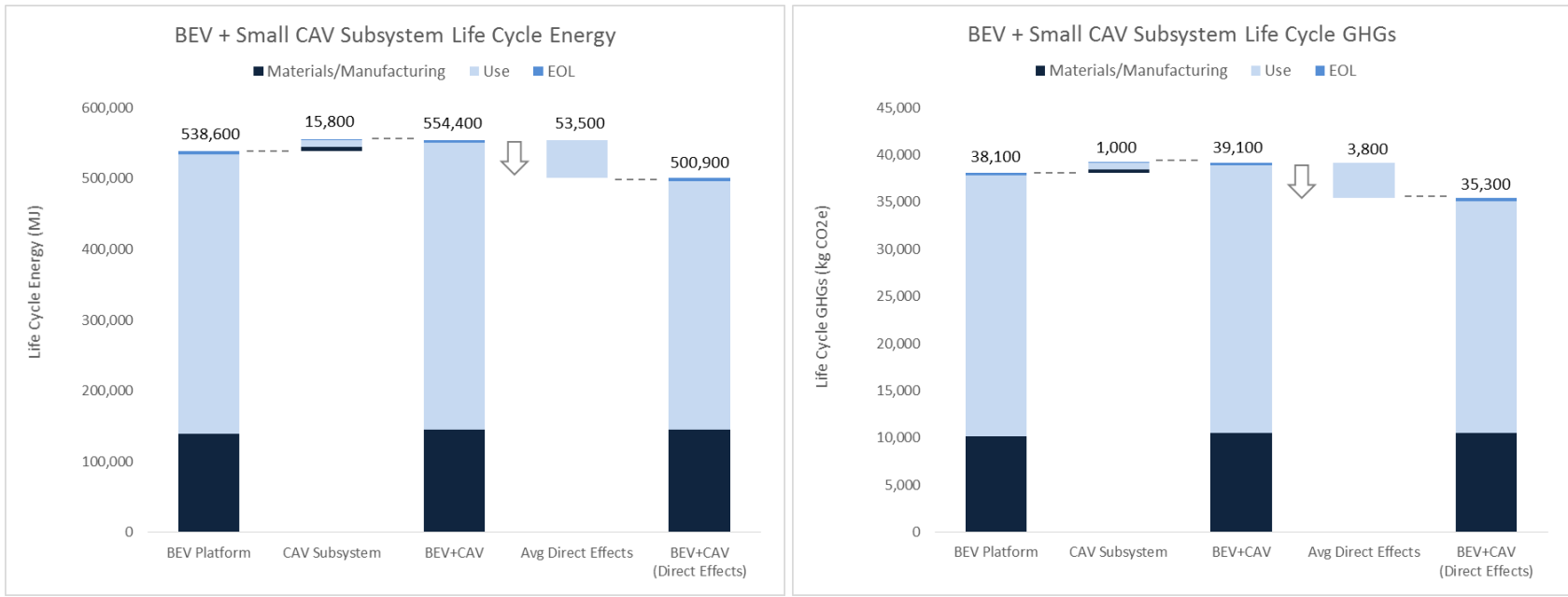


Figure S9. Vehicle-level energy and GHG results for the BEV + Small Subsystem scenario

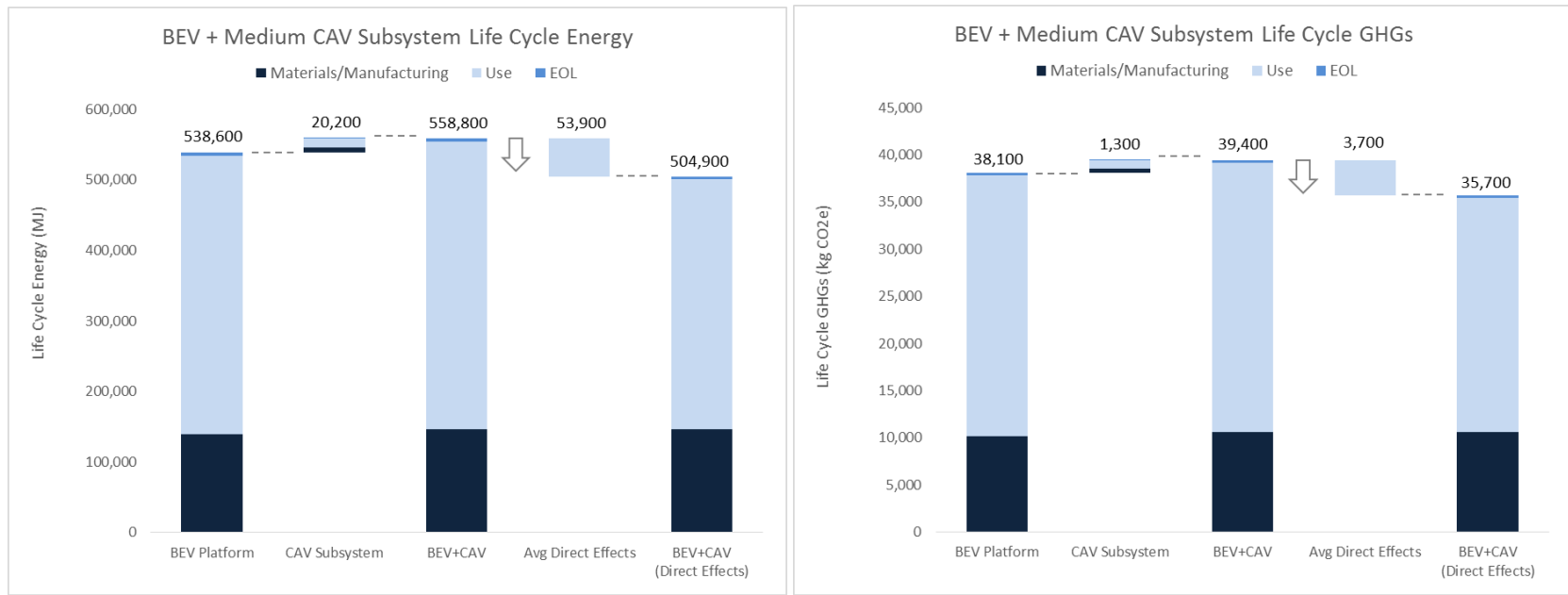


Figure S10. Vehicle-level energy and GHG results for the BEV + Medium Subsystem scenario

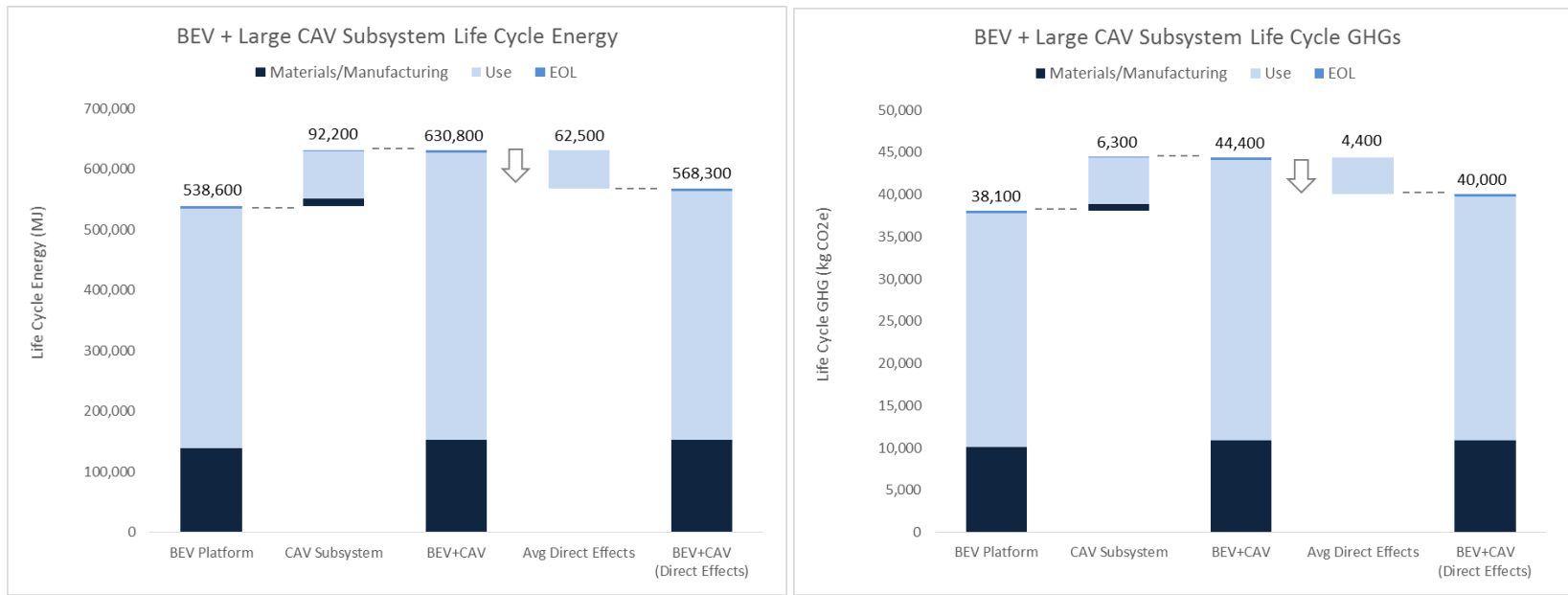


Figure S11. Vehicle-level energy and GHG results for the BEV + Large Subsystem scenario

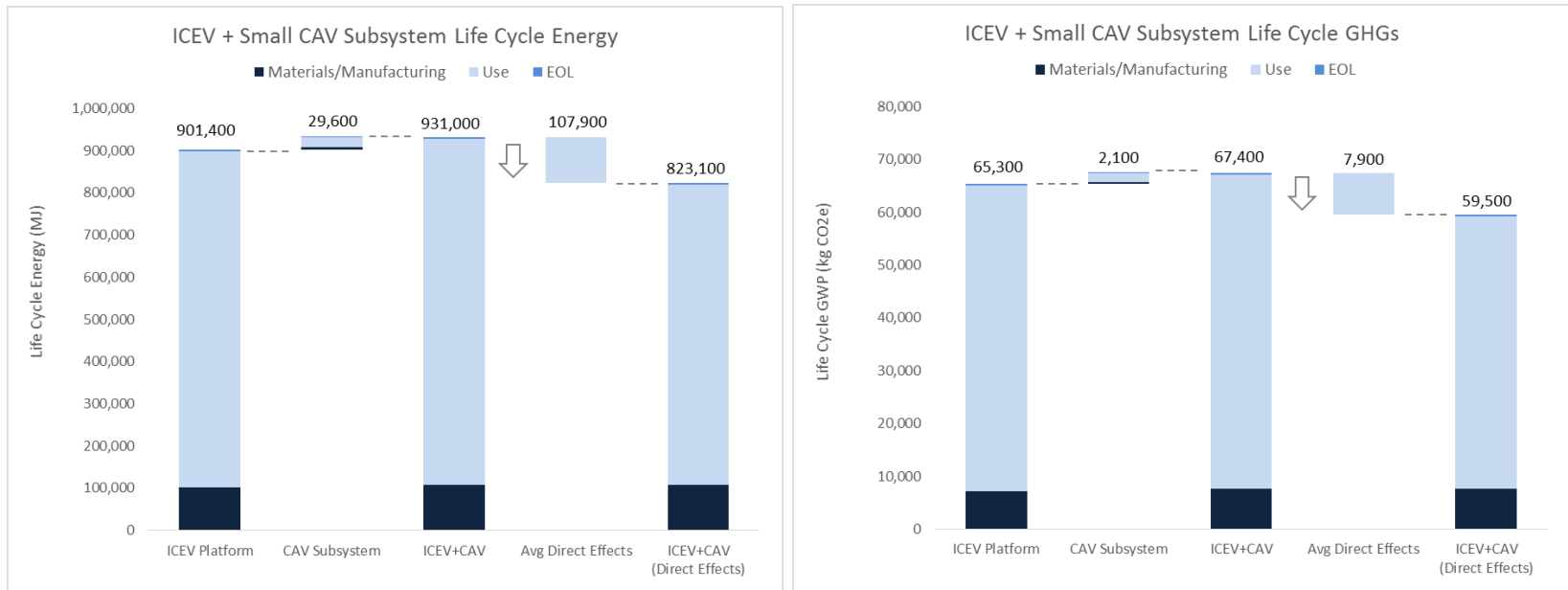


Figure S12. Vehicle-level energy and GHG results for the ICEV + Small Subsystem scenario

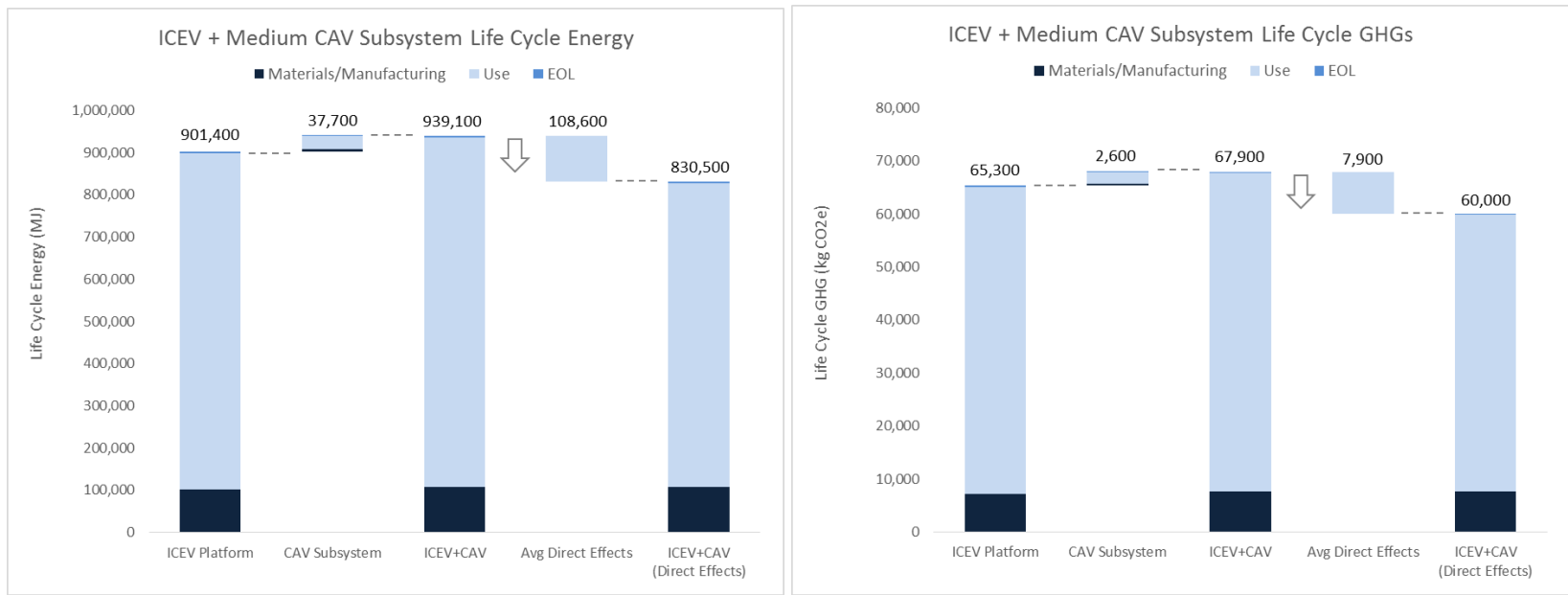


Figure S13. Vehicle-level energy and GHG results for the ICEV + Medium Subsystem scenario

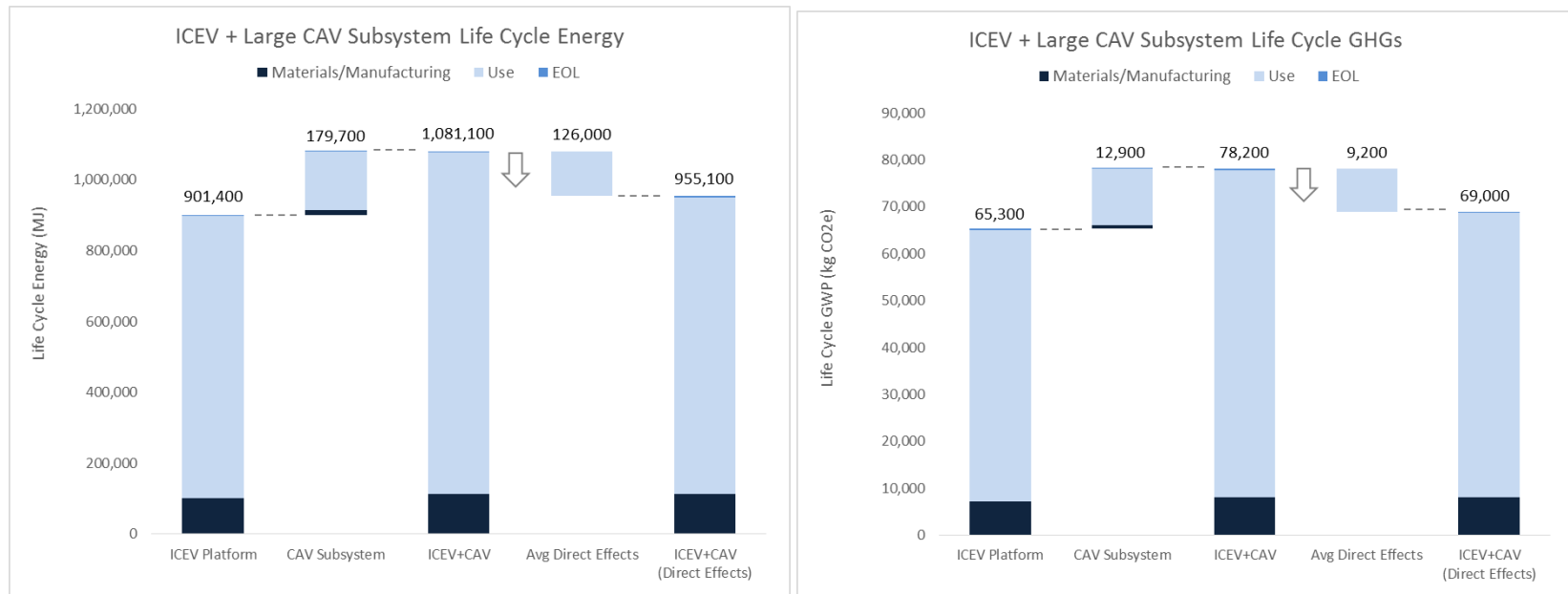


Figure S14. Vehicle-level energy and GHG results for the ICEV + Large Subsystem scenario

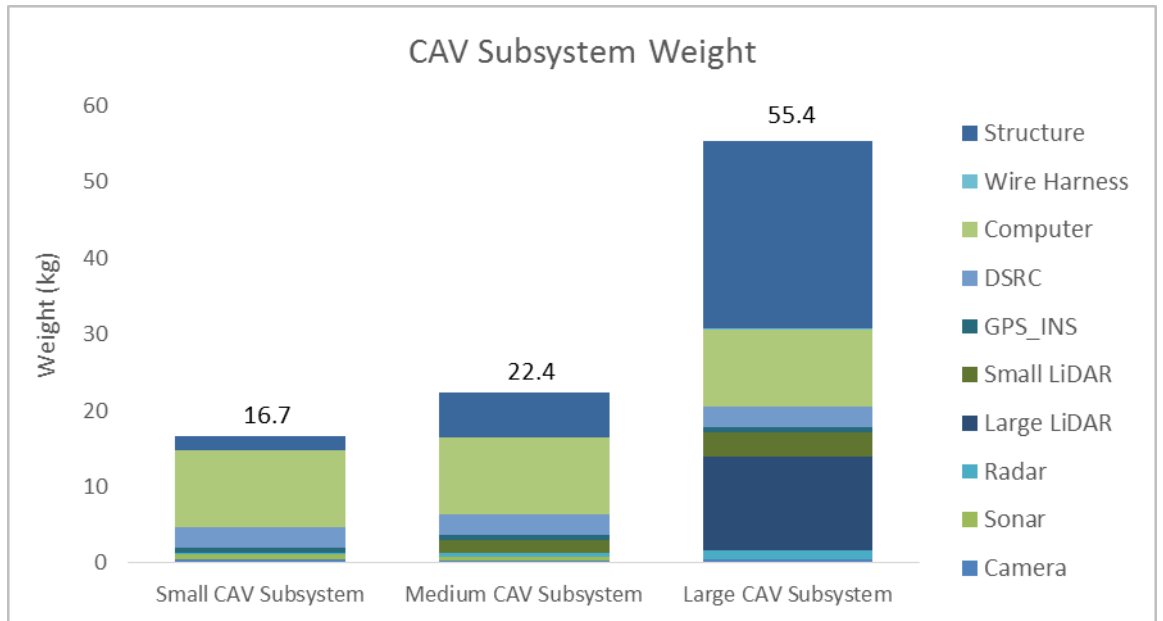


Figure S15. Weight comparison for small, medium, and large CAV sensing and computing subsystems

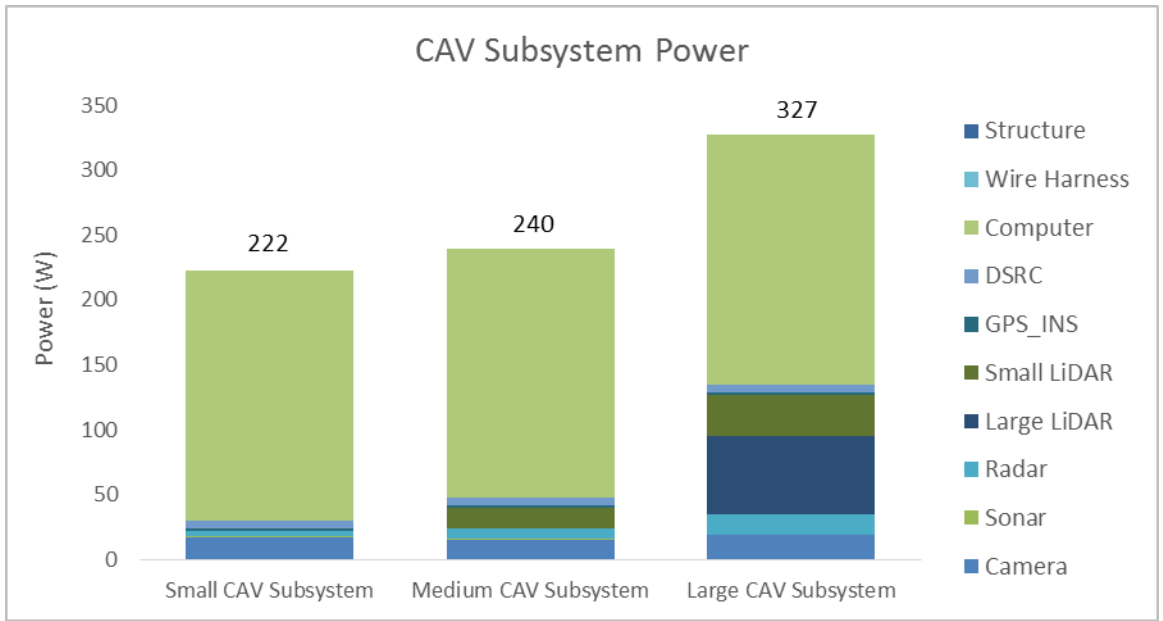


Figure S16. Power consumption comparison for small, medium, and large CAV sensing and computing subsystems

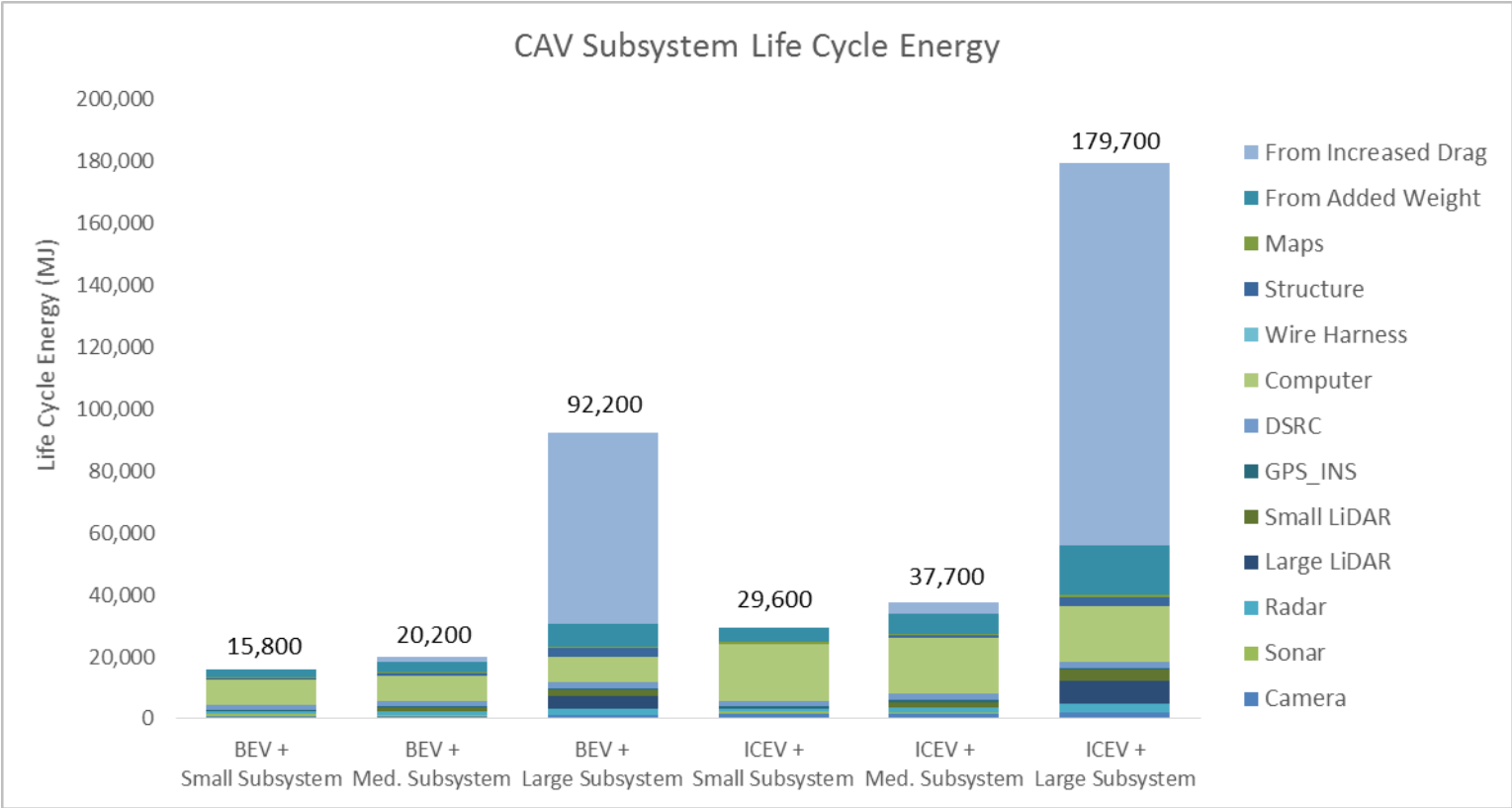


Figure S17. Life cycle energy comparison for the CAV subsystem in all six scenarios

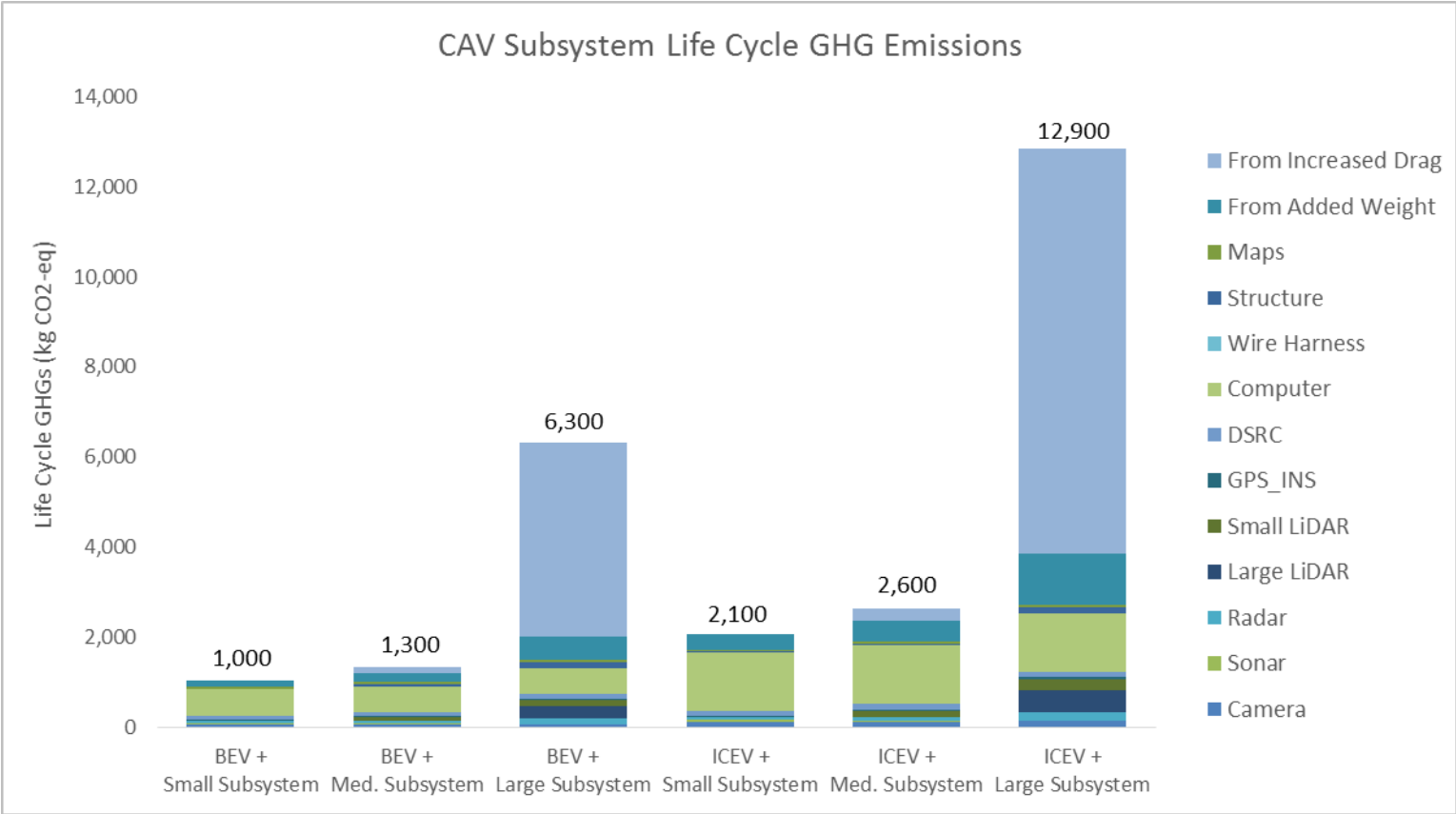


Figure S18. GHG emissions comparison for the CAV subsystem in all six scenarios

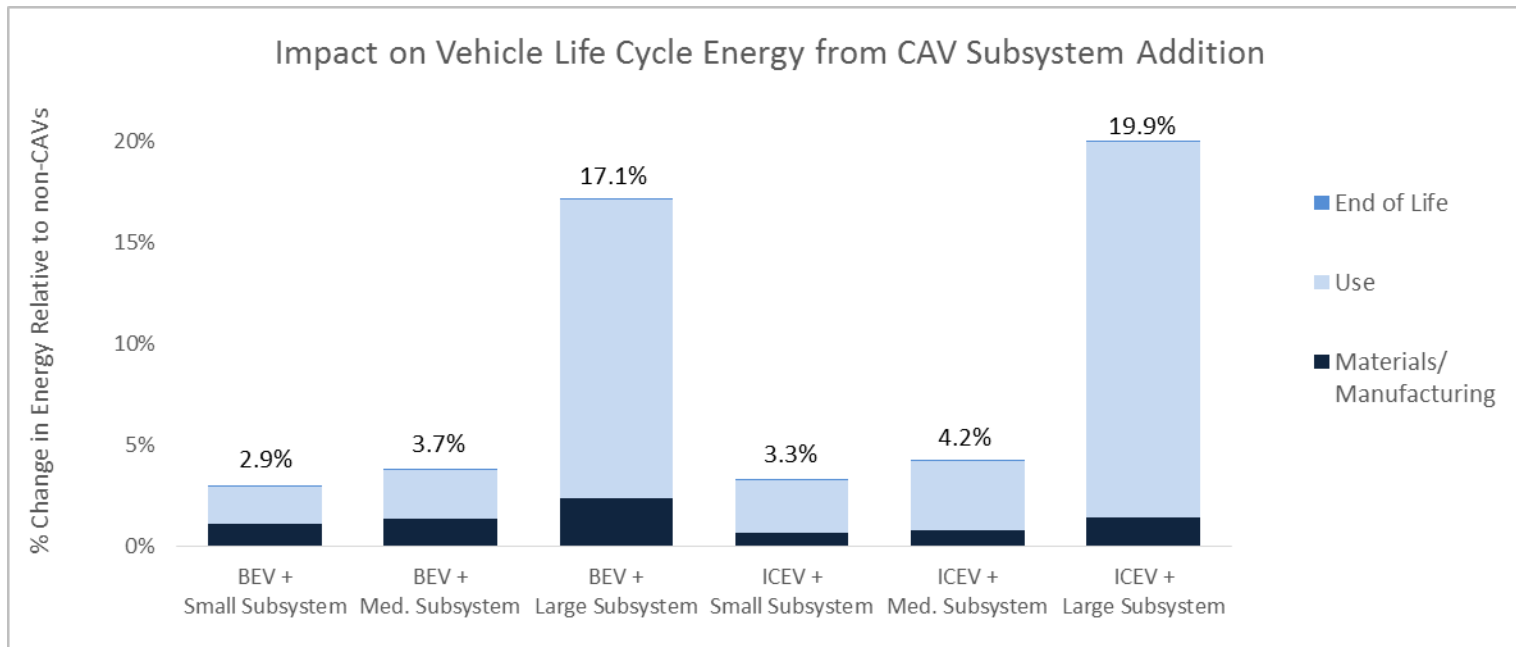


Figure S19. Increase in vehicle life cycle energy when a CAV subsystem is added to the non-CAV platform

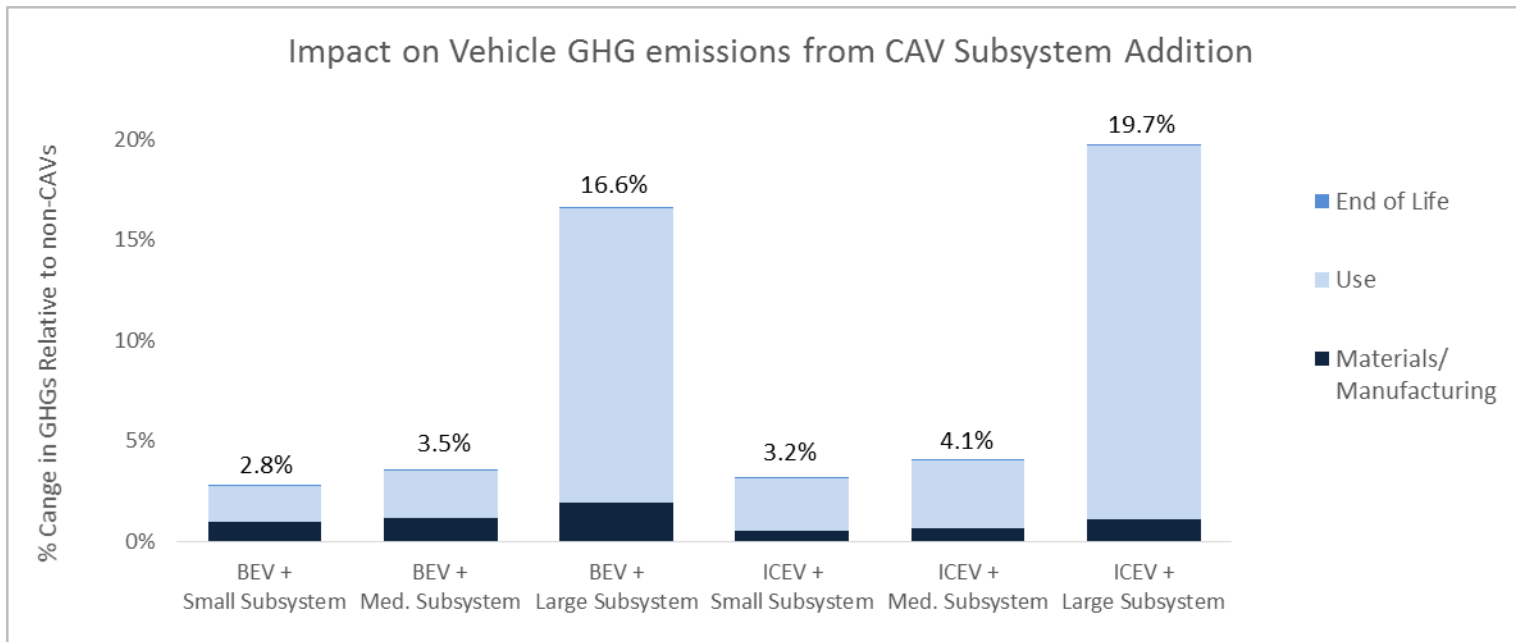


Figure S20. Increase in vehicle GHG emissions when a CAV subsystem is added to the non-CAV platform

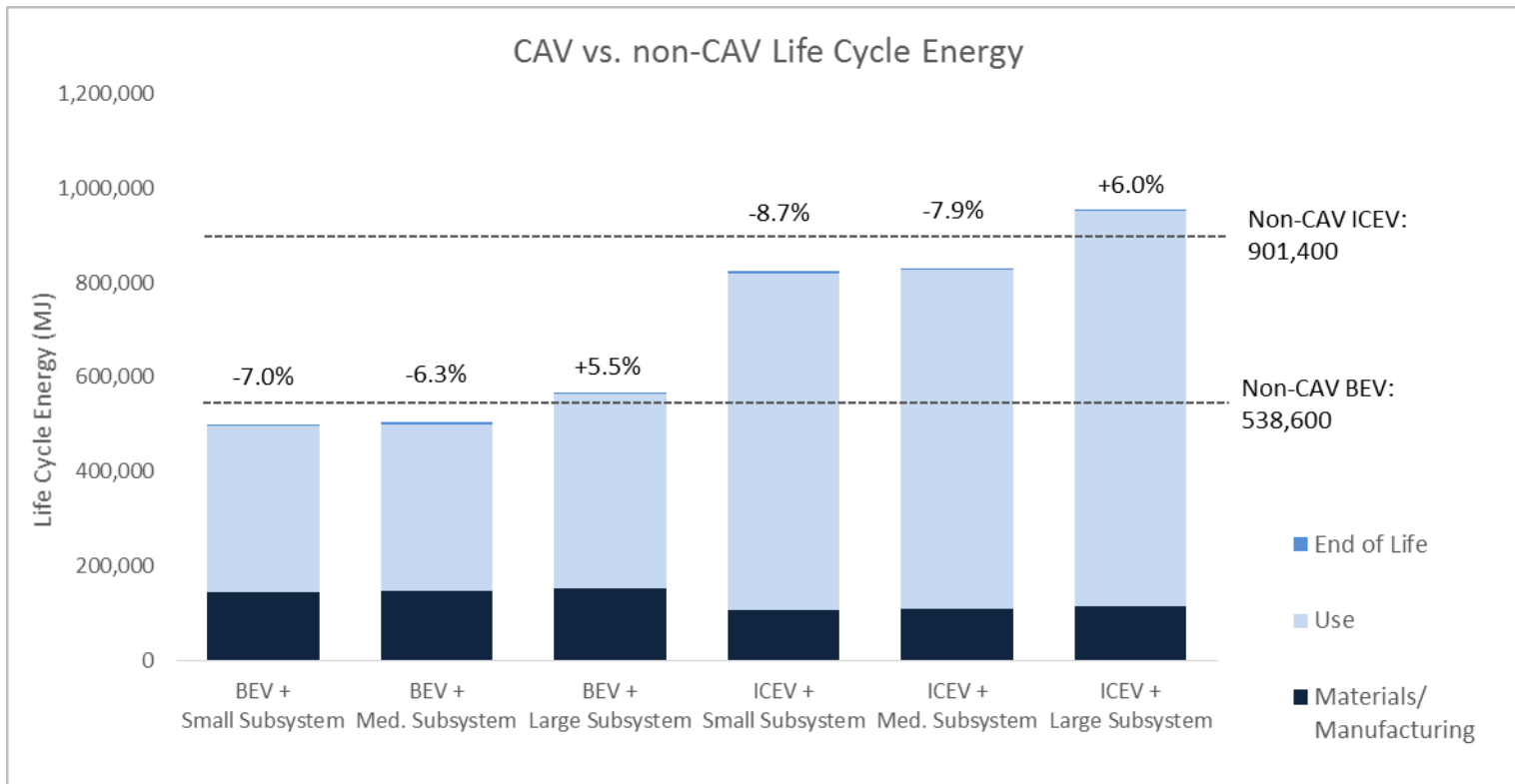


Figure S21. Comparison between vehicle life cycle energy of non-CAVs and CAVs across the six scenarios

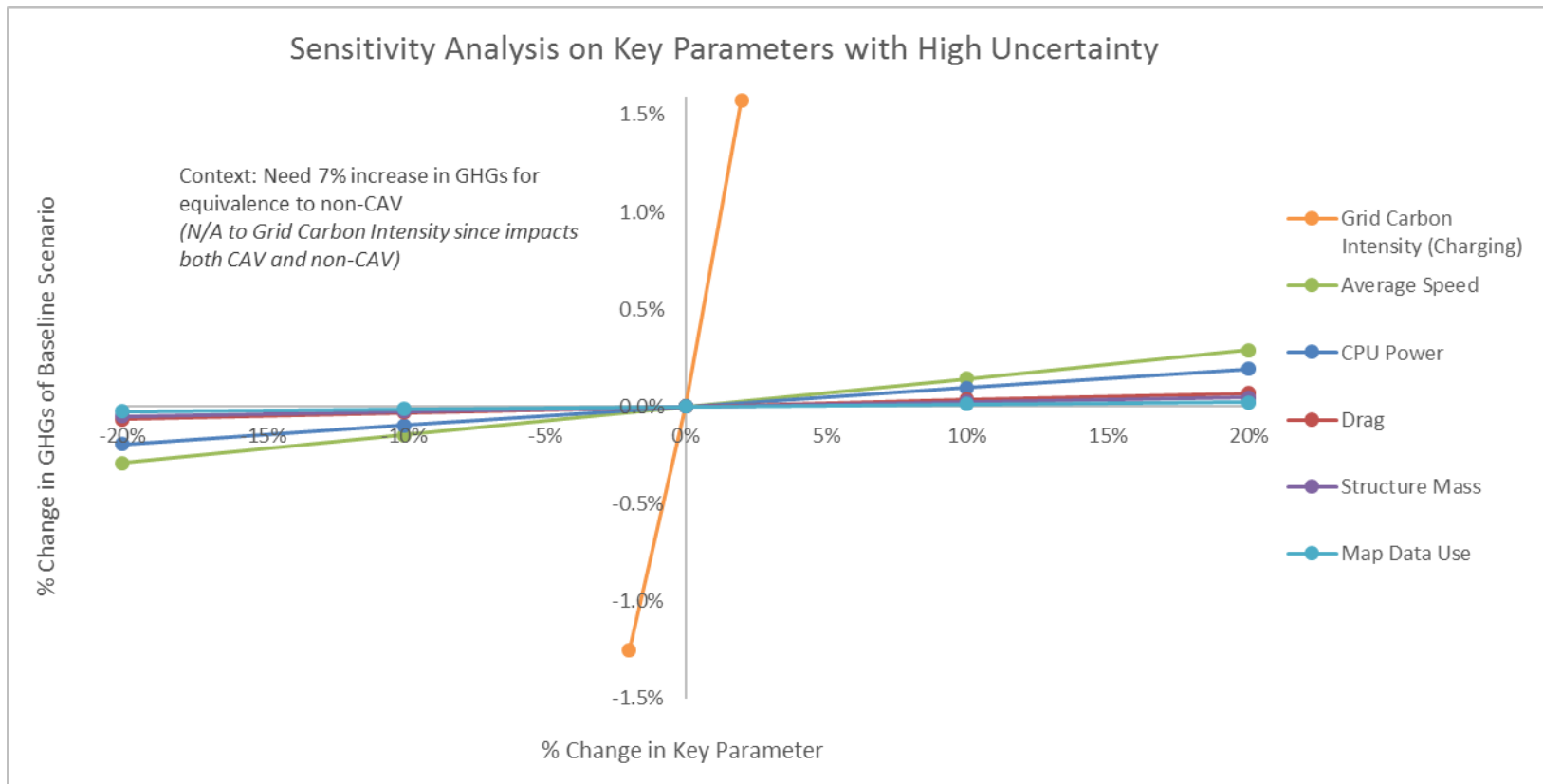


Figure S22. Sensitivity analysis on the baseline scenario for six key parameters

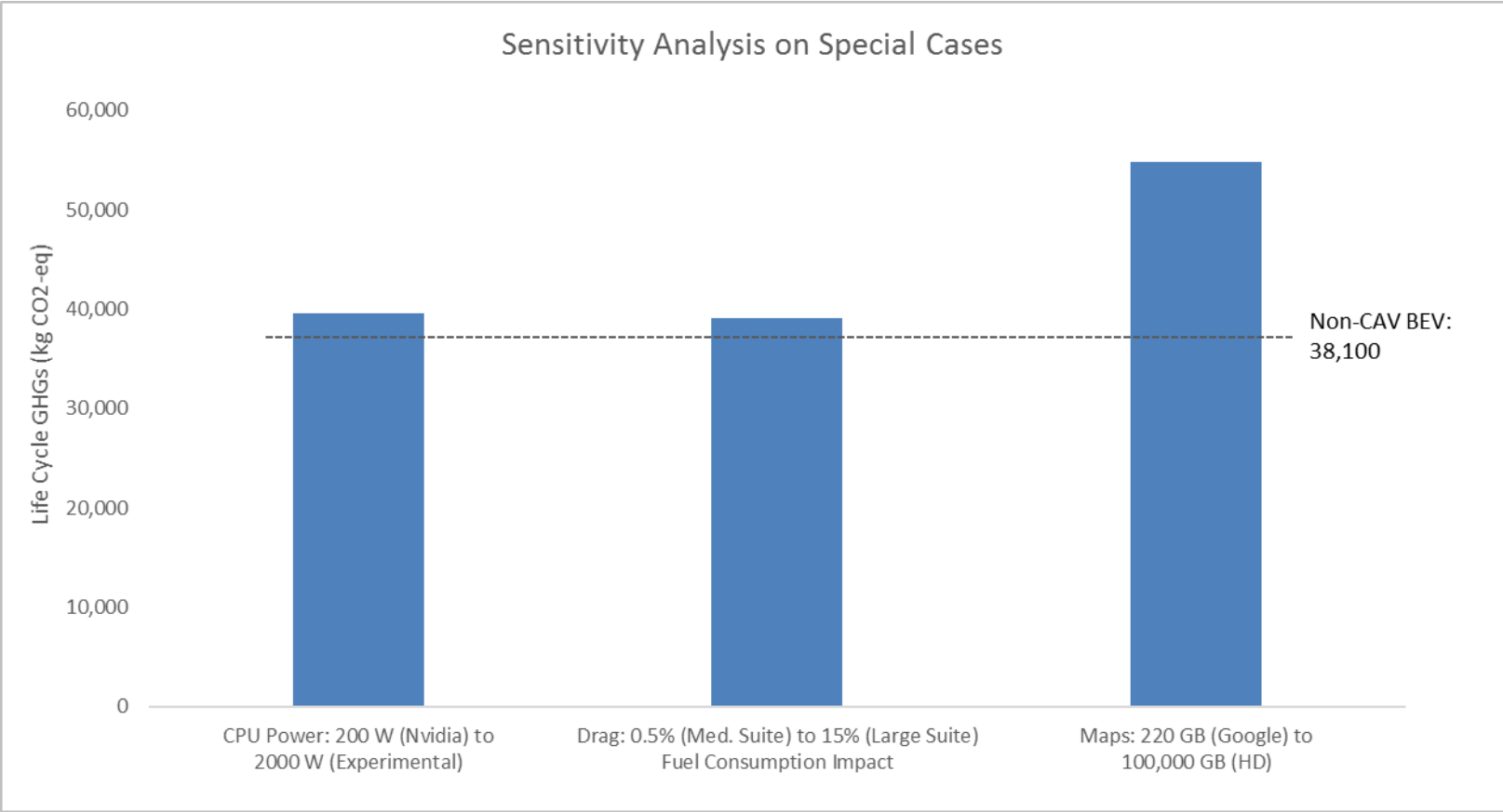


Figure S23. Sensitivity special cases on the baseline scenario illustrating the potential for environmental benefits to be eliminated

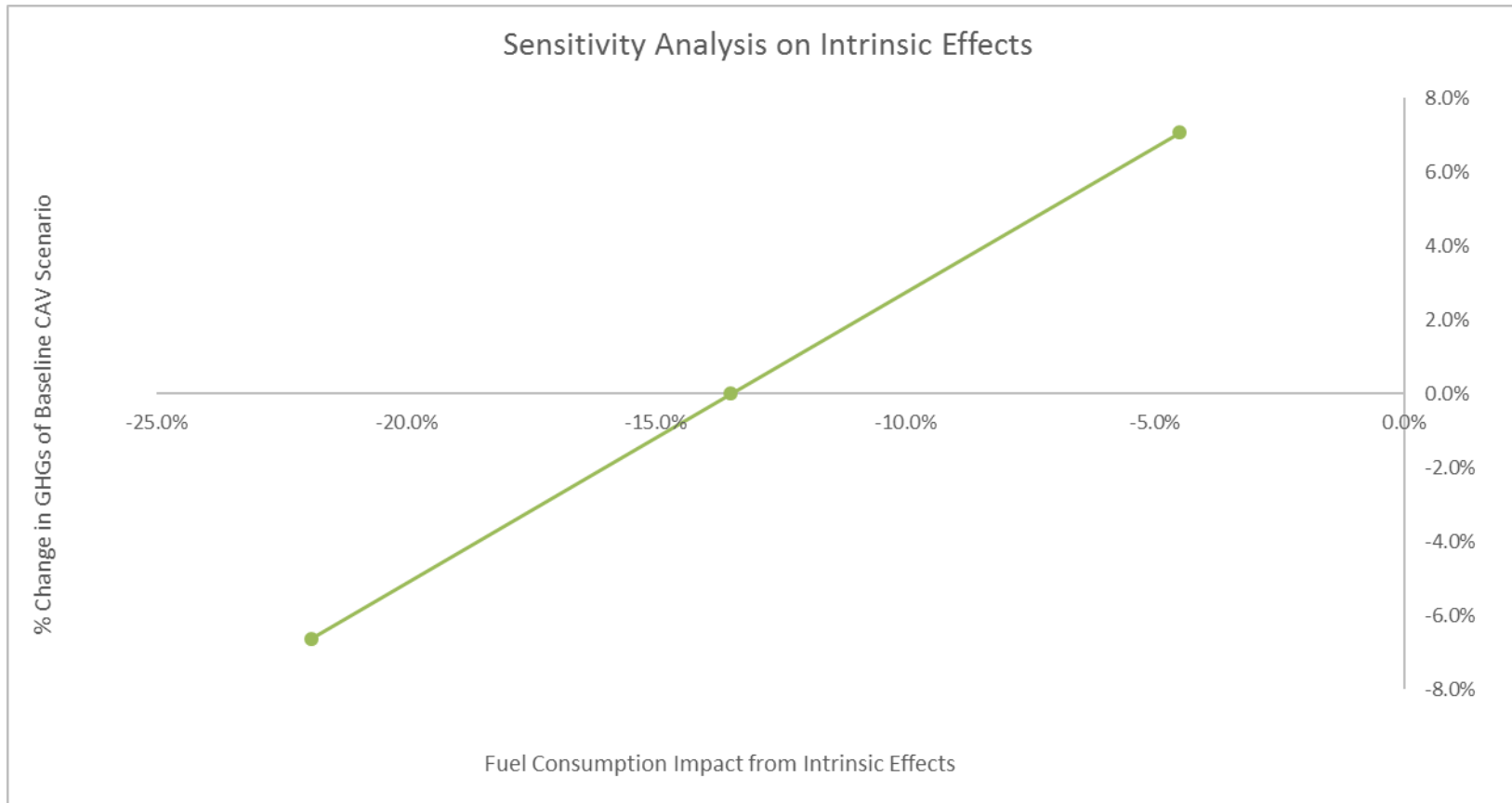


Figure S24. Impacts on GHG results for the baseline scenario as intrinsic effects are varied from -5% to -22%; -14% is the average

References

- (1) Kim, H. C.; Wallington, T. J. Life Cycle Assessment of Vehicle Lightweighting: A Physics-Based Model To Estimate Use-Phase Fuel Consumption of Electrified Vehicles. *Environ. Sci. & Technol.* 2016, 50 (20), 11226–11233; DOI 10.1021/acs.est.6b02059
- (2) Kim, H. C.; Wallington, T. J.; Arsenault, R.; Bae, C.; Ahn, S.; Lee, J. Cradle-to-Gate Emissions from a Commercial Electric Vehicle Li-Ion Battery: A Comparative Analysis. *Environ. Sci. & Technol.* 2016, 50 (14), 7715–7722; DOI 10.1021/acs.est.6b00830
- (3) U.S. Department of Energy and U.S. Environmental Protection Agency Model Year 2015 Fuel Economy Guide; <https://www.fueleconomy.gov/feg/download.shtml>.
- (4) A look at Tesla’s new Autopilot hardware suite; <https://electrek.co/2016/10/20/tesla-new-autopilot-hardware-suite-camera-nvidia-tesla-vision/>
- (5) Building Ford's Next-Generation Autonomous Development Vehicle; <https://medium.com/@ford/building-fords-next-generation-autonomous-development-vehicle-82a6160a7965>
- (6) Introducing Waymo's suite of custom-built, self-driving hardware; <https://medium.com/waymo/introducing-waymos-suite-of-custom-built-self-driving-hardware-c47d1714563>
- (7) Autonomous Vehicle Uses Dragonfly2 and Firefly MV Cameras for Vision; <https://www.ptgrey.com/case-study/id/10393>
- (8) NvidiaAI Driving Platform and SI Supercomputer Xavier; <https://www.gputechconf.jp/assets/files/1062.pdf>
- (9) LRR3: 3rd generation Long-Range Radar Sensor; http://products.bosch-mobility-solutions.com/media/db_application/downloads/pdf/safety_1/en_4/lrr3_datenblatt_de_2009.pdf
- (10) AWG Copper Wire Size Table and Data Chart; http://www.engineersedge.com/copper_wire.htm
- (11) CohdaWireless MK5 OBU Specification Version 1.4; www.cohdawireless.com
- (12) Hacking Automotive Ultrasonic Sensors; <http://www.instructables.com/id/Hacking-Automotive-Ultrasonic-Sensors/>
- (13) DSRC Spring Mounted Mobile Antennas 5.9 GHz; www.mobilemark.com
- (14) Antennas Pinwheel OEM Version 5; www.Novatel.com
- (15) Enclosures PwrPak7-E1 Version 0B; www.Novatel.com
- (16) Dragonfly2 Technical Reference Manual Revision 2.5; www.ptgrey.com
- (17) SavariSW-1000 Road-Side-Unit (RSU); www.savari.net

(18) Ultrasonic Sensor; http://products.bosch-mobility-solutions.com/en/de/_technik/component/CO_PC-CV_DA_Side-View-Assist_CO_CV_Driver-Assistance_2197.html?compId=1157

(19) Puck Hi-Res; www.velodynelidar.com

(20) HDL-64E; www.velodynelidar.com

(21) Teehan, P.; Kandlikar, M. Comparing Embodied Greenhouse Gas Emissions of Modern Computing and Electronics Products. *Environ. Sci. & Technol.* 2013, 47 (9), 3997–4003; DOI 10.1021/es303012r

Appendix B – Phase 2 Supporting Information

Appendix A: Supplementary Material

Electrical Grid Carbon Intensity Predictions

Table A1 provides the U.S. Mix electrical grid carbon intensity and primary energy predictions for the years 2015 to 2050 sourced from [ANL \(2016a\)](#). The GHG emissions reported here include both upstream and downstream emissions. The nuclear primary energy was adapted to include upstream inefficiencies according to the US LCI Database provided by NREL. The percentage reductions from 2015 are also provided.

Table A1: U.S. Mix electrical grid carbon intensity and primary energy predictions for the years 2015 to 2050

Parameter	2015	2020	2025	2030	2035	2040	2045	2050
U.S. Mix Carbon Intensity (kg CO ₂ eq/MJ)	0.15097	0.13502	0.12149	0.11332	0.11189	0.10923	0.10720	0.10590
Reduction from Year 2015	-	11%	20%	25%	26%	28%	29%	30%
U.S. Mix Primary Energy (MJ/MJ)	2.63798	2.42755	2.34144	2.28889	2.24802	2.21381	2.17116	2.13229
Reduction from Year 2015	-	8%	11%	13%	15%	16%	18%	19%

The percentage reductions from the U.S. Mix scenario were applied to the 2015 U.S. Central and Southern Plains electrical grid carbon intensity sourced from [ANL \(2016a\)](#) and primary energy to produce the predictions shown in **Table A2**. These predictions were used as the conservative scenario for the Austin, TX electrical grid.

Table A2: Conservative Austin electrical grid carbon intensity and primary energy predictions for the years 2015 to 2050

Parameter	2015	2020	2025	2030	2035	2040	2045	2050
Conservative Austin Carbon Intensity (kg CO ₂ eq/MJ)	0.20363	0.18211	0.16387	0.15285	0.15092	0.14733	0.14459	0.14283
Conservative Austin Primary Energy (MJ/MJ)	2.75288	2.53328	2.44342	2.38858	2.34593	2.31023	2.26572	2.22516

The percentage reductions from the “Stretch Tech, CP20” scenario reported in Appendix A of [U.S. DOE \(2017\)](#) were applied to the 2015 U.S. Central and Southern Plains electrical grid carbon intensity to produce the predictions shown in **Table A3**. These predictions were used as the optimistic scenario for the Austin, TX electrical grid.

Table A3: Optimistic Austin electrical grid carbon intensity predictions for the years 2015 to 2050

Parameter	2015	2020	2025	2030	2035	2040	2045	2050
Optimistic Austin Carbon Intensity (kg CO ₂ eq/MJ)	0.20363	0.11179	0.06388	0.04791	0.03593	0.02395	0.01996	0.01597
Reduction from Year 2015	-	45%	69%	76%	82%	88%	90%	92%

CAV Subsystem Computer Power Consumption

Table A4 provides the conservative predictions for the CAV subsystem computer power consumption between 2020 and 2050. The power consumption begins at 2000 W in 2020 and decreases to 192 W in 2039, after which it remains constant through 2050 due to diminishing returns. These beginning and ending values were chosen based on the sensitivity analysis bounds from [Gawron et al. \(2018\)](#). The rate of decrease is based on a doubling of computer energy efficiency every 2.7 years ([Koomey et al., 2017](#)). However, to account for an assumed increase in computational requirements as Level 4 software matures this decay rate is instead modeled as a doubling of efficiency every 5.4 years..

Table A4: Conservative CAV subsystem computer power consumption predictions for the years 2020 to 2050

Parameter	2020	2025	2030	2035	2040	2045	2050
Computer Power Consumption (Watts)	2000	1079	577	314	192	192	192

Table A5 provides the optimistic predictions. The power consumption begins at the same starting value of 2000 W in 2020, but declines at a rate of 50% over 2.7 years to a final value of 192 W in 2030.

Table A5: Optimistic CAV subsystem computer power consumption predictions for the years 2020 to 2050

Parameter	2020	2025	2030	2035	2040	2045	2050
Computer Power Consumption (Watts)	2000	620	192	192	192	192	192

Expansions of Groups C, D, and E

An expansion of Group C is provided in **Figure A1** to show the main differences between Scenarios 5 and 6. There is a small increase in vehicle burden due to the 4% increase in fleet VKT caused by more empty miles from the smaller fleet in Scenario 6. The charging-infrastructure burden increases since there is a 900% increase in the burden per charger when using DC fast chargers, which is partially offset by the 45% decrease in the total number of chargers required. Finally, there is a decrease in the parking burden due to the 31% decrease in the AT fleet size. Overall, the life-cycle GHG emissions increase by 3% when transitioning from Scenario 5 to Scenario 6.

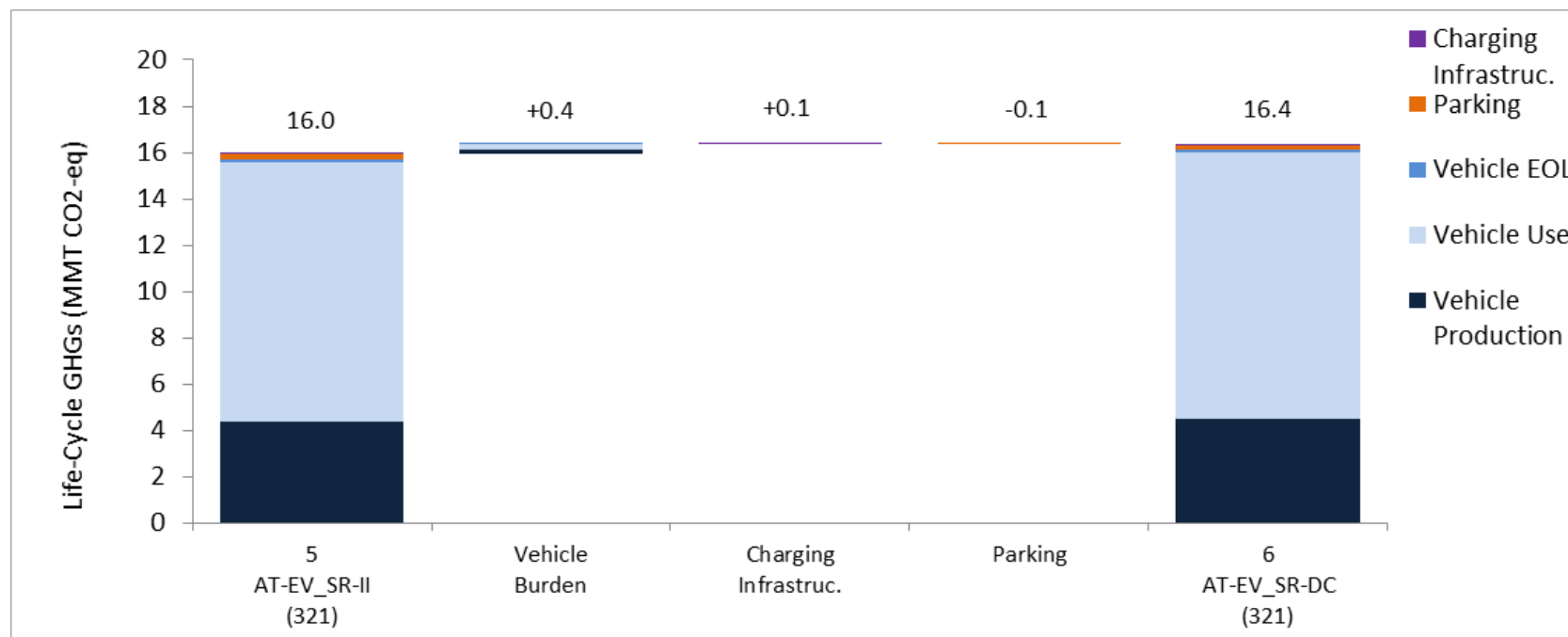


Figure A1: Expansion of Group C showing the impacts of transitioning from the Level II to DC fast charging scenario.

An expansion of Group D is provided in **Figure A2** to show the main differences between Scenarios 7 and 8. The waterfall follows a similar pattern when compared to Group B. Overall, the cumulative life-cycle GHG emissions decrease by 10% when transitioning from Scenario 7 to Scenario 8 with the 643,738 km lifetime.

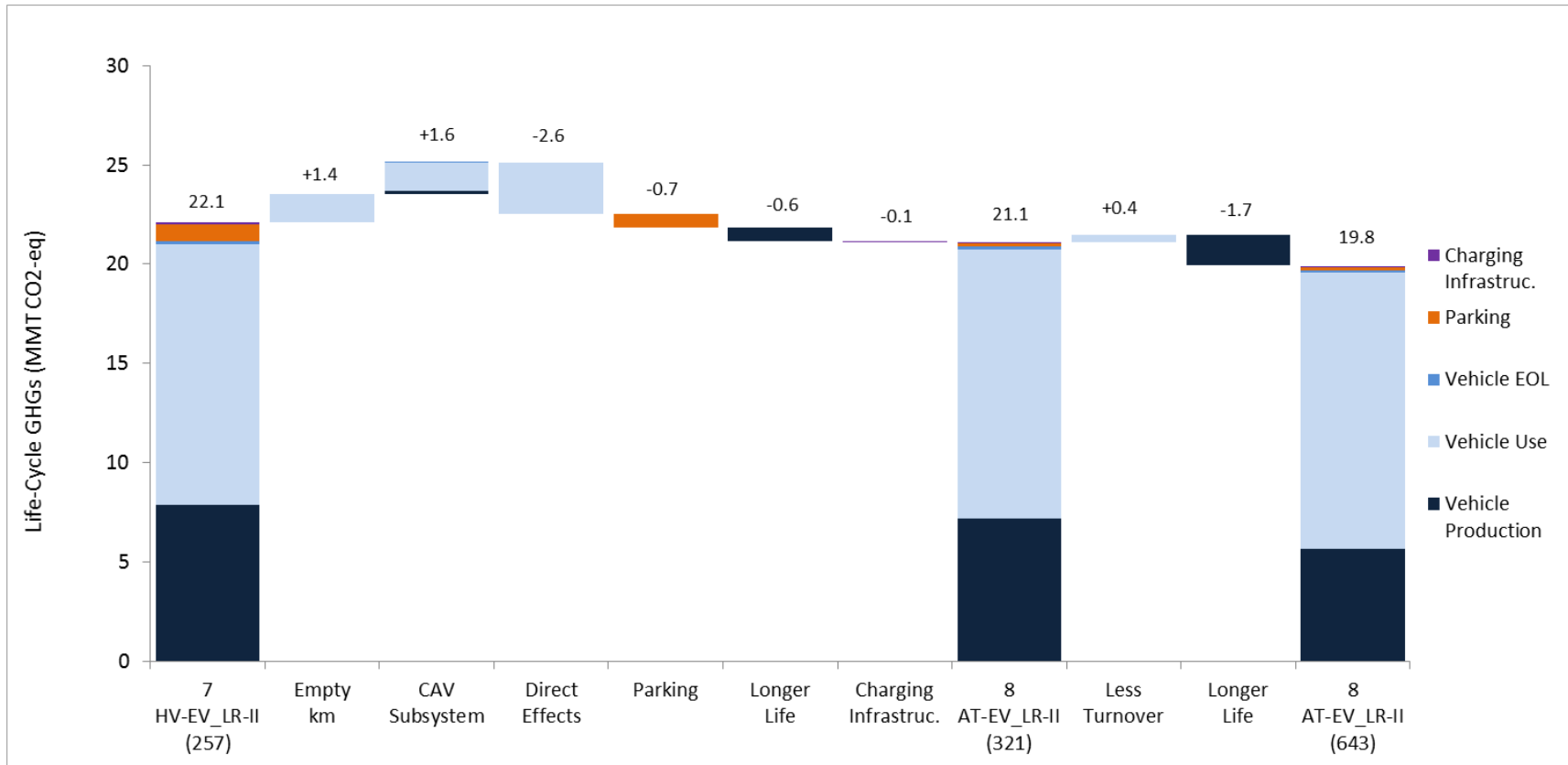


Figure A2: Expansion of Group D showing the impacts of direct and indirect effects specific to long range BEV powertrains. Includes Scenarios 7 and 8, as well as a special sensitivity case for Scenario 8 with a 643,738 km lifetime.

An expansion of Group E is provided in **Figure A3** to show the differences between Scenarios 8 and 9. The waterfall follows a different pattern compared to Group C since there is a 2% decrease in GHG emissions as opposed to a 3% increase. There is a small decrease in vehicle burden due to the 2% decrease in fleet VKT caused by fewer empty kilometers from reduced charging trips. The charging infrastructure burden decreases since the 900% increase in the burden per charger when using DC fast chargers is fully offset by the 85% decrease in the total number of chargers required. Finally, there is a decrease in the parking burden due to the 22% decrease in the AT fleet size.

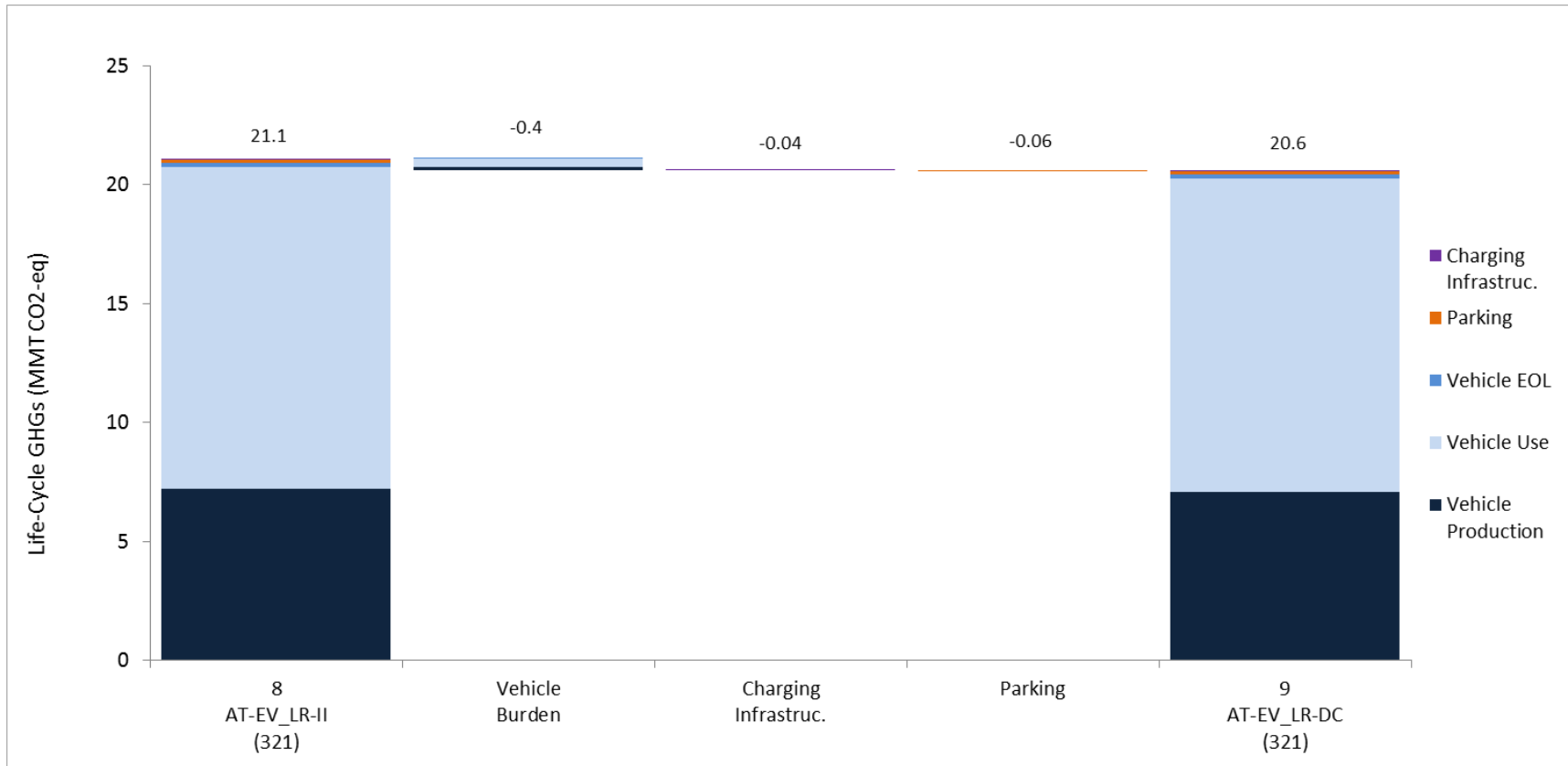


Figure A3: Expansion of Group E showing the impacts of transitioning from the Level II to DC fast charging scenario with long-range BEVs.

Life Cycle Energy Results

The monthly life-cycle energy consumption in a time series from 2020 to 2050 is provided in **Figure A4**.

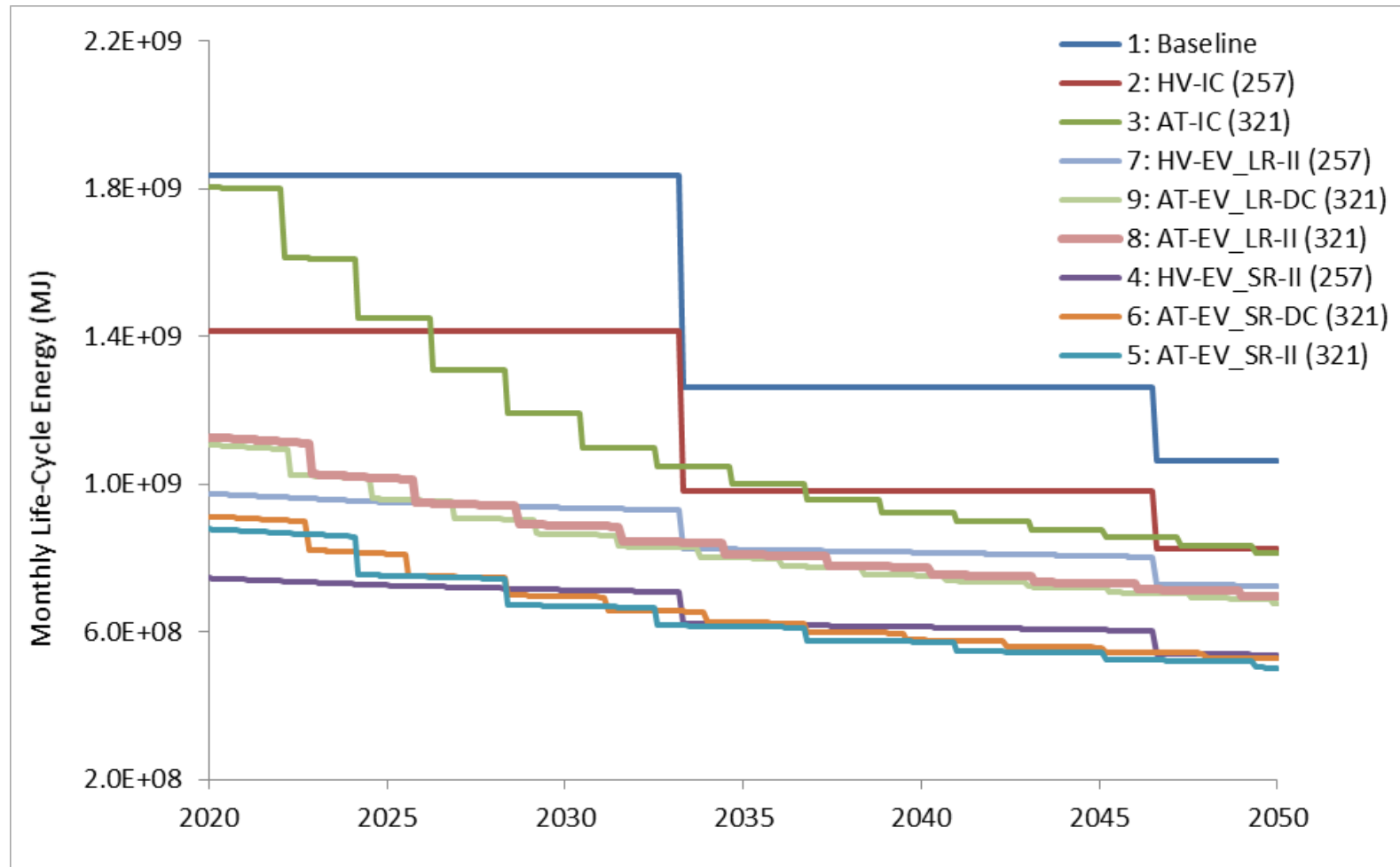


Figure A4: Monthly life-cycle energy consumption from 2020 to 2050 modeled using the conservative fleet turnover and electrical grid decarbonization inputs for the base case. Legend listed in order of decreasing energy consumption.

The cumulative life-cycle energy consumption for each scenario over the 30-year scenario timeframe is provided in **Figure A5**. The results are broken out by life-cycle phase as well as the contributions from parking and charging infrastructure.

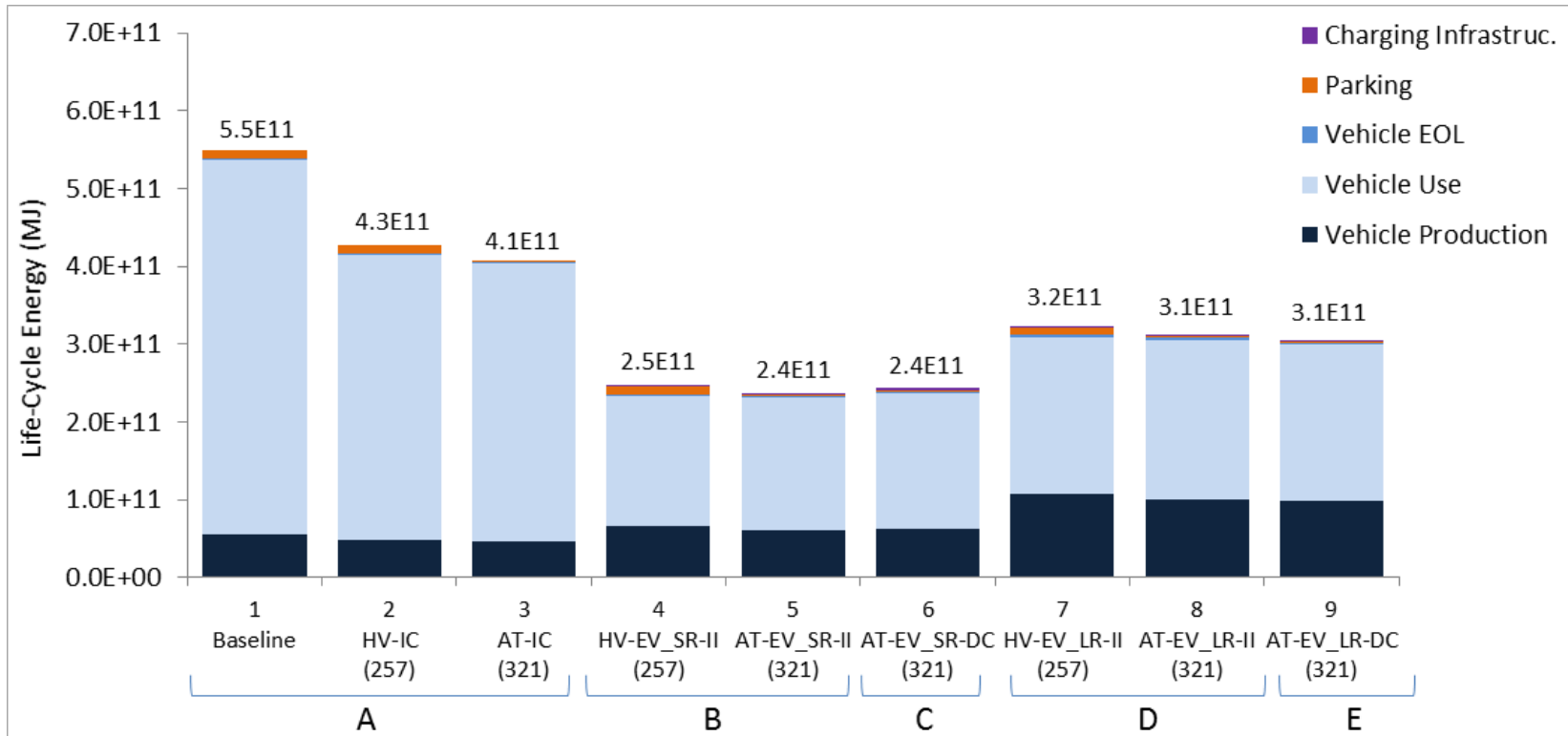


Figure A5: Cumulative fleet life-cycle energy consumption over 30 year scenario timeframe broken out by life-cycle phase

Dynamic Ride-Share

The results of including dynamic ride-sharing within Scenario 5 of the base case are provided in **Figure A6**. Scenarios 5.2, 5.3, and 5.4 vary the AT ride-share capacity at levels of 2, 3, and 4, respectively. Higher AT capacity allows for more passenger trips to be combined, reducing both VKT and fleet size.

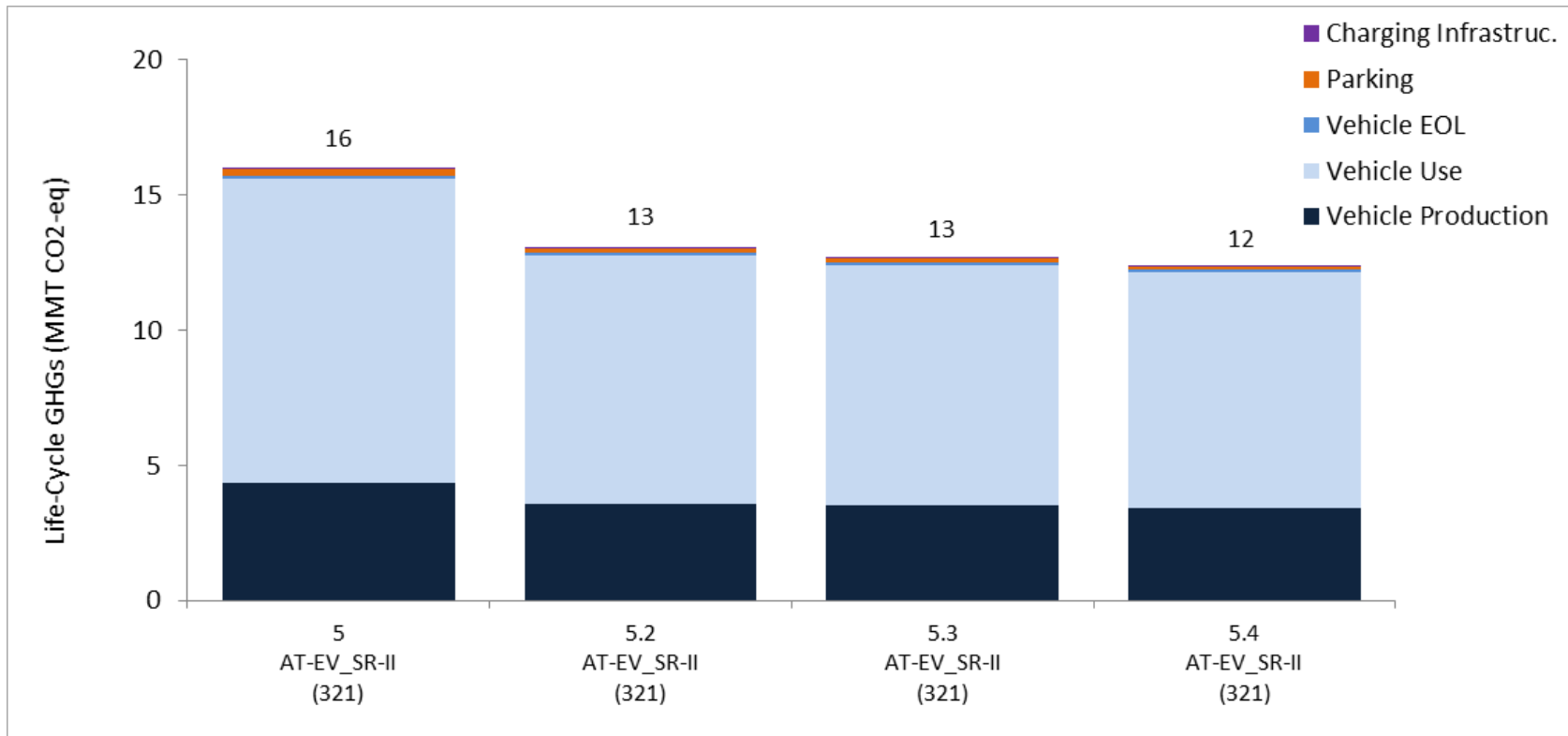


Figure A6: Sensitivity analysis results when adding dynamic ride-sharing to Scenario 5

Sensitivity Analysis

The results of using the optimistic AT lifetime of 643,738 km instead of the conservative lifetime of 321,869 km in the base case are provided in **Figure A7**.

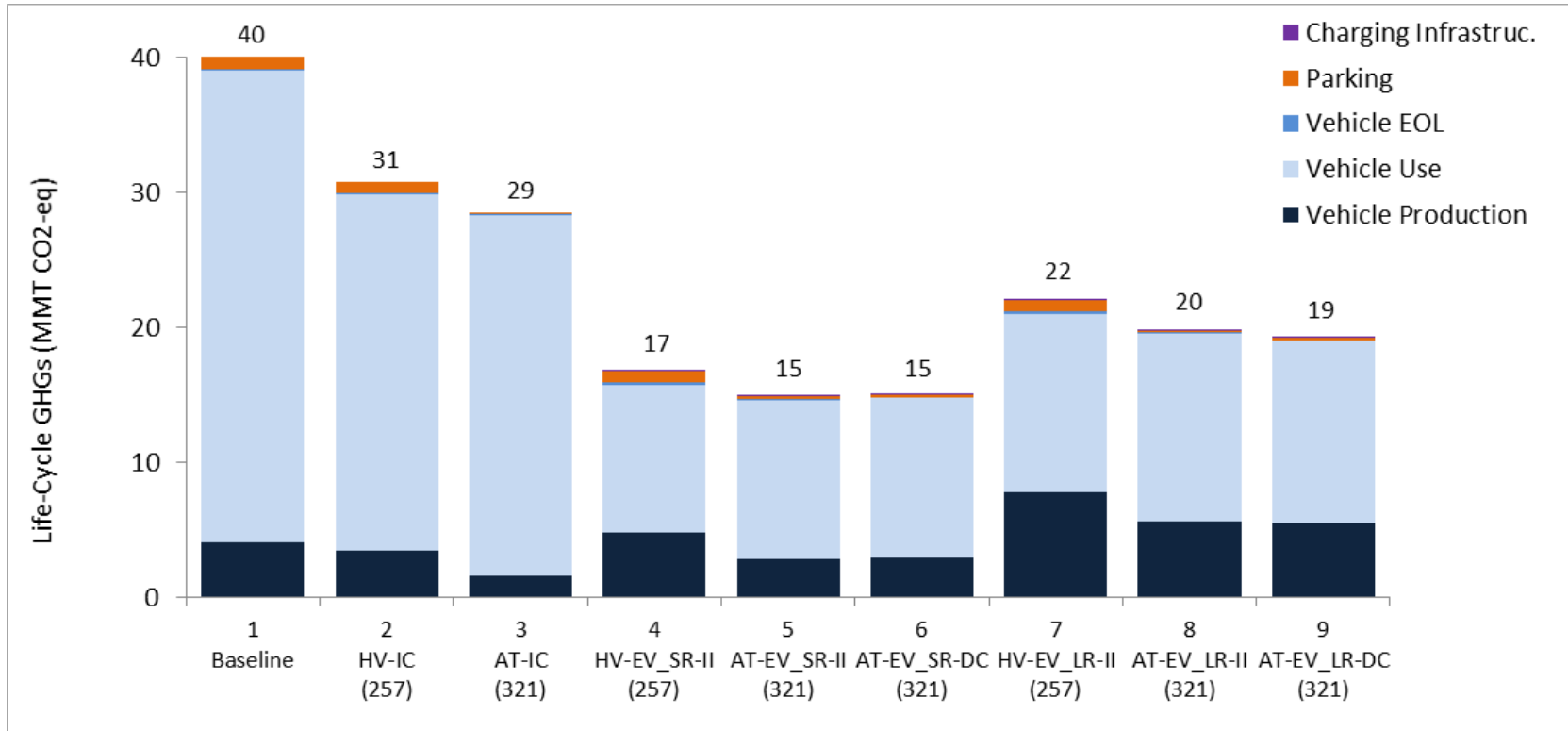


Figure A7: Sensitivity analysis results when changing the AT lifetime from the conservative 321,869 km to the optimistic 643,738 km

The results of using the optimistic annual new-vehicle fuel-consumption rate reduction instead of the conservative reductions within the base case are provided in **Figure A8**.

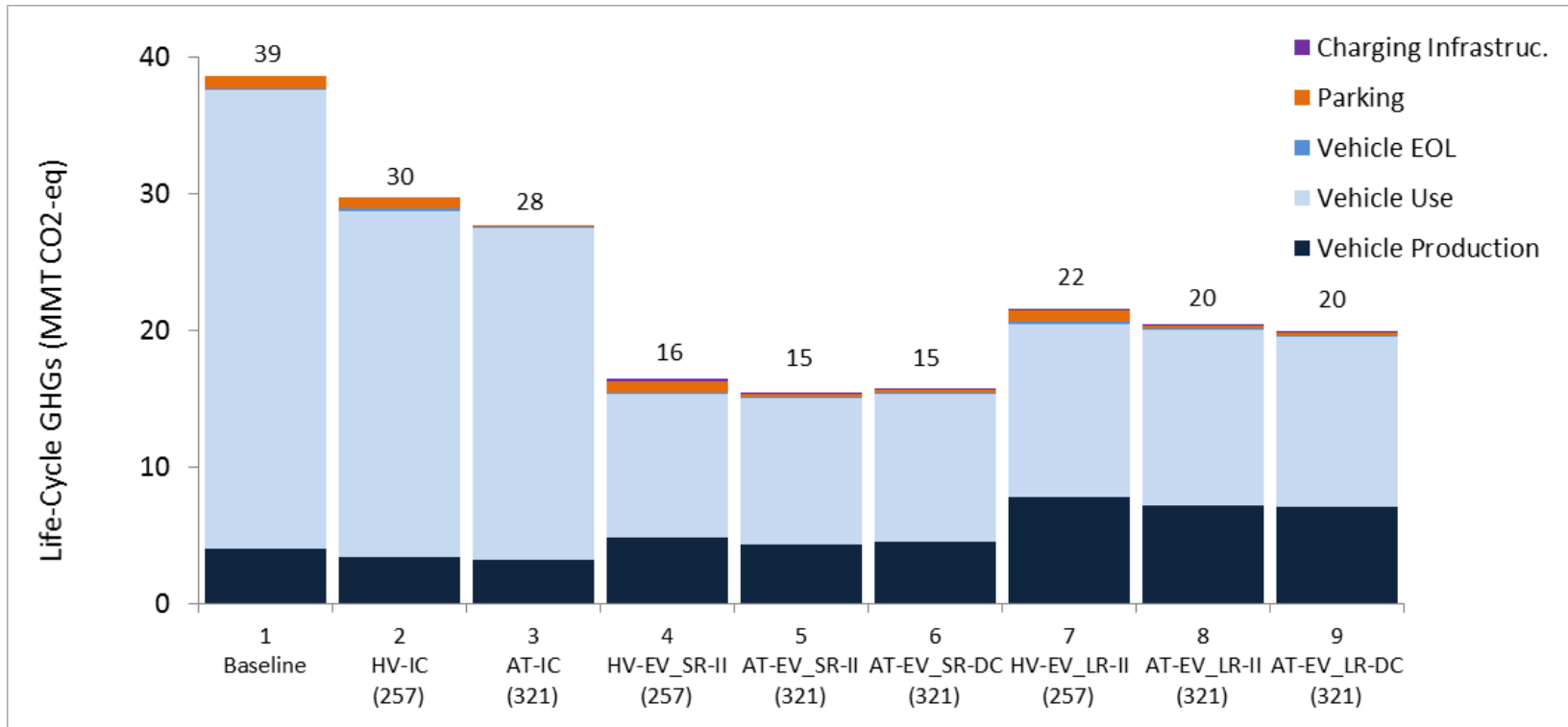


Figure A8: Sensitivity analysis results when changing the annual new-vehicle fuel-consumption rate reduction from the conservative scenario to optimistic in the base case

The results of using the optimistic electrical-grid decarbonization rate instead of the conservative reductions within the base case are provided in **Figure A9**.

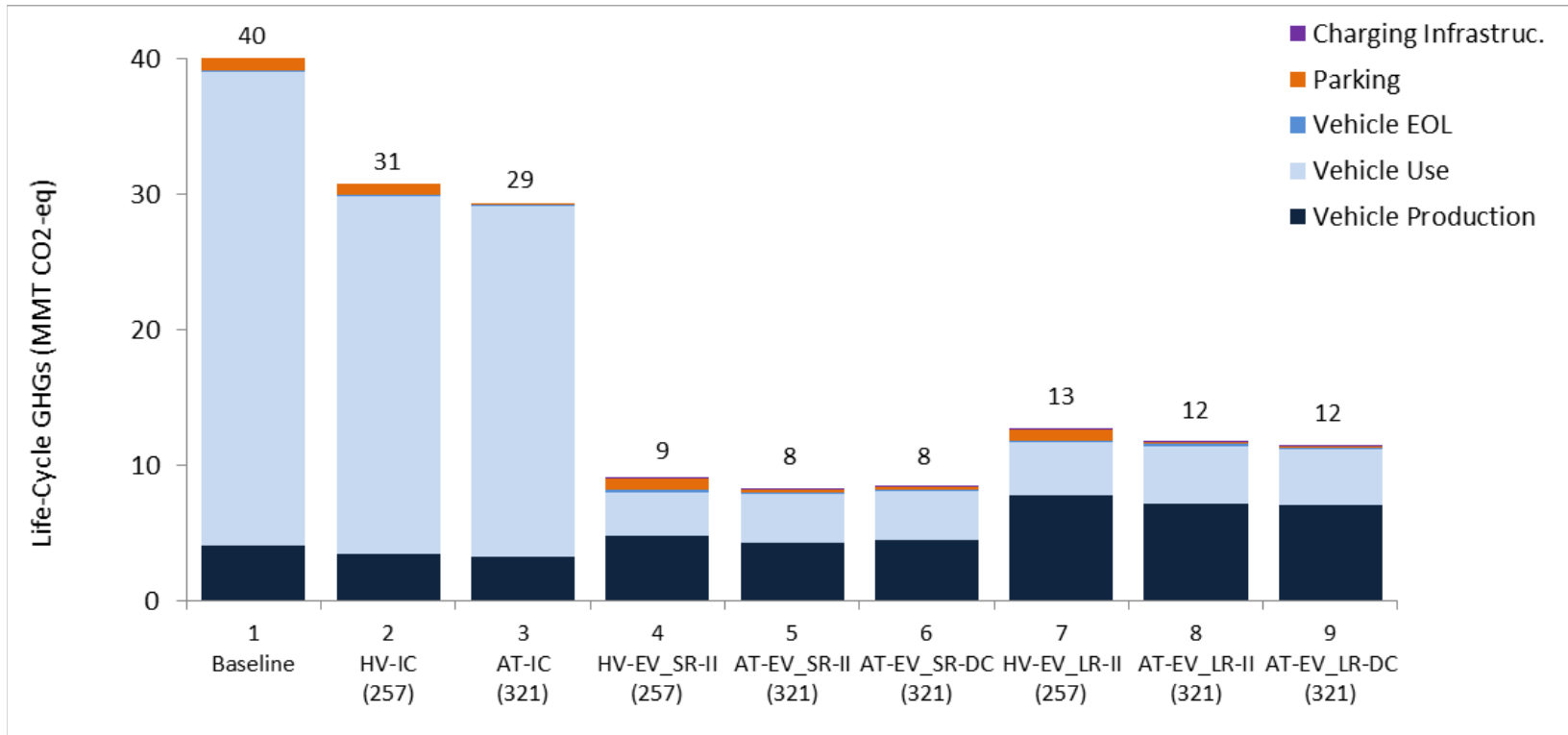


Figure A9: Sensitivity analysis results when changing the electrical grid decarbonization rate from the conservative scenario to optimistic in the base case

The results of using the optimistic CAV-subsystem computer power consumption instead of the conservative reductions within the base case are provided in **Figure A10**.

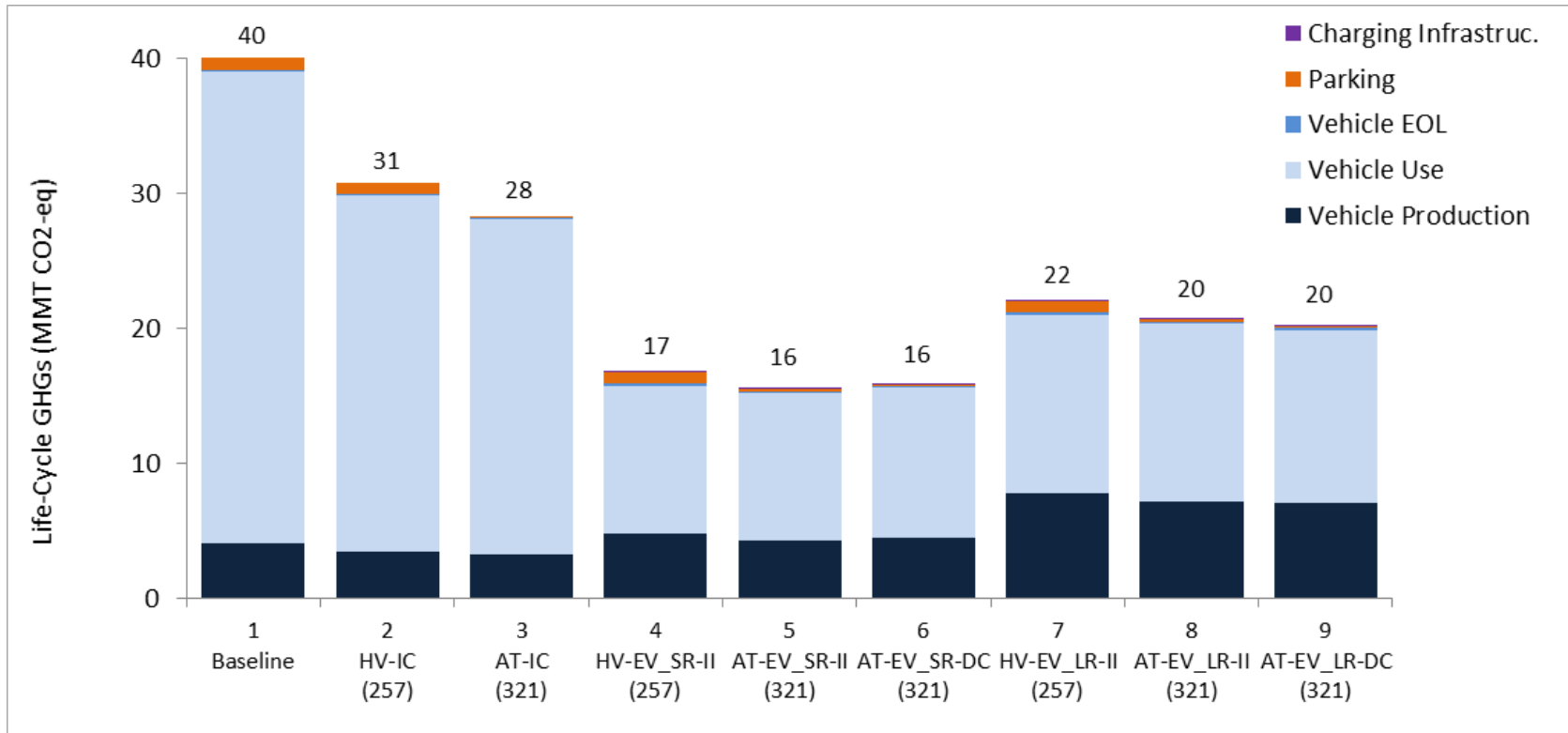


Figure A10: Sensitivity analysis results when changing the computer power consumption from the conservative scenario to optimistic in the base case

The results of combining the optimistic AT lifetime of 643,738 km, optimistic annual new-vehicle fuel-consumption rate reductions, optimistic electrical-grid decarbonization rate, and optimistic CAV-subsystem computer power consumption are provided in **Figure A11**.

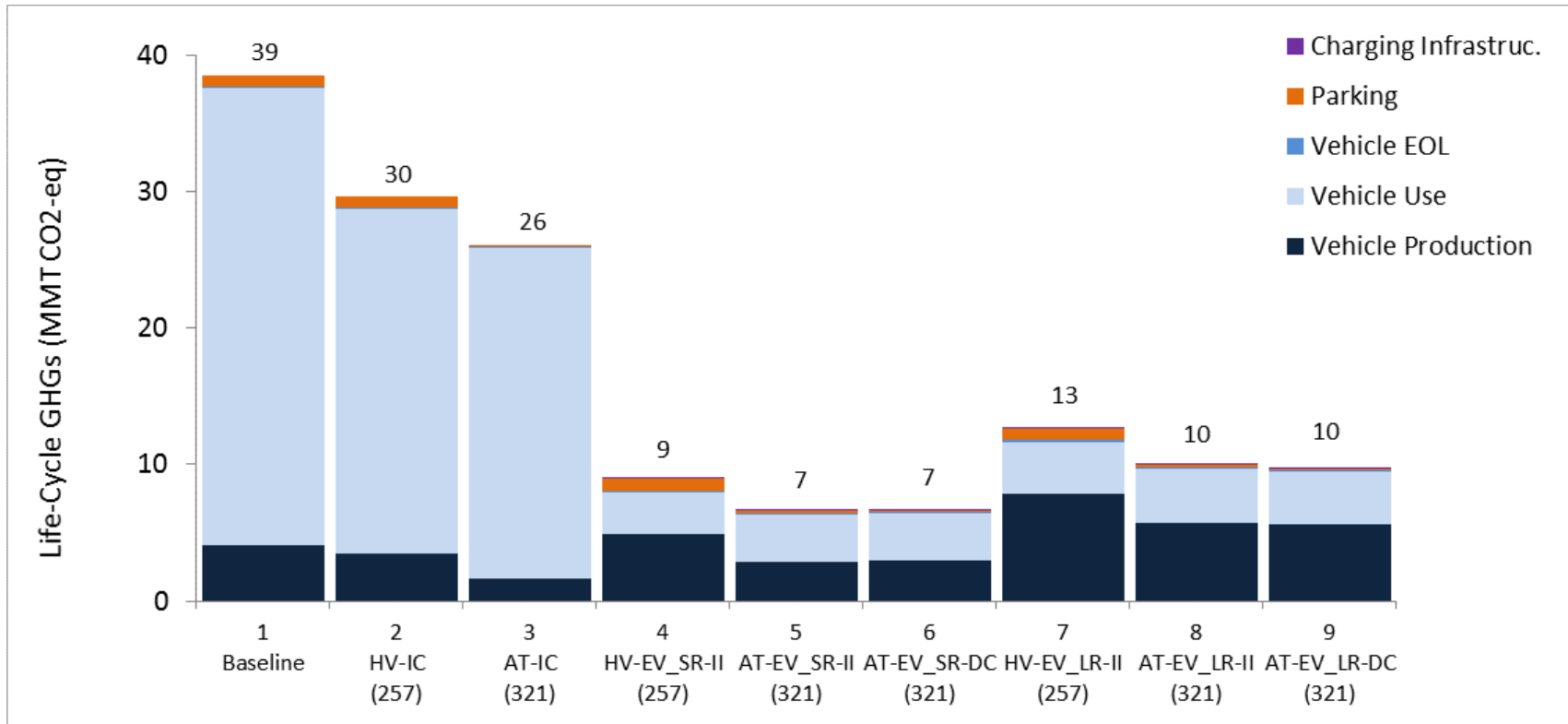


Figure A11: Sensitivity analysis results when combining optimistic lifetimes, annual new-vehicle fuel-consumption rate reductions, computer-power consumption, and electrical-grid decarbonization rates

A summary of the results contained in **Figures A6-A11** is provided in **Figure A12**.

The results are provided in units of kg-CO₂eq in rows 2 to 7 and correspond to those reported in **Figures A7-A11**. Scenarios 5.2, 5.3, and 5.4 are included in accordance with Figure A6.

The percent reductions from the Base Case (row 2) reported in rows 8 to 13 show the impact of changing a parameter from conservative to optimistic. Each case study scenario is impacted differently by the sensitivity analysis. For example, Scenario 2 is not affected by the optimistic lifetime in row 9 since it is only applicable to AT fleets, while Scenario 6 has an 8% reduction.

The percent reductions from the Baseline (column C) are reported in rows 14 to 19 and show the impacts of transitioning from the current fleet of human-driven vehicles to any one of the case study scenarios. The emission benefits of the transitions differ depending on the sensitivity analysis scenario. For example, transitioning from the Baseline to Scenario 5 in the Base Case (row 14) results in a 60% reduction in GHG emissions. However, the benefit increases to 87% in the combined sensitivity analysis scenario with dynamic ride-share (row 19).

	A	B	C	D	E	F	G	H	I	J	K	L	M	N
1		Case Study Scenario	1 Baseline	2 HV-IC (257)	3 AT-IC (321)	4 HV-EV_SR-II (257)	5 AT-EV_SR-II (321)	5.2 AT-EV_SR-II (321)	5.3 AT-EV_SR-II (321)	5.4 AT-EV_SR-II (321)	6 AT-EV_SR-DC (321)	7 HV-EV_LR-II (257)	8 AT-EV_LR-II (321)	9 AT-EV_LR-DC (321)
		Sensitivity Analysis Scenario												
2	GHGs (kg CO ₂ eq)	Base Case	4.01E+10	3.08E+10	2.94E+10	1.69E+10	1.60E+10	1.30E+10	1.27E+10	1.24E+10	1.64E+10	2.21E+10	2.11E+10	2.06E+10
3		A7: Optimistic Lifetime of 643,738 km	4.01E+10	3.08E+10	2.85E+10	1.69E+10	1.49E+10	1.21E+10	1.17E+10	1.14E+10	1.51E+10	2.21E+10	1.98E+10	1.92E+10
4		A8: Optimistic Annual Fuel-Consumption Rate Reduction	3.86E+10	2.97E+10	2.77E+10	1.64E+10	1.54E+10	1.25E+10	1.22E+10	1.19E+10	1.58E+10	2.16E+10	2.03E+10	1.98E+10
5		A9: Optimistic Electrical-Grid Decarbonization Rate	4.01E+10	3.08E+10	2.94E+10	9.16E+09	8.26E+09	6.75E+09	6.55E+09	6.40E+09	8.51E+09	1.28E+10	1.18E+10	1.15E+10
6		A10: CAV-Subsystem Computer Power Consumption	4.01E+10	3.08E+10	2.84E+10	1.69E+10	1.56E+10	1.27E+10	1.24E+10	1.21E+10	1.60E+10	2.21E+10	2.07E+10	2.02E+10
7		A11: A7 + A8 + A9 + A10	3.86E+10	2.97E+10	2.61E+10	9.08E+09	6.67E+09	5.39E+09	5.19E+09	5.05E+09	6.76E+09	1.27E+10	9.98E+09	9.68E+09
8		% Reduction from Base Case	Base Case	0%	0%	0%	0%	0%	0%	0%	0%	0%	0%	0%
9	A7: Optimistic Lifetime of 643,738 km		0%	0%	3%	0%	6%	7%	8%	8%	8%	0%	6%	6%
10	A8: Optimistic Annual Fuel-Consumption Rate Reduction		4%	4%	6%	3%	4%	4%	4%	4%	4%	2%	4%	4%
11	A9: Optimistic Electrical-Grid Decarbonization Rate		0%	0%	0%	46%	48%	48%	48%	48%	48%	42%	44%	44%
12	A10: CAV-Subsystem Computer Power Consumption		0%	0%	3%	0%	2%	2%	2%	2%	2%	0%	2%	2%
13	A11: A7 + A8 + A9 + A10		4%	4%	11%	46%	58%	59%	59%	59%	59%	42%	53%	53%
14	% Reduction from Baseline	Base Case	0%	23%	27%	58%	60%	67%	68%	69%	59%	45%	47%	49%
15		A7: Optimistic Lifetime of 643,738 km	0%	23%	29%	58%	63%	70%	71%	72%	62%	45%	50%	52%
16		A8: Optimistic Annual Fuel-Consumption Rate Reduction	0%	23%	28%	57%	60%	67%	68%	69%	59%	44%	47%	49%
17		A9: Optimistic Electrical-Grid Decarbonization Rate	0%	23%	27%	77%	79%	83%	84%	84%	79%	68%	71%	71%
18		A10: CAV-Subsystem Computer Power Consumption	0%	23%	29%	58%	61%	68%	69%	70%	60%	45%	48%	50%
19		A11: A7 + A8 + A9 + A10	0%	23%	32%	76%	83%	86%	87%	87%	82%	67%	74%	75%

Figure A12: Summary of sensitivity analysis results

The impact of varying the CAV sensing and computing subsystem between the small and large versions described in [Gawron et al. \(2018\)](#) is shown in **Figure A13**. The figure shows the percentage change from the medium CAV subsystem results for both the ICEV and BEV scenarios. The impact ranges from <1% for the small CAV subsystem to 8-10% for the large CAV subsystem.

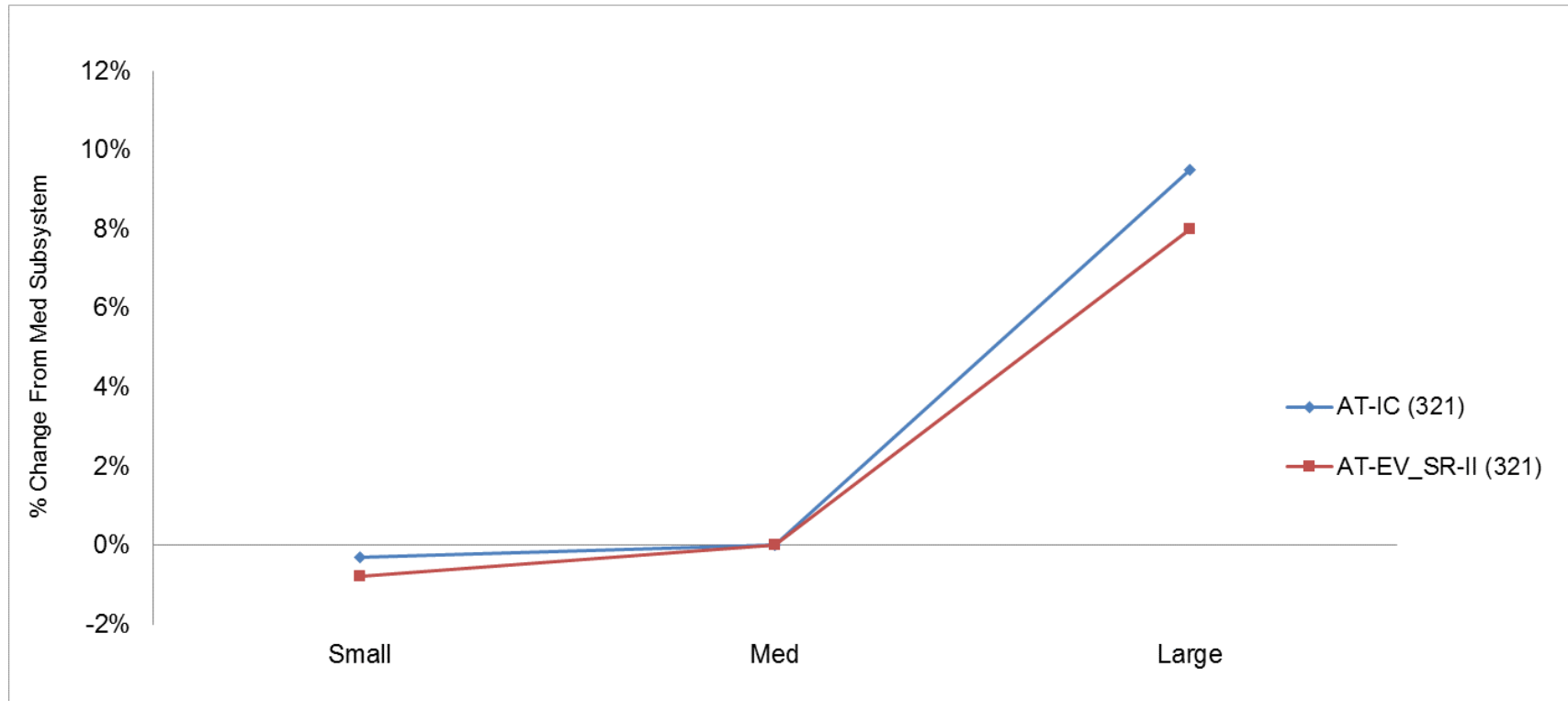


Figure A13: Sensitivity analysis results when varying the size of the CAV sensing and computing subsystem

The impact of varying the CAV direct effects between the minimum of 9% fuel consumption reduction to the maximum of 19% described in [Stephens et al. \(2016\)](#) is shown in **Figure A14**. The figure shows the percentage change from the base case results that use the 14% fuel consumption reduction. The impact is approximately $\pm 5\%$.

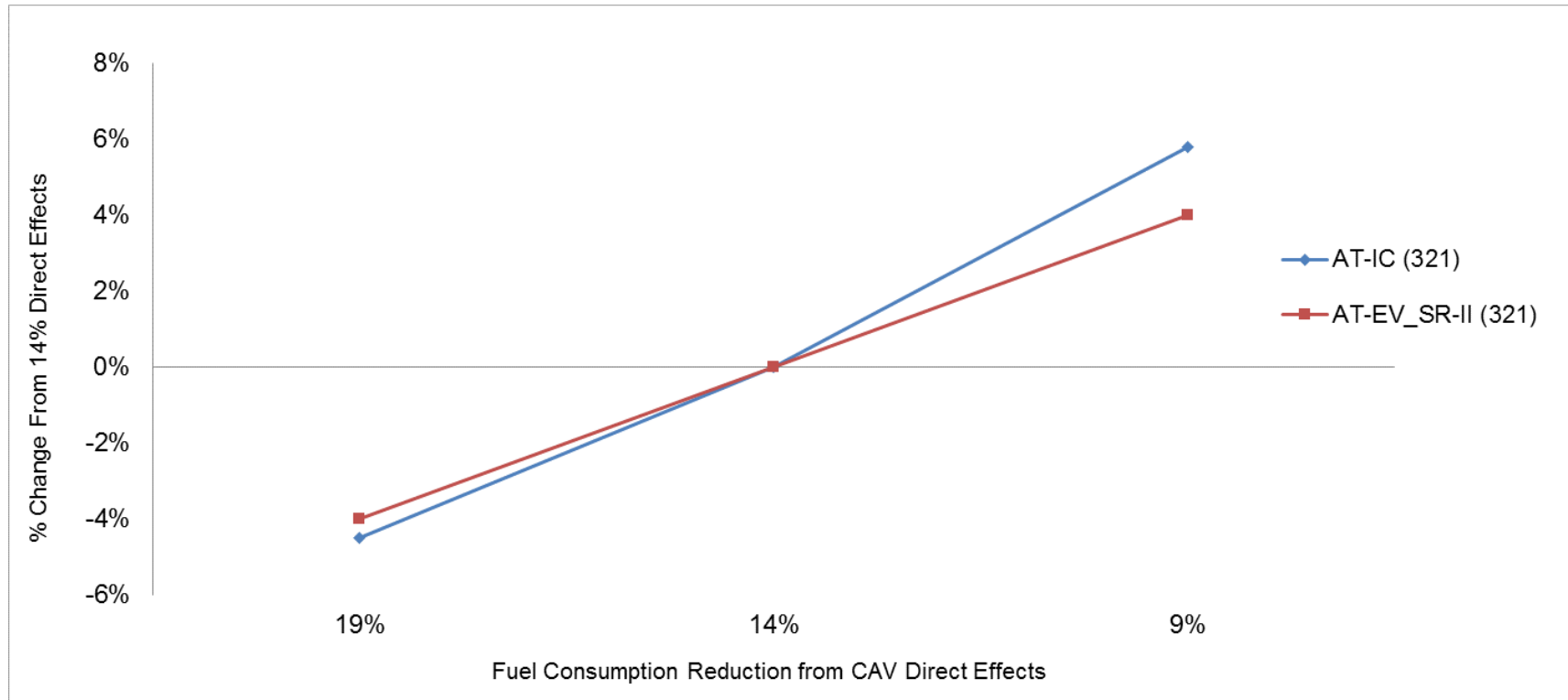


Figure A14: Sensitivity analysis results when varying the fuel consumption reduction from CAV direct effects

References

Argonne National Laboratory (ANL). (2016a). The Greenhouse Gases, Regulated Emissions, and Energy Use in Transportation (GREET) Model Software: GREET 1. Version 2011 Copyright © 1999 UChicago Argonne, LLC.

Gawron, J. H., Keoleian, G. A., Kleine, R. D., Wallington, T. J., & Kim, H. C. (2018). Life Cycle Assessment of Connected and Automated Vehicles: Sensing and Computing Subsystem and Vehicle Level Effects. *Environmental Science & Technology*, 52(5), 3249-3256.
doi:10.1021/acs.est.7b04576

Koomey, J, and Naffziger, S. (2015, March 31). Moore's Law Might Be Slowing Down, But Not Energy Efficiency. Retrieved September 15, 2018 from <https://spectrum.ieee.org/computing/hardware/moores-law-might-be-slowing-down-but-not-energy-efficiency>

Stephens, T. S., Gonder, J., Chen, Y., Lin, Z., Liu, C., & Gohlke, D. (2016). Estimated Bounds and Important Factors for Fuel Use and Consumer Costs of Connected and Automated Vehicles. NREL (National Renewable Energy Laboratory (NREL), Golden, CO (United States)). Retrieved from <http://www.nrel.gov/docs/fy17osti/67216.pdf>

U.S. Department of Energy (COE). (2017). Energy CO2 Emissions Impacts of Clean Energy Technology Innovation and Policy. Retrieved May 2, 2018 from <https://www.energy.gov/sites/prod/files/2017/01/f34/Energy%20CO2%20Emissions%20Impacts%20of%20Clean%20Energy%20Technology%20Innovation%20and%20Policy.pdf>